

Chapter 6

Detectability of curves in sea level relative to a local datum

6.1 Introduction

In chapter 4 the detectability of specific curves in individual sea-level height series has been investigated. Only variations in relative sea-level heights have been examined, i.e., sea-level changes relative to the local tide gauge bench mark. Changes in height of the tide gauge itself have not been considered. The main conclusion based on these individual time series was that the detectability of curves in these series is limited by the occurrence of long-periodic fluctuations in the data. As a result, estimates of trend values stabilise only after a large observation period (of the order of 80 to 100 years). Consequently, a change in trend at the beginning of the time series cannot be detected. How many years of observations are required to detect greenhouse-gas induced warming at the end of the time series depends on (knowledge of) the resulting pattern and the extent of the acceleration.

In this chapter, the detectability of a common curve for a group of tide gauges will be examined. Of interest is whether or not the availability of more data sets containing similar sea-level height data will reduce the time required to reliably estimate the underlying sea-level variation pattern. It will also be examined whether the detectability of patterns is reduced by inaccuracies in height connections between tide gauges. Considered will be the influence of, e.g., time span between measurement campaigns, precision of measurements, and the method used to correct for obtained variations in height.

Since tide gauges measure sea-level heights relative to their tide gauge bench marks, any local vertical movements of these tide gauge bench marks will have introduced inconsistencies between the individual time series. These inconsistencies impair the quality of a common sea-level variation curve determined for a group of tide gauges. By connecting the tide gauge bench marks in height, inconsistencies between individual sea-level height series introduced by height changes of the tide gauges themselves, can be eliminated.

Nowadays, it is preferred to connect tide gauges in height by means of (permanent) GPS observations. However, in the past, no direct height connections were made between tide gauge bench marks. Usually, the tide gauge bench marks have been connected to a local height system, (hopefully) on a regular basis. Therefore, in this chapter, common sea-level variation curves relative to the local height datum will be considered, for a group of tide gauges situated along the Dutch coast.

For this chapter it is assumed that all tide gauges included in the data set refer to the same vertical datum. Therefore, vertical movements of this vertical reference system will not be considered. If a sea-level variation pattern needs to be established for a group of tide gauges situated in different datum zones, vertical movements of the reference surfaces will introduce inconsistencies between the (groups of) time series. These inconsistencies can be removed by connecting the local datums in height. This so-called vertical datum connection will be discussed in chapter 7.

Methods (and their inherent errors) that can be used to connect tide gauge bench marks to a local reference frame have been discussed in chapter 5. Based on this information, a reasonable estimate of the quality expected from local height connections can be made. Unfortunately, this only holds for new surveys and height connections performed over the last few decades.

For large parts of obtainable (long) sea-level height records only scant information is available on when tide gauge bench marks have been part of measuring campaigns, how changes in height of these bench

marks have been treated, and whether possible changes in the local reference system have been converted into height changes of the tide gauges. Therefore, instead of trying to approximate the actual height connection history for the various tide gauges, a number of possible configurations will be simulated. Height connections as considered in this chapter will be described in section 6.2.3.

Analogous to chapter 4, to examine the detectability of sea-level variation curves, simulated data sets will be used. These data sets contain a specific variation curve (e.g., one trend throughout the time series) in combination with periodic fluctuations and height connection errors (inconsistencies between the individual time series introduced by inaccuracies in the height connections). Since the (common) sea-level variation curve in the data set is known, it can be examined how well this curve can be detected if individual sea-level height series are contaminated by different types of height connection errors.

For this chapter it will be assumed that all tide gauges experience the same variations in absolute sea level. Spatial variations in sea level rise will be discussed in chapter 8. The detectability of a single trend throughout the time series will be discussed in section 6.3. In section 6.4, transition to a higher slope value at the beginning of the time series will be examined. Finally, in section 6.5, detectability of changes in trend at the end of the time series will be treated. First, in the next section, the general structure of the data sets used will be explained.

6.2 General structure of simulated data sets

All data sets considered in this chapter, consist of sea-level height time series simulated for a group of six tide gauges. It is assumed that all six time series start in 1865 and contain data up to 1996, except for section 6.5, in which data sets up to 2100 will be used.

The individual time series in the data sets are based on three components. Firstly, they consist of a signal part, which is the sea-level variation curve that needs to be detected. Secondly, they contain periodic fluctuations and measuring noise of the tide gauge system. These two effects are considered as one group, since, for annual mean values these two effects are difficult (and not really necessary) to distinguish. Finally, simulated sea-level signals contain height connection errors. These are inconsistencies between the individual time series introduced by inaccuracies in the height connections. Based on knowledge of actual sea-level variations (and especially due to our lack of knowledge of what has really occurred) a wide range of possibilities can be considered to simulate the three parts of the time series.

6.2.1 Simulated sea-level variation curves

In this chapter, only a small group of six tide gauges, situated along the Dutch coast will be used. As has been shown in section 3.4, there is a large similarity between the time series obtained by these tide gauges. Therefore, it will be assumed that all six tide gauges experience the same sea-level variation curve. Differences in sea-level variation curves will only be examined for a larger group of tide gauges scattered all around the North Sea area; see chapter 8.

In this chapter, linear sea-level variations equal to those introduced in chapter 4 will be used, i.e.,

- a specific trend throughout the time series
- transition to a higher trend value at the beginning of the time series
- transition to a higher trend value at the end of the time series

In chapter 4, slope values of either 1.0, 1.5, 2.0, or 2.5 mm/yr have been used to simulate a consistent trend throughout the time series. However, in chapter 4 it has been concluded that the actual trend value used is of no influence on the detectability of a linear pattern in a time series containing periodic fluctuations. Therefore, in this chapter, all simulated data sets considered will be based on a sea-level rise with a slope value of 1.5 mm/yr.

If a change in trend at the beginning of the time series is required, analogous to chapter 4, it will be assumed that “pre-industrial” sea-level rise has a 0.8 mm/yr lower trend value than present-day sea-level increase. For the onset year of the sea level rise acceleration, again, the year 1885 will be used. In this chapter, only an abrupt increase in slope value will be considered, since, as discussed in chapter 4, a 0.8 mm/yr increase in slope value at the beginning of a time series containing long-periodic fluctuations cannot (or hardly) be detected.

Analogous to chapter 4, greenhouse-gas induced warming will be simulated by a sea-level rise acceleration yielding either a 20, 49, or 86 cm sea-level increase for the year 2100 (relative to 1990). Starting in 1991, simulated time series contain an abrupt increase in slope value to 1.8, 4.5, or 7.8 mm/yr respectively.

6.2.2 Simulated periodic fluctuations and measuring noise

Periodic fluctuations and measuring noise (of the tide gauge equipment) are treated as one group, because of the method used to simulate these signals. Either detrended time series are used, or periodic fluctuations are based on (at least) the highest components resulting from SSA decomposition of actual tide gauge data. These highest components usually contain mainly measuring noise.

In chapter 4, data sets composed of the full range of periodic fluctuations as present in actual tide gauge data have been used. In addition, time series containing only short-periodic fluctuations, or even no periodic fluctuations at all have been examined. As it is not very realistic to assume that (long) periodic fluctuations can be eliminated from the sea-level height series, all time series as considered in this chapter consist of both long- and short-periodic fluctuations.

For the group of six tide gauges situated in a local area, three different types of periodic patterns will be considered:

- all time series experience the same periodic fluctuations
- all time series contain the same long-periodic pattern, but different short-periodic fluctuations
- different time series experience different short- and long-periodic fluctuations

Same periodic fluctuations For this scenario it will be assumed that all six time series are basically equal, except for inconsistencies introduced by height connections between tide gauges. Periodic fluctuations used for all six data sets are those for tide gauge Den Helder. Detrended annual mean sea-level heights have been used to simulate this periodic pattern.

Different short-periodic fluctuations All six tide gauges experience the same long-periodic fluctuations (e.g., due to proximity of the stations). However, as a result of local circumstances, short-periodic patterns differ for the various tide gauges. As explained in section 4.3, time series containing either long- or short-periodic fluctuations are created by applying SSA analysis to actual tide gauge data and, subsequently, using reconstructions based on only specific principal components.

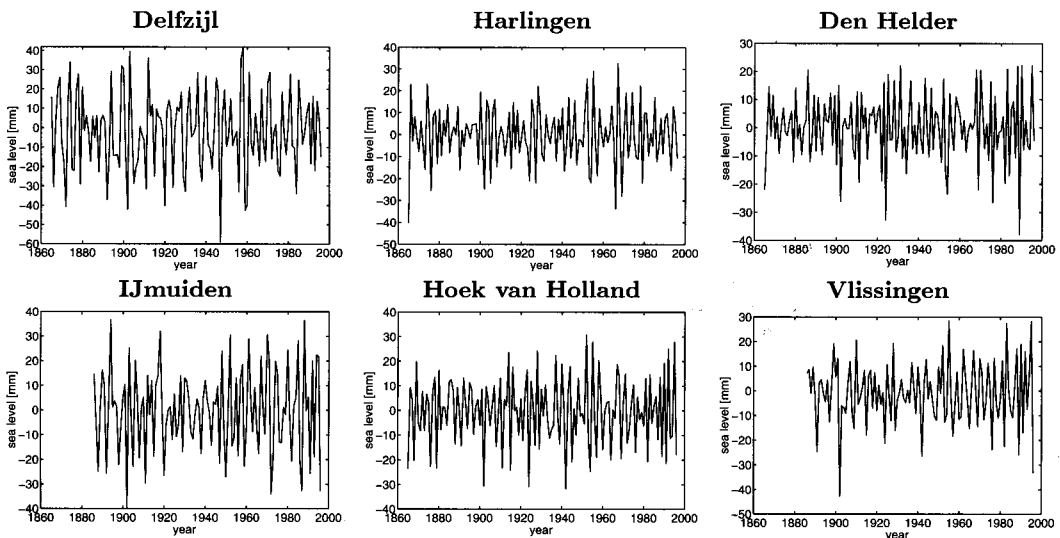


Fig. 6.1 Simulated short-periodic fluctuations based on specific combinations of SSA components. For tide gauges Vlissingen and IJmuiden data starting in 1887 has been used.

Figure 6.1 shows short-periodic fluctuations based on (a number of) the higher components following from SSA analysis of sea-level height data for six Dutch tide gauges. As explained in chapter 3, time series

for IJmuiden and Vlissingen contain significantly deviating sea-level heights at the beginning of the data sets. Consequently, for these two tide gauges, time series have only been used starting in 1887. Their periodic patterns have been repeated in order to create data sets starting in 1865.

The long-periodic patterns of all six time series are identical, i.e., they all use the long-periodic fluctuations for tide gauge Den Helder. These long-periodic fluctuations result from SSA analysis in which a window size of 20 years has been used. Signal is reconstructed based only on the first seven (detrended) principal components.

Different periodic fluctuations Finally, a situation will be considered in which different tide gauges experience a somewhat different (short and long) periodic pattern. Periodic signals are simulated by using detrended annual mean sea-level values corresponding to actual tide gauge data. Resulting periodic patterns are shown in figure 6.2. Again, for data from tide gauges IJmuiden and Vlissingen, only data starting in 1887 has been used and complete data sets have been created by repeating the periodic patterns.

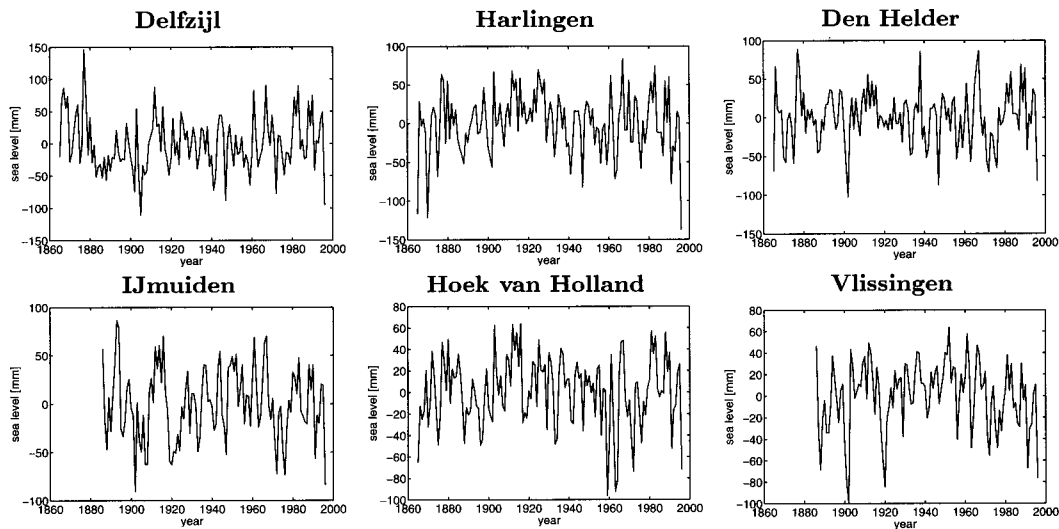


Fig. 6.2 Simulated periodic fluctuations based on detrended annual mean sea-level heights. For tide gauges Vlissingen and IJmuiden only data starting in 1887 has been used.

6.2.3 Simulated height connection scenarios

All actual sea-level data used in this chapter originates from Dutch tide gauges. Consequently, it will be assumed that all tide gauges considered are connected to the local Dutch height system, nowadays, NAP. Unfortunately, this height system has not been constant throughout the time span over which sea-level heights are available. For example, NAP was introduced in 1875. According to Waalewijn (1987), local disagreements with the old system (AP) could be as large as 10 to 20 cm. As another example, due to reconstruction works in 1955, the last bench mark on which the original AP and NAP systems were based, was removed and the zero of the Dutch height system was transferred to an underground bench mark.

Changes in reference surface complicate the possibilities to reconstruct the actual history of height changes between tide gauges. In addition, it seems difficult to ascertain when specific tide gauge bench marks have been measured. Therefore, the influence of inaccuracies in height connections will be examined based on a number of potential height connection methods. Considered will be:

- Height connections cause no additional errors in sea-level values.
- Height connections introduce normally distributed random noise on annual values.
- Height connections are performed on a regular basis (every 10, 20, or 30 years). Errors in determined tide gauge heights are described by normally distributed random values.
- Height connections are performed on an irregular basis (in 1885, 1940, 1960, 1980 and 1996). Errors in determined tide gauge heights are described by normally distributed random values.

The above mentioned height connection methods can be applied with a wide range of values for the standard deviations of the height connection noise. Table 6.1 gives an overview of the scenarios that will be considered in this chapter to simulate height connection errors. A more detailed description is given in the remainder of this section. In principle, all errors in determined tide gauge heights are simulated by normally distributed random values with zero mean and specific standard deviations.

scenario	short explanation	height differences based on following parameters
<i>no-error</i>	errorless height connection	
<i>annual</i>	yearly connection of heights	different standard deviations: $\sigma : 5 \text{ mm}$, $\sigma : 1 \text{ cm}$, $\sigma : 2 \text{ cm}$
<i>regular</i>	height connection every: 10, 20, or 30 years	$N = 10$, $N = 20$, or $N = 30$ years different standard deviations: $\sigma : 1 \text{ cm}$, $\sigma : 2 \text{ cm}$
<i>irregular</i>	height connections in: 1885, 1940, 1960, 1980, 1996	same precision for all connections different standard deviations: $\sigma : 1 \text{ cm}$, $\sigma : 2 \text{ cm}$, $\sigma : 5 \text{ cm}$
<i>historical</i>	height connections in: 1885, 1940, 1960, 1980, 1996	subsequent connections have better precisions <i>set 1</i> : 1885 $\sigma : 3 \text{ cm}$, 1940 $\sigma : 2 \text{ cm}$, 1960 $\sigma : 2 \text{ cm}$, 1980 $\sigma : 1.5 \text{ cm}$, 1996 $\sigma : 1.5 \text{ cm}$ (<i>pessimistic</i>) <i>set 2</i> : 1885 $\sigma : 2 \text{ cm}$, 1940 $\sigma : 1.5 \text{ cm}$, 1960 $\sigma : 1.5 \text{ cm}$, 1980 $\sigma : 1 \text{ cm}$, 1996 $\sigma : 1 \text{ cm}$ <i>set 3</i> : 1885 $\sigma : 1.5 \text{ cm}$, 1940 $\sigma : 1 \text{ cm}$, 1960 $\sigma : 1 \text{ cm}$, 1980 $\sigma : 0.8 \text{ cm}$, 1996 $\sigma : 0.8 \text{ cm}$ (<i>optimistic</i>)

Table 6.1 Overview of height connection scenarios as used in this chapter.

Errorless height connection (*no-error*) In the simplest case, it will be assumed that height connections between tide gauges can be performed without introducing additional errors. This is not a very realistic assumption, but these results will be used for comparison with those obtained from more realistic height connection scenarios.

Annual connection of heights (*annual*) If height connections have been performed on (at least) a yearly basis, height connection errors can be described as normally distributed random values that have to be added to the annual mean sea levels. Nowadays, this high rate of height connections can be achieved by means of GPS. However, it is not likely that bench marks have been connected at least once a year in the (far) past. Therefore, these results will, again, be used as reference for other scenarios.

Constant time span between connections (*regular*) Height measurements have been performed every 10, 20, or 30 years. Furthermore, height connections are assumed at the same time for all tide gauges. For these time spans between the measurements, connections have allegedly been performed in:

N = 10 1856, 1866, 1876, 1886, 1896, 1906, 1916, 1926, 1936, 1946, 1956, 1966, 1976, 1986, and 1996.

N = 20 1856, 1876, 1896, 1916, 1936, 1956, 1976, and 1996.

N = 30 1846, 1876, 1906, 1936, 1966, and 1996.

Inaccuracies in height measurements lead to fictitious height differences represented by normally distributed random noise. If these height differences are distributed over sea-level values obtained between height connections, this will introduce errors in annual sea-level values as shown in figure 6.3. These examples have been based on normally distributed random errors with a standard deviation of 1 cm.

Different time spans between connections (*irregular*) In the Netherlands, first-order levelling campaigns have been performed between 1875 and 1885, 1926 and 1939, 1950 and 1959, 1965 and 1978, and, finally the fifth primary levelling from 1996 to 1999. Based on this information, connections are assumed in 1885, 1940, 1960, 1980, and 1996; at the same time for every tide gauge. Fictitious height differences will be represented by normally distributed random noise with various standard deviations. The same precision is assumed for all subsequent height connections performed for all tide gauges.

Long before the first primary levelling, height measurements have been performed in the Netherlands. However, they often did not refer to the same height datum, included only a specific (small) region

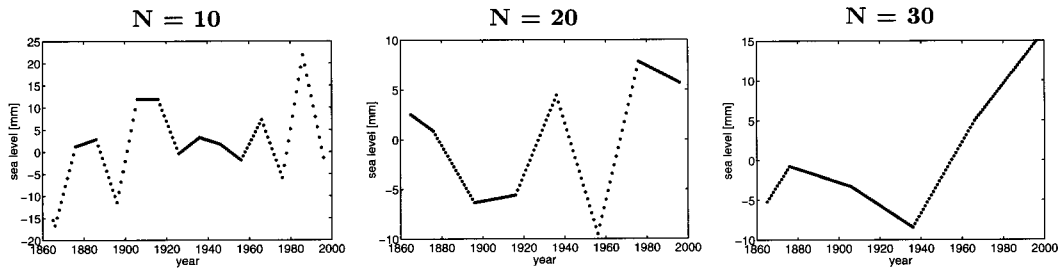


Fig. 6.3 Simulated errors in sea-level values, introduced by inconsistencies in height connections; *regular*, $\sigma : 1$ cm. Past measurements have been corrected for fictitious height differences.

and their quality is difficult to discern. Therefore, it will be presumed that station velocities can only be determined after the second height connection in 1940. These velocities are used to correct measurements over the period between 1865 up to 1940.

Subsequent height connections have better precisions (*historical*) Again, height connections corresponding to the history of first-order levellings in the Netherlands are used, i.e., connections in 1885, 1940, 1960, 1980, and 1996. However, for this scenario it is assumed that subsequent height connections have been performed with a better quality. Unfortunately, it is difficult to estimate realistic height connection precisions. Internal precisions of primary levelling networks are known, but tide gauge bench marks have often only been included in secondary levelling networks. In addition, it is difficult to ascertain when tide gauge bench marks have been included in levelling campaigns. Therefore, the following three sets of precisions have simply been selected:

- *set 1* Height connection in 1885: $\sigma = 3$ cm, 1940: $\sigma = 2$ cm, 1960: $\sigma = 2$ cm, 1980: $\sigma = 1.5$ cm, 1996: $\sigma = 1.5$ cm. *Pessimistic*.
- *set 2* Height connection in 1885: $\sigma = 2$ cm, 1940: $\sigma = 1.5$ cm, 1960: $\sigma = 1.5$ cm, 1980: $\sigma = 1$ cm, 1996: $\sigma = 1$ cm.
- *set 3* Height connection in 1885: $\sigma = 1.5$ cm, 1940: $\sigma = 1$ cm, 1960: $\sigma = 1$ cm, 1980: $\sigma = 0.8$ cm, 1996: $\sigma = 0.8$ cm. *Optimistic*.

For all six tide gauges, the same set of standard deviations will be used. In figure 6.4, examples are shown of (fictitious) height corrections resulting from (a specific realization of) height connection errors. Height connection errors are simulated by normally distributed random values using one of the three above mentioned sets of standard deviations.

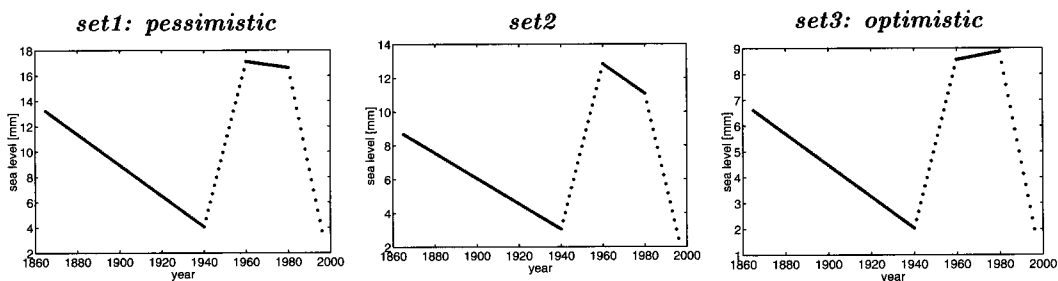


Fig. 6.4 Simulated errors in sea-level values, introduced by height connections; *historical*, 3 different sets of standard deviations. Past measurements have been corrected for fictitious height differences.

6.2.4 Methods for correcting determined height differences

Errors are not only introduced by inaccuracies in height connections, but can also result from incorrect adaptation of sea levels to determined height differences. Actual height changes can be rather abrupt (e.g., due to relocation of the tide gauge or reconstruction works in the area), or follow a more secular pattern (e.g., due to sedimentation). In addition, two methods can be applied to correct sea-level values

for measured height changes of the tide gauge bench mark. The first approach is to distribute height changes over the sea-level measurement for the elapsed period between height connections. The second method simply corrects measurements only after the height difference is discovered. Since information on which procedure has been applied, and what type of height changes might have occurred is very scarce, the following scenarios will be treated:

- Tide gauges follow secular movements and determined height differences are distributed over the elapsed period between height connections.
- Tide gauges follow secular movements, but, height changes are corrected intermittently.
- One tide gauge bench mark has experienced an abrupt change in height, but, determined height differences are distributed over the elapsed period between height connections.

These last two scenarios will introduce (additional) errors into the individual sea-level height time series.

Intermittent correction of heights Height differences as determined at a new height connection are only used to correct subsequent sea-level measurements. This seems not a very good method to correct sea-level height data obtained from tide gauges experiencing secular height changes. However, this might have happened in the past.

It is assumed that all six tide gauge bench marks undergo secular movements that can be described by a simple linear trend. Figure 3.11, as published by Lorenz *et al.* (1991), shows velocities of underground bench marks based on the 2nd, 3rd, and 4th first-order levelling in the Netherlands. Unfortunately, these underground bench marks do not correspond with sites as used in this chapter.

Velocities of tide gauge bench marks have been simulated based on known velocities of underground bench marks in the area. Two different sets of station velocities have been chosen. One set in which station velocities of all six tide gauges have values close to each other, and one set with relatively large differences in station velocities. Selected values are shown in table 6.2.

	tide gauge					
	Delfzijl	Harlingen	Den Helder	IJmuiden	Hoek van Holland	Vlissingen
<i>case 1</i>	-0.38	-0.33	-0.32	-0.31	-0.38	-0.27
<i>case 2</i>	-0.38	-0.22	-0.42	-0.06	-0.48	0.00

Table 6.2 Station velocities (in mm/yr) based on velocities of underground bench marks.

Examples of errors introduced by intermittent correction of height differences, using secular movements as presented in table 6.2, are shown in figure 6.5. The two figures have been based on height connections in 1885, 1940, 1960, 1980, and 1996. For subsequent height connections increasing precisions are assumed (i.e., height connection scenario *historical* with *pessimistic* precisions).

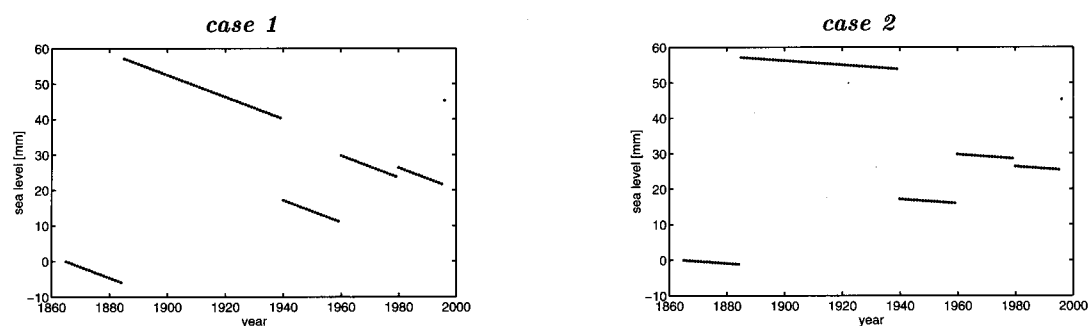


Fig. 6.5 Simulated errors in sea levels, introduced by uncorrected secular movements (tide gauge IJmuiden) and intermittent correction of fictitious heights in 1885, 1940, 1960, 1980, 1996; *pessimistic* set of st. dev.

Abrupt change in height Errors will also be introduced if determined height differences are distributed over all measurements obtained in the elapsed period between height connections, while in reality a more or less abrupt change in height has occurred.

As can be seen from figure 6.6, if abrupt changes in height are divided over the complete period of time between height connections, sea-level values before the jump has occurred receive an erroneous correction, while corrections to sea-level heights after the jump has occurred are to small.

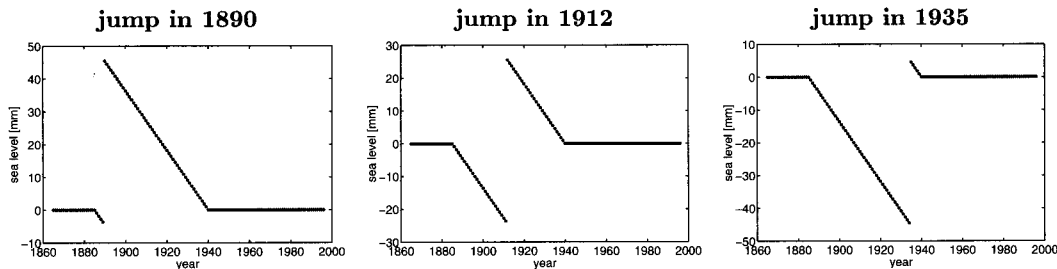


Fig. 6.6 Simulated errors in sea-level values, introduced by both a 5 cm jump in sea-level height and erroneous correction of this jump. Height connections in 1885, 1940, 1960, 1980, 1996.

6.3 Same trend throughout the time series

In this section, it is assumed that the sea-level variation curve can be adequately described by a simple linear trend. As explained in section 6.2, all simulated time series will be based on a linear trend of 1.5 mm/yr throughout the time series. In addition, time series contain periodic fluctuations that are either the same for all time series, different for all time series, or only short periodic fluctuations will vary.

In the following sections, results based on different height connection scenarios will be described. These height connection scenarios have been described in detail in section 6.2.3. An overview of the labels used to indicate the various height connection scenarios is given in table 6.3.

scenario	short explanation	height differences based on following parameters
<i>no-error</i>	errorless height connection	
<i>annual</i>	yearly connection of heights	different standard deviations: σ : 5 mm, σ : 1 cm, σ : 2 cm
<i>regular</i>	height connection every: 10, 20, or 30 years	N = 10, N = 20, or N = 30 years different standard deviations: σ : 1 cm, σ : 2 cm
<i>irregular</i>	height connections in: 1885, 1940, 1960, 1980, 1996	same precision for all connections different standard deviations: σ : 1 cm, σ : 2 cm, σ : 5 cm
<i>historical</i>	height connections in: 1885, 1940, 1960, 1980, 1996	subsequent connections have better precisions set 1: 1885 σ : 3 cm, 1940 σ : 2 cm, 1960 σ : 2 cm, 1980 σ : 1.5 cm, 1996 σ : 1.5 cm (<i>pessimistic</i>) set 2: 1885 σ : 2 cm, 1940 σ : 1.5 cm, 1960 σ : 1.5 cm, 1980 σ : 1 cm, 1996 σ : 1 cm set 3: 1885 σ : 1.5 cm, 1940 σ : 1 cm, 1960 σ : 1 cm, 1980 σ : 0.8 cm, 1996 σ : 0.8 cm (<i>optimistic</i>)

Table 6.3 Height connection scenarios used to examine the detectability of one linear trend.

If height connections are not performed at least once a year, the method used for correcting height differences (see section 6.2.4) becomes important. In section 6.3.3, height connection scenarios *regular*, *irregular*, or *historical* will be applied. It is assumed that tide gauges follow secular movements and determined height differences are distributed over the elapsed period between the height connections. This implies that, apart from inconsistencies introduced by inaccuracies in the height connections, no additional errors are introduced into the time series.

In section 6.3.4 it is assumed that tide gauges follow secular movements, but height changes are corrected intermittently; applying height connection scenario: *historical*. The effects of an abrupt change in height for one tide gauge will be examined in section 6.3.5; using height connection scenario: *irregular*. As explained in section 6.2.4, both these methods will introduce additional errors into the time series.

6.3.1 Errorless height connection

As a reference for other sections, first results will be shown for “ideal” height connections, i.e., connection of tide gauges in height does not introduce inconsistencies in the sea-level height series relative to one another. As a result, simulated time series for the six tide gauges in the data set are exactly the same, except for possible differences in (short) periodic fluctuations. No additional measuring noise (of the tide gauge equipment) is added to the time series, since, this would yield the same effect as height connection noise introduced by annual connection of tide gauge heights, and this will be discussed in the next section.

In chapter 4, it has been shown that for a signal containing periodic fluctuations based on actual tide gauge data, of the order of 90 years of observations are required before estimates of the trend stabilise around its actual value. Since no additional information is introduced, result are exactly the same for a group of six tide gauges based on the same periodic pattern; see left-most graph in figure 6.7.

If the six time series contain different short periodic fluctuations, trend estimates stabilise around a slightly higher value. This is a side-effect of the method used (SSA) to create the time series containing only short periodic fluctuations; see chapter 4 for more details on this effect. Since short periodic fluctuations contain measuring errors as well, different time series contain different errors. These errors will be strongly reduced when combining the six data sets. However, the long periodic fluctuations are the same for all six time series. The long observation period required for trend estimates to stabilise is due to long periodic information in the data and not caused by (random) errors in the time series. Consequently, the curve of trend estimates does not change much (at least as a significant number of observations has been included).

If long periodic fluctuations are based on actual sea-level data for six tide gauges along the Dutch coast, the curve of estimated trend values changes significantly; see right-most graph of figure 6.7. But although the oscillations in slope values are highly reduced, a relatively large dip in trend (to approx. 1.3 mm/yr) is still found if around 90 years of observations have been included. This is not surprisingly. As shown in section 3.4, there is a large similarity between the time series obtained by tide gauges along the Dutch coast. As a result, by adding more of these time series to a data set, only (a small) part of the influence of the long periodic fluctuations will be reduced.

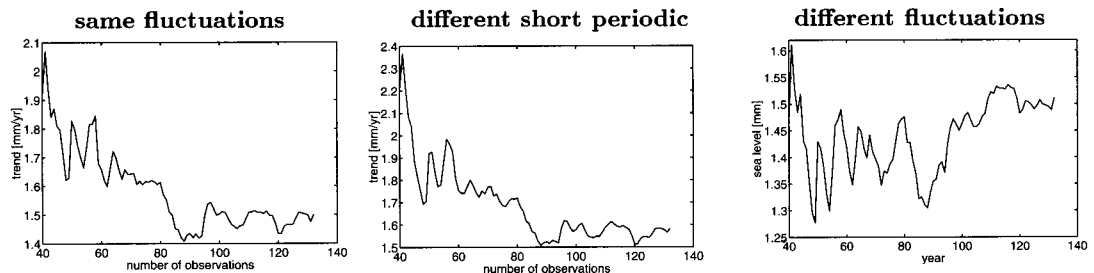


Fig. 6.7 Estimated trend versus the number of observations used; based on 6 time series (left-most estimate based on data for 1957-1996, right-most estimate on data from 1865 up to 1996). All series contain a trend of 1.5 mm/yr, with (possibly different) periodic fluctuations. Height connection: *no-error*.

As explained in section 3.4, the ratio between the first and second (and other) singular value, following from a singular value decomposition (SVD), can be used as a measure of similarity between the individual time series. A reconstruction based on only the first singular value will show the “common” pattern in the time series, while reconstructions based on higher singular values contain deviations from this common pattern.

As an example, figure 6.8 shows reconstructions based on the first three principal components for a group of tide gauges containing different short periodic fluctuations. The reconstruction based on the first singular value contains the majority of the signal. This reconstruction shows the common pattern, i.e., the trend, and periodic fluctuations that are (more or less) common. Reconstructions based on higher singular values show a “noise-like” behaviour; they represent the short periodic fluctuations that differ between the time series.

For a data set with both different long and short periodic fluctuations, reconstructions based on specific singular values are shown in figure 6.9. Analogous to figure 6.8, the reconstruction based on the

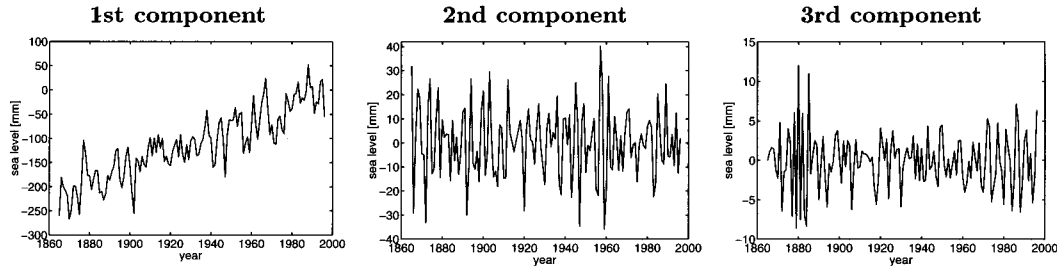


Fig. 6.8 Reconstructions (1st station) based on resp. 1th, 2nd and 3rd principal component. Height connection: *no-error*. Short periodic fluctuations based on different tide gauges.

first singular value not only shows the trend common to all time series, but also periodic fluctuations. From this it can be concluded that there is a significant similarity between the periodic patterns for the different time series. However, since the reconstructions based on higher singular values also contain a lot of information, there are major differences between the time series as well.

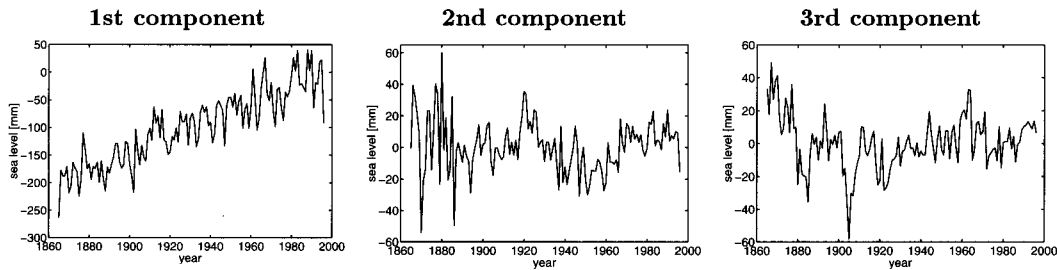


Fig. 6.9 Reconstructions (1st station) based on resp. 1th, 2nd and 3rd principal component. Height connection: *no-error*. Periodic fluctuations based on different tide gauges.

6.3.2 Annual connection of heights

For this section, data sets have been generated in which all time series are the same (with the possible exception of variations in periodic patterns), except for normally distributed random values added to the annual mean sea-level heights. This random noise can be viewed as height connection noise resulting from (at least) annual connection of tide gauge bench marks. As an alternative, this noise can also be interpreted as measuring noise introduced by the tide gauge equipment itself. For all six time series the same standard deviation will be used to represent the height connection noise.

Same absolute sea-level signal for all tide gauges

In section 6.3.1, it has been shown that for a group of 6 tide gauges, containing exactly the same periodic pattern, of the order of 90 years of observations are required before trend estimates stabilise around their actual value. If inconsistencies in height connections between tide gauges yield normally distributed noise that can be added to annual mean values, curves of trend estimates do not change very much.

Figure 6.10 shows estimated trends for time series containing the same periodic fluctuations and height errors represented by normally distributed random noise on annual mean values. This figure shows that for relatively large noise levels (standard deviations 5 or 10 cm), oscillations in estimated trend values increase if only up to 70 years of data is used. However, even for these large noise levels, comparison with figure 6.7 shows that this type of height connection noise no longer really hampers the estimation of trends, if estimates are based on at least 90 years of data.

Trend estimates as shown in figure 6.10 have been based on one particular realization of height connection noise. A different set of error values will lead to (slightly) different results. For 100 sets of simulated random noise values, estimated trend curves are shown in figure 6.11. Mean value and range of trend

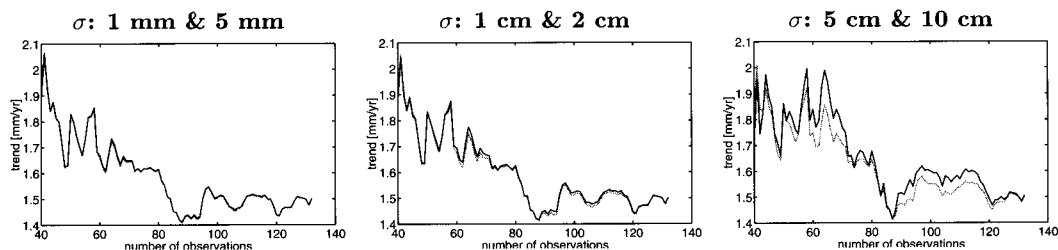


Fig. 6.10 Estimated trend versus the number of observations used (left-most estimate based on data for 1957-1996, right-most estimate on data from 1865 up to 1996). Height connection: *annual*; 6 noise levels. All time series contain the same periodic fluctuations.

estimates based on the complete data sets (i.e., 132 observations, from 1865 up to 1996) for these 100 realizations are given in table C.3 in appendix C.2.

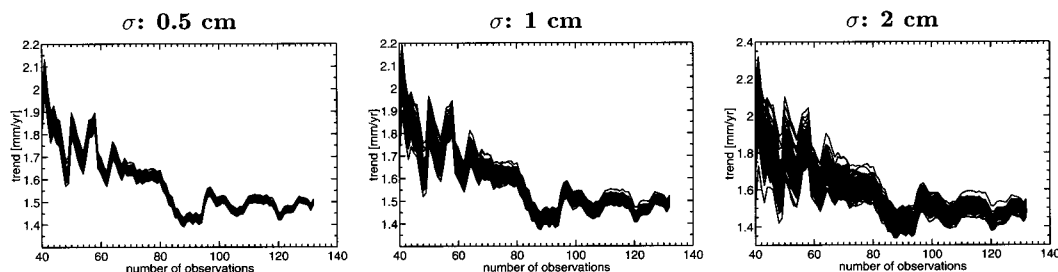


Fig. 6.11 Estimated trend versus number of observations used (left-most estimate based on data for 1957-1996, right-most estimate on data from 1865 up to 1996). Height connection: *annual*; 3 noise levels. For 100 realizations of connection noise. All time series contain the same periodic fluctuations.

From table C.3 it is clear that the mean value of trend estimates based on 132 years of data does not change if the amount of connection noise increases. However, as can be seen from both this table and figure 6.11, the spread in estimated trend values increases significantly with increasing height connection noise level. For a standard deviation of 5 mm, curves of estimated trends are similar for the different realizations of noise functions. Trend estimates based on a standard deviation of 2 cm show a larger variety. However, even for a noise level of 2 cm, trend estimates (based on at least 90 years of observations) are within 10% of the actual trend value (1.5 mm/yr) present in the data.

If the time series contain the same sea-level signal with normally distributed random noise added to the yearly values, the first singular value is still relatively large; at least for low noise levels. The higher the noise level, the smaller the ratio between first and second singular value; see table C.1 in appendix C.1. This is not surprisingly, since, with increasing noise level the similarity between the time series will reduce. Consequently, less signal will be common to all time series (represented by the 1st singular value), and more information will be transferred to the higher principal components.

As an example, in figure 6.12, reconstructed signals based on only the second singular value are shown for (one specific realization of) height connection noise with standard deviations of 0.1, 1, and 10 cm. For the low noise levels, the influence of the reconstructions based on the second singular value is rather small as compared to the signal represented by the first singular value. If the large noise level applies (σ 10 cm), the signal represented by the second principal component is significant.

Same long periodic fluctuations, different short periodic fluctuations

Figure 6.13 shows estimated trends for 100 realizations of height connection noise, based on standard deviations of 0.5, 1, or 2 cm. Mean value and range of the trend estimates (for data from 1865 up to 1996) based on these 100 realizations, are again given in table C.3 in appendix C.2.

Results as presented in table C.3, for data sets containing different high-frequency oscillations are similar to those based on the same periodic pattern. However, it can clearly be seen that although the

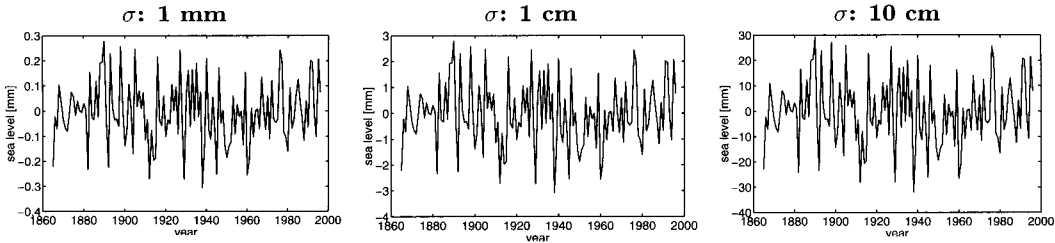


Fig. 6.12 Reconstructions (1st station) based on second principal component. Height connection: *annual*; noise level: 1 mm, 1 cm, or 10 cm. All time series contain the same periodic fluctuations.

spread in trend estimates is similar, values are systematically high. As indicated in the preceding (and in chapter 4), this is a side-effect of the method used (SSA) to generate the short periodic signals.

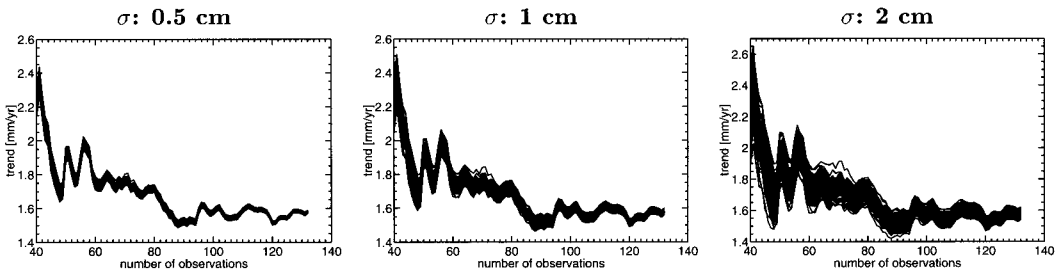


Fig. 6.13 Estimated trend versus number of observations used (left-most estimate based on data for 1957-1996, right-most estimate on data from 1865 up to 1996). Height connection: *annual*; 3 noise levels. For 100 realizations of connection noise. Time series contain different short periodic fluctuations.

Periodic fluctuations based on different sea-level height time series

Figure 6.14 shows that, again, the spread in estimated trend curves increases significantly with increasing height connection noise level. However, even for connection noise with a standard deviation of 2 cm, trend estimates (based on at least 90 years of data) are within 10% of the actual trend in the time series. Mean value and range of the trend estimates (for data from 1865 up to 1996) based on these 100 realizations of connection noise, are presented in table C.3 in appendix C.2. The results seem slightly better than those based on the data set containing the same periodic pattern.

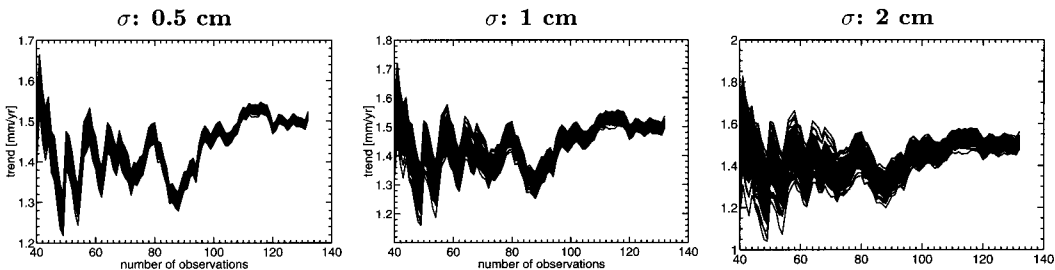


Fig. 6.14 Estimated trend versus number of observations used (left-most estimate based on data for 1957-1996, right-most estimate on data from 1865 up to 1996). Height connection: *annual*; 3 noise levels. For 100 realizations of connection noise. Time series contain different periodic fluctuations.

6.3.3 Height connections determined in specific measuring campaigns

In this section, a height connection scenario will be used in which tide gauges experience secular movements and have been connected to the local reference frame in specific measuring campaigns. To simulate

inconsistencies introduced by the height connections, one of the following three scenarios will be used: *regular*, *irregular*, or *historical*; see table 6.3 or section 6.2.3 for more details on these height connection scenarios. It is assumed that tide gauges follow secular movements and determined height differences are distributed over the elapsed time between the height connections.

For all tide gauges it is assumed that height connections have been performed at the same time with the same measurement precision. Errors introduced by inaccuracies in height connections are described by normally distributed random noise with a specific standard deviation.

Same absolute sea-level signal for all tide gauges

regular First, it is assumed that all height connection errors can be represented by normally distributed random values with a standard deviation of 1 cm. For height connections performed every 10, 20 or 30 years trend estimates are shown in figure 6.15, based on 100 different realizations of measuring noise.

Comparison of the graphs in figure 6.15 shows that increasing the elapsed time between height connections from 10 to 20 years leads to a somewhat larger spread between estimated trend values based on different realizations of height connection noise. A further increase in time span to height connections every 30 years hardly changes the estimated trends.

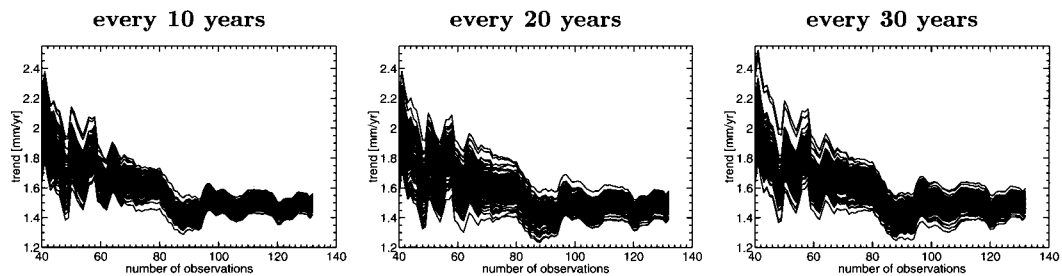


Fig. 6.15 Estimated trend versus number of observations used (left-most estimate based on data for 1957-1996, right-most estimate on data from 1865 up to 1996). Height connection: *regular*; $N = 10, 20, \text{ or } 30$; $\sigma = 1$ cm. For 100 realizations of connection noise. All time series contain the same periodic fluctuations.

If height connections can only be performed with a standard deviation of 2 cm, variations in estimated trends based on different realizations of height connection noise increase significantly; see figure 6.16. This effect is even more pronounced for the simulated data sets based on larger time spans between subsequent height connections. The larger the time span between the height connections, the larger the spread in estimated trend values based on different realizations of connection noise.

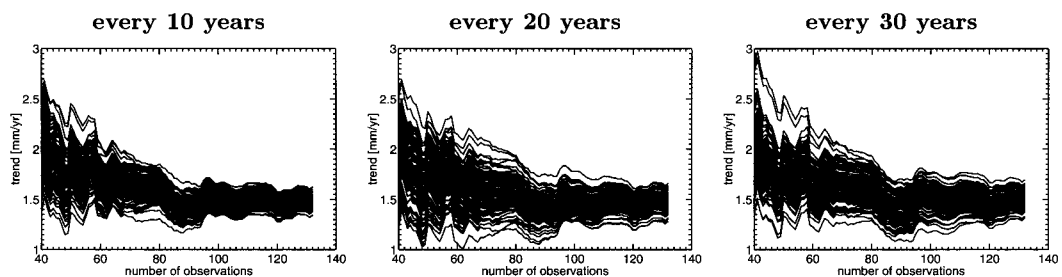


Fig. 6.16 Estimated trend versus number of observations used (left-most estimate based on data for 1957-1996, right-most estimate on data from 1865 up to 1996). Height connection: *regular*; $N = 10, 20, \text{ or } 30$; $\sigma = 2$ cm. For 100 realizations of connection noise. All time series contain the same periodic fluctuations.

Comparison of figures 6.15 and 6.16 shows that if height connections are performed every 10 years, increasing the noise level from 1 to 2 cm yields a larger spread in estimated trend values. However, if a large enough number of observations is included, trend values still stabilise more or less within 10 % of their actual value. This is confirmed by table C.4 in appendix C.2, which gives a range of trend estimates (based on 132 years of data) of 1.42 - 1.56 mm/yr for a noise level of 1 cm. If connection noise is based on a standard deviation of 2 cm, trend estimates range between 1.34 and 1.63 mm/yr.

With increasing period between subsequent connections, the difference that might occur between the actual slope value and the value around which trend estimates stabilise becomes larger. This implies that the risk increases of estimating trends that are systematically too high or low, if longer time spans occur between height connections.

As an example, for one specific realization of connection errors (σ 1 cm), figure 6.17 shows reconstructions based on specific singular values. Results for larger noise levels will not be shown since they are, except for the scale, almost equal to those based on a value of only 1 cm.

The reconstruction based on the first singular value contains the trend and periodic pattern. In reconstructions for higher principal components, errors introduced by height connections are visible. At least, these reconstructions reveal when inconsistencies between time series have been introduced. Consequently, this information could be used to reduce the influence of height connection errors; see chapter 3.

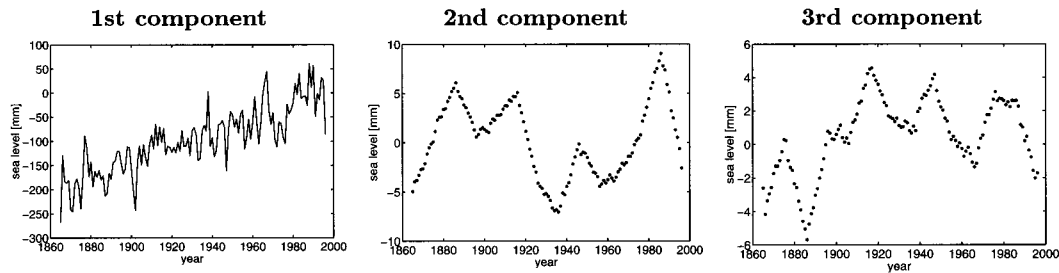


Fig. 6.17 Reconstructions (1st station) based on resp. 1th, 2nd, or 3rd principal component. Height connection: *regular*; $N = 10$, σ : 1 cm. All time series contain the same periodic fluctuations.

If the time span between height connections increases, the pattern in reconstructions based on specific singular values becomes less clear as compared to the results for height connection every 10 years. This is demonstrated by figure 6.18, showing reconstructions based on the first three singular values, for height connections every 30 years.

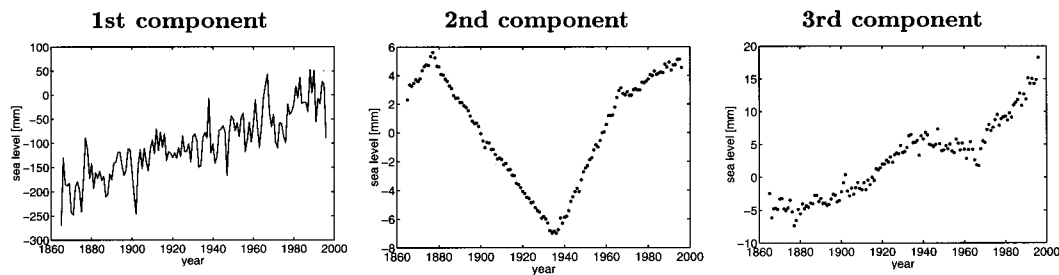


Fig. 6.18 Reconstructions (1st station) based on resp. 1th, 2nd, or 3rd principal component. Height connection: *regular*; $N = 30$, σ : 1 cm. All time series contain the same periodic fluctuations.

irregular Height connections are assumed in 1885, 1940, 1960, 1980, and 1996; yielding four height differences, see section 6.2.3 for more details. It is assumed that tide gauges follow secular movements and determined height differences are distributed over the elapsed period between the height connections. In figure 6.19, estimated trend curves are shown for three different levels of height connection noise. Trend estimates based on a standard deviation of 1 cm are similar to those based on more regular height connections; see figure 6.15. With increasing noise level, the spread in estimated trend values increases significantly. For example, for a noise level of 2 cm, the spread in estimated trend values based on *irregular* height connection is larger than for *regular* height connections every 30 years (see figure 6.16).

historical Instead of using the same precision for all height connections, for subsequent connections lower noise levels are assumed. One of the following sets of standard deviations will be used:

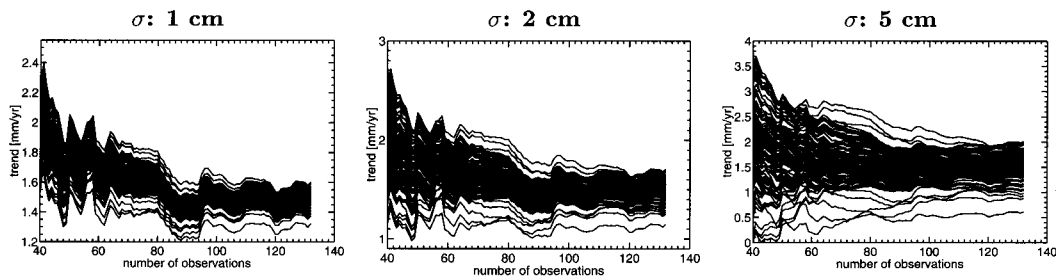


Fig. 6.19 Estimated trend versus number of observations used (left-most estimate based on data for 1957-1996, right-most estimate on data from 1865 up to 1996). Height connection: *irregular*; 3 noise levels. For 100 realizations of connection noise. All time series contain the same periodic fluctuations.

- *set 1* 1885: σ 3 cm, 1940: σ 2 cm, 1960: σ 2 cm, 1980: σ 1.5 cm, 1996: σ 1.5 cm. *Pessimistic*.
- *set 2* 1885: σ 2 cm, 1940: σ 1.5 cm, 1960: σ 1.5 cm, 1980: σ 1 cm, 1996: σ 1 cm.
- *set 3* 1885: σ 1.5 cm, 1940: σ 1 cm, 1960: σ 1 cm, 1980: σ 0.8 cm, 1996: σ 0.8 cm. *Optimistic*.

For these three sets of standard deviations, estimated trends are shown in figure 6.20. After about 80 or 90 years of observations have been included, trend estimates based on the most optimistic set of standard deviations stabilise well within 10% of their actual value. For the two higher noise levels, a somewhat larger amount of observations may be required before trend estimates stabilise. In addition, the higher the noise level, the larger the difference between the actual trend in the data and the value around which slope estimates stabilise.

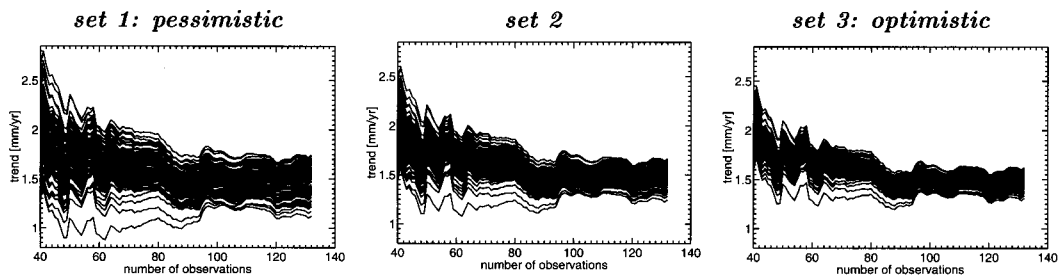


Fig. 6.20 Estimated trend versus number of observations used (left-most estimate based on data for 1957-1996, right-most estimate on data from 1865 up to 1996). Height connection: *historical*; 3 sets of noise levels. For 100 realizations of connection noise. All time series contain the same periodic fluctuations.

Same long periodic fluctuations, different short periodic fluctuations

In the preceding, it has been shown that only if height connections result in errors with a standard deviation of 1 cm, estimated trend values do not deviate much from their actual value (i.e., 1.5 mm/yr). For higher noise levels it was found that the larger the period between height connections, the more estimated trends could deviate from their actual value. The same situation holds for data sets containing different short periodic fluctuations. Plots of estimated trends will, therefore, not be shown.

For data sets with the same periodic pattern, height connection errors could be discerned from reconstructions based on specific singular values. Figure 6.21 shows an example of reconstructions using the first three singular values based on a data set containing different short periodic fluctuations. From these reconstructions, height connection errors are no longer visible.

In the reconstructions as given in figure 6.21, inconsistencies between time series due to height connection errors are completely overshadowed by differences in short periodic fluctuations. If less precise height measurements are assumed (σ 5 cm instead of 1 cm), the effect of height connection noise is more evident in the reconstructions based on specific singular values. From figure 6.22, the effect of corrections to sea-level heights as a result of fictitious height differences is again visible (to plot the data, dots have been used to enhance the effect of the connection errors).

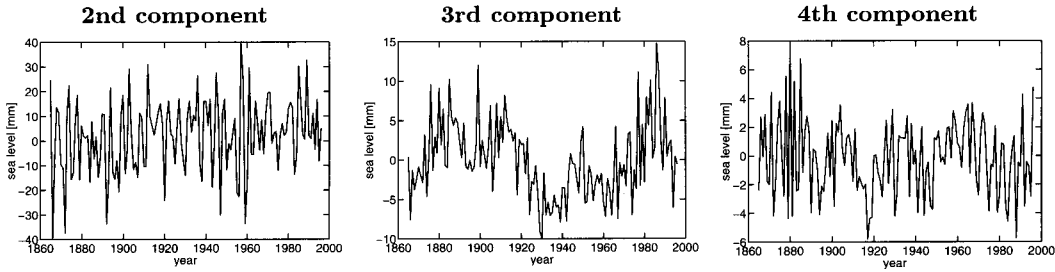


Fig. 6.21 Reconstructions (1st station) based on specific principal components. Height connection: *regular*; $N = 10$, $\sigma = 1$ cm. Time series contain different short periodic fluctuations.

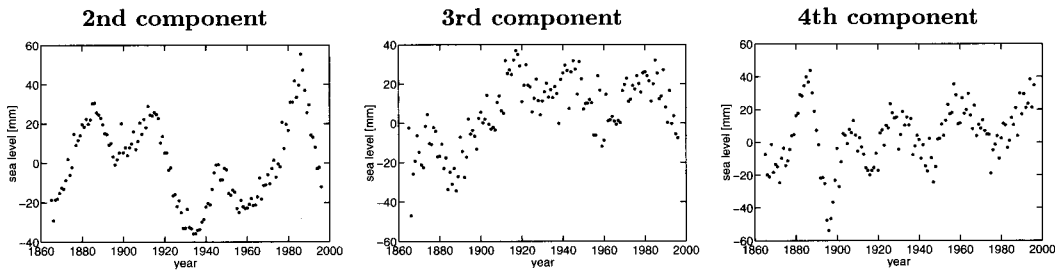


Fig. 6.22 Reconstructions (1st station) based on specific principal components. Height connection: *regular*; $N = 10$, $\sigma = 5$ cm. Time series contain different short periodic fluctuations.

Periodic fluctuations based on different sea-level height time series

In table C.4 in appendix C.2, mean values and ranges of trend estimates are given for data sets containing different periodic patterns. Comparison of these results with those corresponding to data sets with the same periodic fluctuations yields a large similarity, both for mean value and range. After a sufficient amount of observations have been included, plots of trend estimates are also similar to those in which the same periodic pattern is used. Therefore, as an example, trend estimates are only shown for height connections in 1885, 1940, 1960, 1980, and 1996; see figure 6.23.

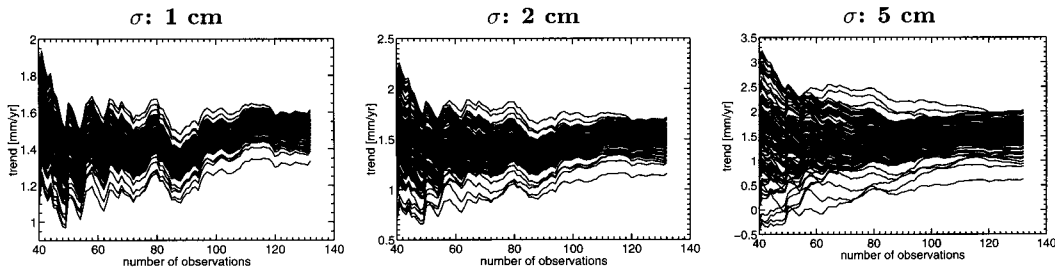


Fig. 6.23 Estimated trend versus number of observations used (left-most estimate based on data for 1957-1996, right-most estimate on data from 1865 up to 1996). Height connection: *irregular*; 3 noise levels. For 100 realizations of connection noise. Time series contain different periodic fluctuations.

As indicated in the preceding, the ratio between the first and second singular value resulting from SVD can be used as a measure of similarity between the time series. As can be seen from table C.2 in appendix C.1, for time series containing the same periodic pattern this ratio decreases rapidly with increasing noise level. If data sets contain different periodic fluctuations, this ratio is much smaller if no (or only small) height connection errors are made.

If relatively large height connection errors are present, similar values are derived for the ratio between first and second singular value, whether the same periodic pattern or different periodic information applies. This suggests that for small noise levels the effects of differences in periodic pattern prevail,

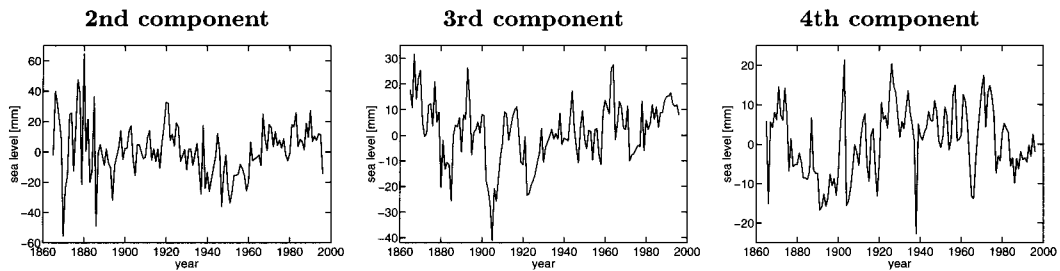


Fig. 6.24 Reconstructions (1st station) based on specific principal components. Height connection: *regular*; $N = 10$, σ : 1 cm. Time series contain different periodic fluctuations.

while for larger standard deviations height connection errors have a major influence. This is confirmed by figures 6.24 and 6.25, in which reconstructions are shown for singular values based on data sets with height connection precisions of resp. 1 and 5 cm. If a noise level of 1 cm applies, reconstructions are dominated by differences in periodic pattern. In reconstructions based on a precision of 5 cm, differences due to height connection errors are visible.

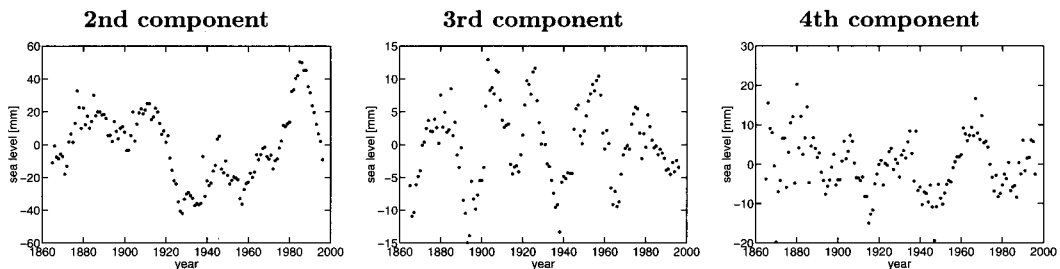


Fig. 6.25 Reconstructions (1st station) based on specific principal components. Height connection: *regular*; $N = 10$, σ : 5 cm. Time series contain different periodic fluctuations.

6.3.4 Intermittent correction of heights

In the preceding, it has been assumed that tide gauges follow secular movements and determined height differences are distributed over measurements obtained during the elapsed period between height connections. In this section, it will be shown how results are influenced if heights are corrected intermittently. As described in section 6.2.3, all six tide gauge are assumed to undergo secular movements, either with values relatively close to each other, or with larger differences between the stations. In addition, all results are based on height connection scenario: *historical*.

Same absolute sea-level signal for all tide gauges

Figure 6.26 shows estimated trends for the scenario in which secular movements of individual tide gauges are more or less similar in size. As compared to results in which height differences have been divided over past measurements (see figure 6.20) trend estimates show a somewhat larger range if more than around 60 years of observations have been included. This larger range in trend values can also be seen from comparing results in table C.4 with those presented in table C.5; both in appendix C.2.

Results in figure 6.26 have been based on data sets in which all six stations show similar secular height changes. If instead a wider range of velocity values applies (see table 6.2), results are derived as presented in figure 6.27. Comparison of these figures shows that larger differences in velocities hardly effect estimated trend curves. However, for the larger differences in velocities, more “extreme” examples of estimated trend curves seem to appear.

For one realization of connection noise, reconstructions based on specific singular values are shown in figure 6.28. Especially from the reconstruction based on the fourth singular value, the pattern of height

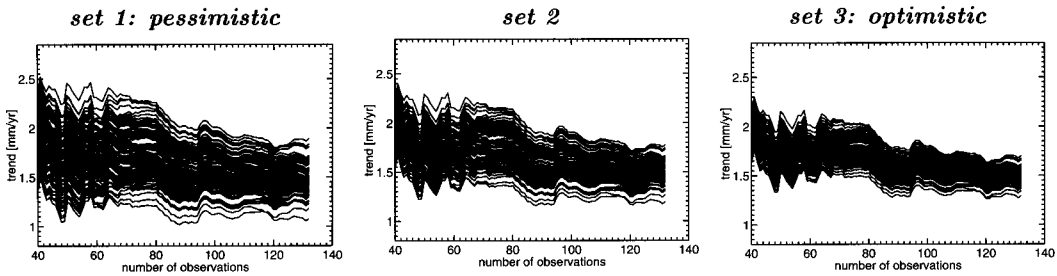


Fig. 6.26 Estimated trend versus number of observations used (left-most estimate based on data for 1957-1996, right-most estimate on data from 1865 up to 1996). Height connection: *historical*; 3 sets of noise levels. For 100 realizations of connection noise. Intermittent correction of heights. *Small* differences in velocities between tide gauges. All time series contain the same periodic fluctuations.

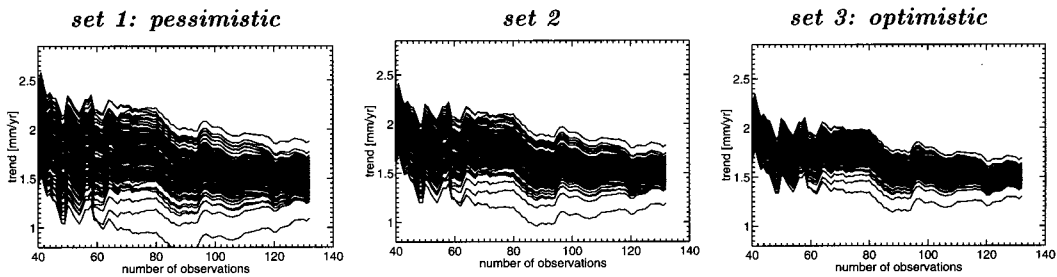


Fig. 6.27 Estimated trend versus number of observations used (left-most estimate based on data for 1957-1996, right-most estimate on data from 1865 up to 1996). Height connection: *historical*; 3 sets of noise levels. For 100 realizations of connection noise. Intermittent correction of heights. *Large* differences in velocities between tide gauges. All time series contain the same periodic fluctuations.

connections is clearly visible. Contrary to results shown in preceding sections, this connection pattern displays jumps, analogous to the pattern of simulated errors as shown in section 6.2.3 (figure 6.5).

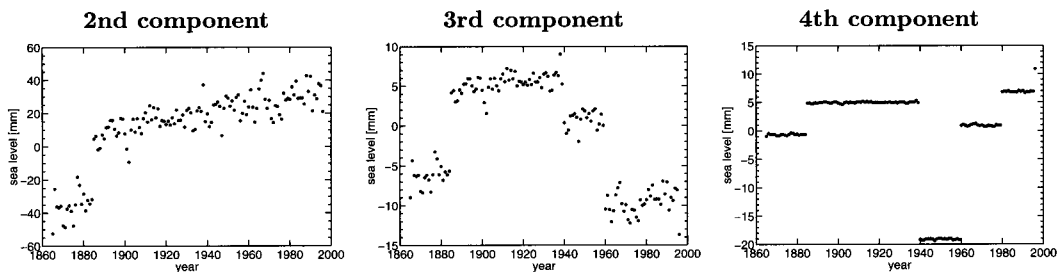


Fig. 6.28 Reconstructions (4th station) based on specific principal components. Height connection: *historical*; *pessimistic* noise levels. Intermittent correction of heights. *Small* differences in velocities between tide gauges. All time series contain the same periodic fluctuations.

Same long periodic fluctuations, different short periodic fluctuations

Results based on data sets in which different time series contain different short periodic fluctuations are both similar to those based on the same periodic pattern and to those shown in section 6.3.3 (data sets contain different short periodic fluctuations; height differences distributed over past measurements).

For data sets with the same periodic pattern, height connection noise was clearly visible from reconstructions based on specific singular values, especially from the 4th singular value. In section 6.3.3 it has been explained that in data sets with different (short) periodic fluctuations, connection noise is only visible if larger noise levels apply.

In figure 6.29, reconstructions from the fourth singular value are shown for data sets based on three different sets of connection noise. Fourth singular value is used, since, these reconstructions show (for these particular experiments) height connection errors the most clearly. Figure 6.29 demonstrates that only for larger values of connection noise, inconsistencies between time series due to the height connections are visible from the reconstructions. However, even for the *pessimistic* set of noise levels, the pattern of connection errors is not really clear.

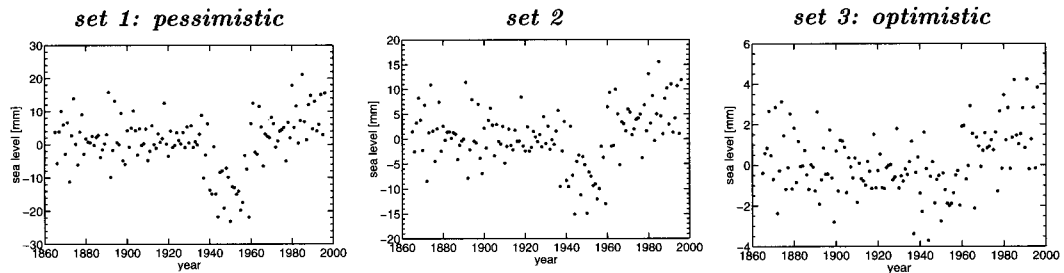


Fig. 6.29 Reconstructions (4th station) based on 4th principal component. Height connection: *historical*; 3 sets of noise levels. Intermittent correction of height. *Small* differences in velocities between tide gauges. Time series contain different short periodic fluctuations.

Periodic fluctuations based on different sea-level height time series

Mean value and range of trend estimates for 100 realizations of connection noise errors are presented in table C.5 in appendix C.2. This table shows that results for data sets in which time series contain different periodic fluctuations are almost equal to those in which all time series are based on the same periodic pattern. This is also clear from comparing trend estimates curves, as shown in figures 6.26 and 6.30; both using data sets in which the tide gauge experience similar vertical movements.

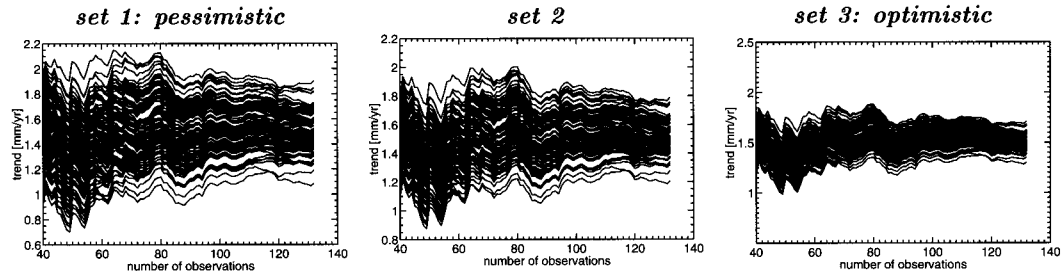


Fig. 6.30 Estimated trend versus number of observations used (left-most estimate based on data for 1957-1996, right-most estimate on data from 1865 up to 1996). Height connection: *historical*; 3 sets of noise levels. For 100 realizations of connection noise. Intermittent correction of heights. *Small* differences in velocities between tide gauges. Time series contain different periodic fluctuations.

Figures with reconstructions based on specific principal components are not shown. Even if time series are based on the *pessimistic* set of standard deviations, inconsistencies introduced by inaccuracies in height connections are no longer visible. This implies that (for these specific simulated time series), inconsistencies resulting from height connection errors are small as compared to variations in periodic fluctuations between the time series.

6.3.5 Abrupt changes in height

In this section, results will be shown for the scenario in which height differences are divided over past measurements, while in reality, one tide gauge has experienced an abrupt change in height. It is preferred to only show results for one specific realization of height connection noise. The reason behind this decision is that in plots with 100 realizations of noise the effects of an abrupt change are difficult to discern due

to the (wide) spread in trend curves. Still, in table C.6 in appendix C.2, mean value and range of trend estimates are given for 100 realizations of height connection errors.

All plots of estimated trends are based on height connections scenario: *irregular* with σ 1 cm. Results will only be shown for data sets in which all time series contain the same periodic pattern. The plots contain two different curves, a black curve representing results based on scenarios with different jumps, a grey curve (for reference) showing trend estimates for one specific realization of connection noise, without an additional jump.

Figure 6.31 shows estimated trends for data sets in which one time series experiences an abrupt vertical movement in 1890. This figure demonstrates that the larger the abrupt vertical movement of the tide gauge, the larger its effect on estimates of a common trend in the group of time series.

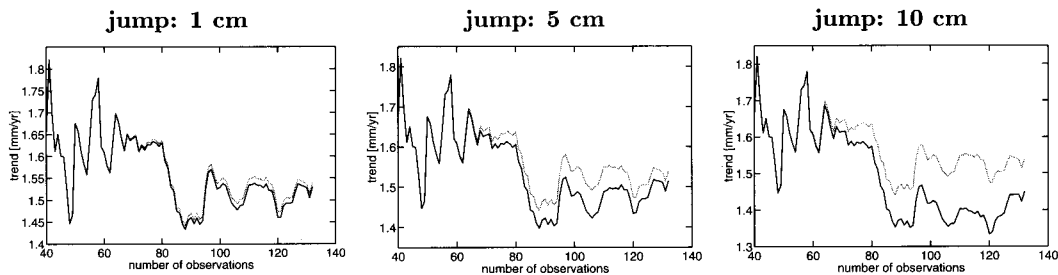


Fig. 6.31 Estimated trend versus number of observations used (left-most estimate based on data for 1957-1996, right-most estimate on data from 1865 up to 1996). Height connection: *irregular*; σ 1 cm. Height differences divided over past measurements. Abrupt change (1st time series) of 1, 5, or 10 cm in 1890.

In figure 6.6 (section 6.2.3), simulated errors resulting from an abrupt change in height have been presented. From these plots it could be discerned that an abrupt change in height occurring shortly after the last connection or shortly before the next height determination yields relatively large errors in the time series. On the other hand, if the jump occurs somewhere in between subsequent height connections, its influence is relatively small. This is confirmed by figure 6.32, in which the first tide gauge experiences an abrupt change in height somewhere in between the first (in 1885) and second (in 1940) height connection.

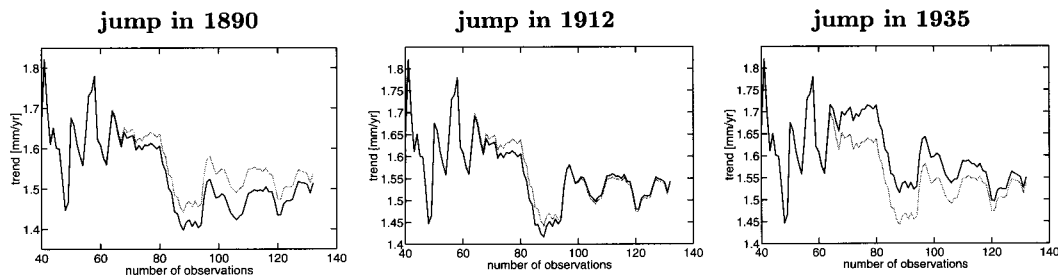


Fig. 6.32 Estimated trend versus number of observations used (left-most estimate based on data for 1957-1996, right-most estimate on data from 1865 up to 1996). Height connection: *irregular*; σ 1 cm. Height differences divided over past measurements. Abrupt change (1st time series) of 5 cm.

6.4 Transition to higher trend at the beginning of the time series

In chapter 4 it has been shown that a 0.8 mm/yr lower slope value at the beginning of the data set could not be discerned from individual time series containing periodic fluctuations based on actual sea-level height series. Smoothing of the time series did not yield a significant improvement. In this section it is investigated whether or not the detectability of a change in trend at the beginning of the sea-level height series improves, if more time series containing this pattern are available.

First, it is assumed that tide gauges are connected in height without introducing additional errors into the measurement series. Trend estimates for data sets containing the same periodic pattern, different short periodic fluctuations, or different short- and long periodic fluctuations, are shown in figure 6.33. For the data set in which all time series contain the same periodic pattern, results are equal to those presented in chapter 4.

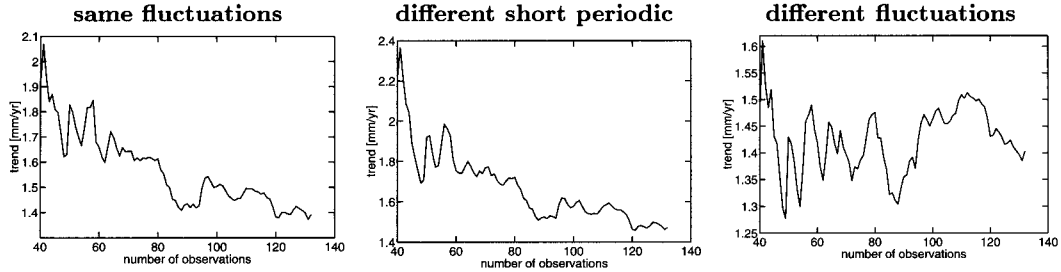


Fig. 6.33 Estimated trend versus number of observations used (left-most estimate based on data for 1957-1996, right-most estimate on data from 1865 up to 1996); 6 time series; (possibly different) periodic fluctuations. First, trend 0.7 mm/yr; in 1885 abrupt increases to 1.5 mm/yr. No errors introduced by height connection.

Comparison of trend curves as shown in figure 6.33 with those given in figure 6.7 (same trend throughout the time series, no additional height connection noise) clearly reveals the lower trend estimates after around 115 years of data have been included. However, based only on results as presented in figure 6.33, lowering of trend estimates due to the actual variation in sea-level increase cannot be discerned from other fluctuations in slope estimates resulting from long periodic information in the data.

Although fluctuations in trend estimates are largely reduced if different time series contain different (long) periodic patterns, the change in trend at the beginning of the time series is still of the same order of magnitude as oscillations in trend estimates. Consequently, adding more time series to the data set does not, significantly, improve the detectability of a change in trend in the beginning of the sea-level height series. Therefore, results based on different height connection scenarios will not be presented.

6.5 Transition to higher trend at the end of the time series

In chapter 4 it has been shown that a small increase in trend value (from 1.5 to 1.8 mm/yr) is difficult to discern from plots of estimated trend values, even if observations up to the year 2100 are used. If sea-level rise acceleration is more severe (e.g., trend increases to 4.5 mm/yr), this change in trend becomes visible if of the order of 30 to 40 years of observations are obtained.

past height connections (up to 1996)		“future” height connections	
scenario	remarks	scenario	remarks
<i>no-error</i>		<i>no-error</i>	
<i>annual</i>	$\sigma : 5 \text{ mm}, \sigma : 1 \text{ cm}, \sigma : 2 \text{ cm}$	<i>annual</i>	$\sigma : 5 \text{ mm}, \sigma : 1 \text{ cm}, \sigma : 2 \text{ cm}$
<i>historical</i>	st. dev. from <i>set 1</i> , <i>set 2</i> , or <i>set 3</i>	<i>annual</i>	$\sigma : 5 \text{ mm}, \sigma : 1 \text{ cm}, \sigma : 2 \text{ cm}$
<i>historical</i>	st. dev. from <i>set 1</i> , <i>set 2</i> , or <i>set 3</i>	<i>regular</i>	$\bar{N} = 5 \text{ or } N = 10 \text{ years}$ $\sigma : 5 \text{ mm}, \sigma : 1 \text{ cm}, \sigma : 2 \text{ cm}$

Table 6.4 Height connection scenarios used to examine the detectability of a change in trend at the end of the time series.

In the following sections, it will be examined how the detectability of a change in trend at the end of the time series is influenced by inconsistencies between the time series introduced by height connection errors. Table 6.4 gives an overview of the height connection scenarios that will be applied. Often, for the complete simulated time series with data up to the year 2100, two separate height connection scenarios will be used. The first scenario applies to data obtained in the past, i.e., height connections performed up to 1996. The second scenario applies to “future” height connections. It is assumed that tide gauges follow secular movements and determined height differences are distributed over the elapsed period between the height connections. Results will be shown for data sets in which the six time series either contain the

same periodic fluctuations, or data sets in which all time series are based on different (long and short) periodic fluctuations.

6.5.1 No inaccuracies in heights between tide gauges

For reference, in this section, estimates of a common trend will be shown for a group of six tide gauges. It is assumed that (past and future) height connections between tide gauges do not introduce additional errors into sea-level height series.

Same absolute sea-level signal for all tide gauges

Figure 6.34 shows estimates for a common trend, based on a group of time series in which sea-level rise increases to resp. 1.8, 4.5, or 7.8 mm/yr. Trends are plotted versus the year up to which observations have been included in the estimation. Results are equal to those presented in chapter 4.

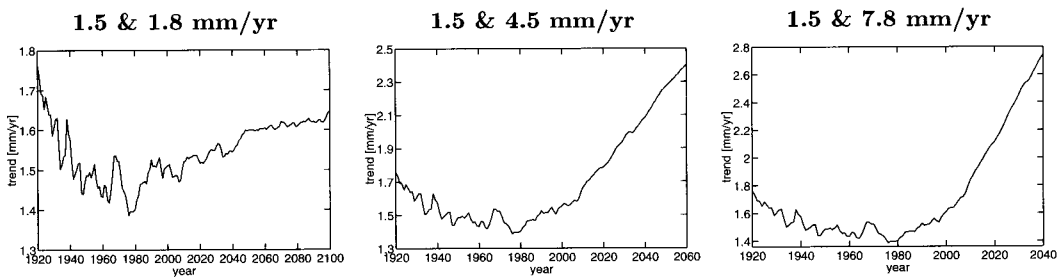


Fig. 6.34 Estimated trend versus the date up to which observations have been used. Past and future height connection: *no-error*. First, trend of 1.5 mm/yr; in 1991 abrupt change to 1.8, 4.5, or 7.8 mm/yr. All time series contain the same periodic fluctuations.

Periodic fluctuations based on different sea-level height time series

If the frequency content of the periodic pattern for the six time series would be completely different, combining the six time series would result in a major reduction of the influence of the periodic fluctuations. However, as already indicated in section 6.3.1, there is significant correlation between the frequency contents of data sets for the six tide gauges on which the simulated time series used in this chapter have been based. Consequently, combining the six time series will only reduce part of the influence of the long periodic fluctuations on the trend estimates.

This is confirmed by figure 6.35. Compared to figure 6.34, trend estimates show somewhat less variations if data up to around 1980 is used. As a result, the effect of sea-level rise acceleration is somewhat clearer, even for a small increase in slope value to only 1.8 mm/yr.

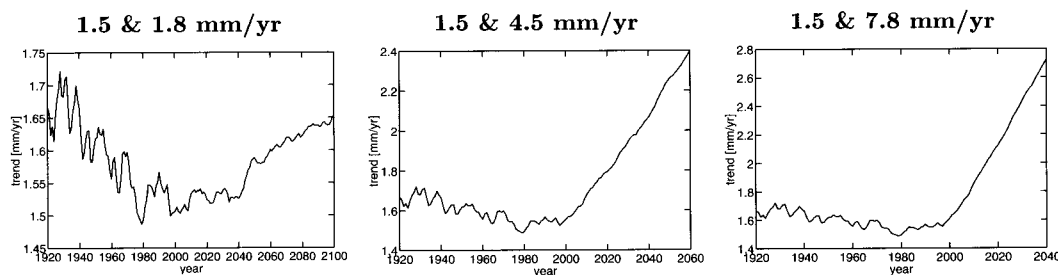


Fig. 6.35 Estimated trend versus the date up to which observations have been used. Past and future height connection: *no-error*. First, trend of 1.5 mm/yr; in 1991 abrupt change to 1.8, 4.5, or 7.8 mm/yr. Time series contain different periodic fluctuations.

6.5.2 Annual connection of all heights

As reference for the two following sections, it will be assumed that inconsistencies introduced by height connections can be represented, for the complete time span (from 1865 up to 2100), by normally distributed random errors on annual mean values. Same standard deviations are used throughout the time series and for all six tide gauges.

Same absolute sea-level signal for all tide gauges

As an example, figure 6.36 shows estimated trends for data sets in which sea-level increase accelerates to 1.8 mm/yr. For the two smallest standard deviations, spread in trend estimates is rather small. Only if a precision of 2 cm applies, trend estimates show some more variation. However, as can be seen from table C.8 in appendix C.2, if observations up to the year 2050 (or 2100) are used, the range in trend values does not increase much with decreasing precision of height connections. Even for a standard deviation of 5 cm, trend estimates for the year 2050 range only between 1.51 and 1.66 mm/yr.

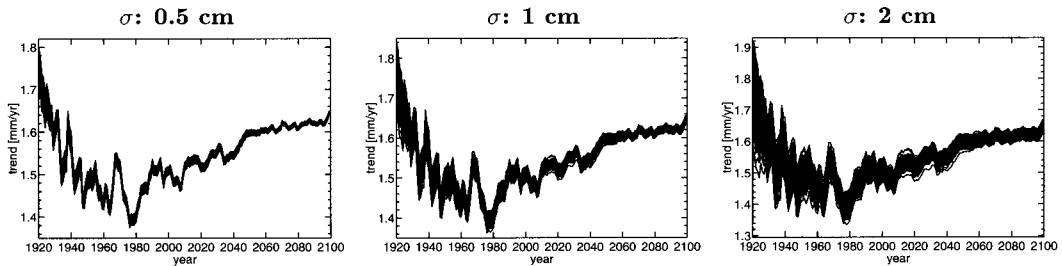


Fig. 6.36 Estimated trend versus the date up to which observations have been used. Past and future height connection: *annual*; 3 noise levels. For 100 realizations of measuring noise. First, trend of 1.5 mm/yr; in 1991 abrupt change to 1.8 mm/yr. All time series contain the same periodic fluctuations.

Periodic fluctuations based on different sea-level height time series

Analogous to the data set without height connection noise, visibility of sea-level increase to 1.8 mm/yr improves a little as compared to the data sets based on the same periodic fluctuations; see figure 6.36. Even for height connection errors with a standard deviation of 2 cm, trend curves seem to stabilise followed by a slow increase in slope values.

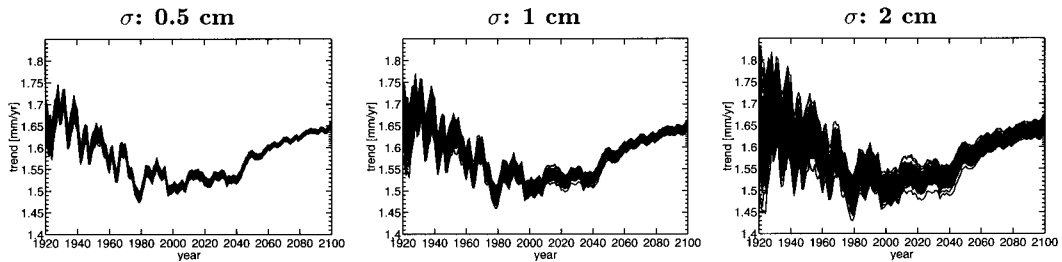


Fig. 6.37 Estimated trend versus the date up to which observations have been used. Past and future height connection: *annual*; 3 noise levels. For 100 realizations of measuring noise. First, trend of 1.5 mm/yr; in 1991 abrupt change to 1.8 mm/yr. Time series contain different periodic fluctuations.

6.5.3 Permanent monitoring of future height changes

For data up to 1996, height connections are assumed that, more or less, correspond to the history of Dutch first order levellings; i.e., height connection scenario: *historical*. It is assumed that tide gauges follow secular movements and determined height differences are distributed over the elapsed period between the height connections. Connection errors are represented by normally distributed random noise with one of the following sets of standard deviations:

- *set 1* 1885: σ 3 cm, 1940: σ 2 cm, 1960: σ 2 cm, 1980: σ 1.5 cm, 1996: σ 1.5 cm. *Pessimistic*.
- *set 2* 1885: σ 2 cm, 1940: σ 1.5 cm, 1960: σ 1.5 cm, 1980: σ 1 cm, 1996: σ 1 cm.
- *set 3* 1885: σ 1.5 cm, 1940: σ 1 cm, 1960: σ 1 cm, 1980: σ 0.8 cm, 1996: σ 0.8 cm. *Optimistic*.

From 1996 on, permanent monitoring of height changes applies, or height measurements are performed on (at least) a yearly basis. Consequently, future height connections (after 1996) introduce errors that can be described by normally distributed random values added to annual mean sea-level heights.

A small increase in trend value (from 1.5 to 1.8 mm/yr) is already difficult to detect in time series containing no additional height connection errors. Therefore, results presented in this section are based on data sets with a sea-level rise acceleration to 4.5 mm/yr.

Same absolute sea-level signal for all tide gauges

First, the *pessimistic* set of precisions will be assumed for height connections performed in the past. Figure 6.38 shows estimated trends versus the year up to which observations are assumed available. For future height connections, three different noise levels are used.

As can be seen from figure 6.38 (and table C.10), curves of estimated trends are not (significantly) influenced by the precision of height connections after 1996. Due to the low precision and long time spans between height connections in the past, whether future connections have a standard deviation of 5 mm or 2 cm, does not change the results.

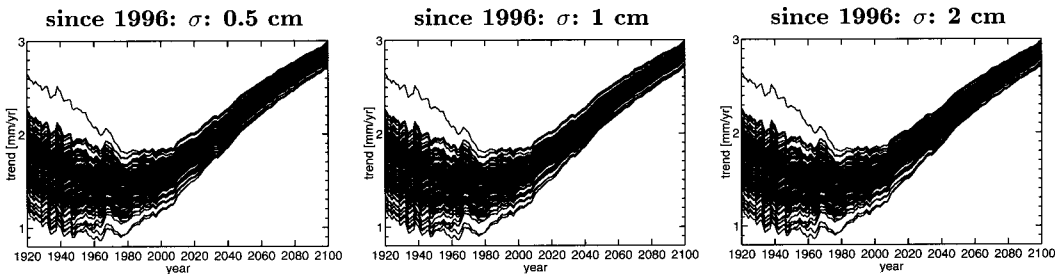


Fig. 6.38 Estimated trend versus date up to which observations have been used. Past height connection: *historical*, *pessimistic* noise level. Future height connection: *annual*; 3 noise levels. First, trend of 1.5 mm/yr; in 1991 abrupt change to 4.5 mm/yr. All time series contain the same periodic fluctuations.

From estimated trends as shown in figure 6.38, it is clear that sea-level rise is increasing. However, a rather long range of future measurements might be required before this sea-level rise acceleration becomes clearly visible. In addition, it is difficult to estimate the onset time of the acceleration.

Sea-level rise acceleration is difficult to discern from the plots of estimated trend values due to the relatively low precision of height connections in the past. This is confirmed by figure 6.39, in which all estimated trends have been based on future height connections with a noise level of 5 mm, while for past connections different sets of standard deviations have been used.

Comparison of the results in figure 6.39, clearly shows that the spread in estimated trend values significantly decreases if better precisions are assumed for past height connections. From plots of estimated trends based on the *optimistic* set of standard deviations, sea-level rise acceleration is already clearly visible after only a limited amount of future observations has been included.

As a final example, different noise levels are assumed for future height monitoring, while for past height connections the *optimistic* set of standard deviations is used. Estimated trends versus the year up to which observations are assumed available are shown in figure 6.40. The three plots, based on different future noise levels are (more or less) identical. Consequently, if measurements obtained in the past have to be included, changing the precision of future height measurements hardly has any effect.

Why historical height connections have a much larger influence can be explained as follows. A (very) long time span is assumed between some height connections performed in the past. As a result, errors in these connections yield inconsistencies in the time series that are systematic over large parts of the data set. Errors in future height connections are assumed random on a yearly basis. Therefore, even for

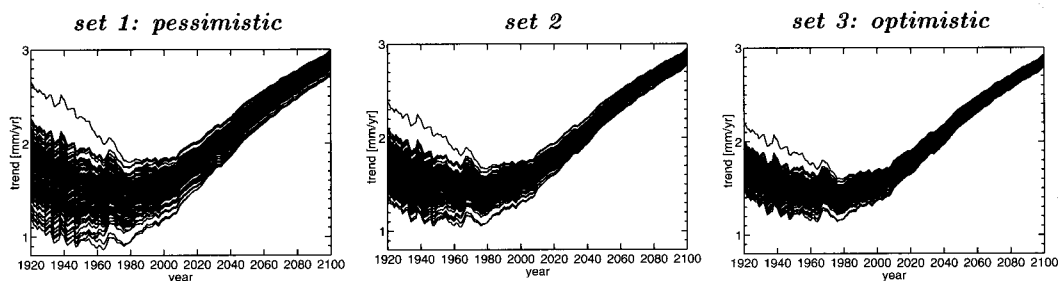


Fig. 6.39 Estimated trend versus date up to which observations have been used. Past height connection: *historical*, 3 sets of noise levels. Future height connection: *annual*; σ : 5 mm. First, trend of 1.5 mm/yr; in 1991 abrupt change to 4.5 mm/yr. All time series contain the same periodic fluctuations.

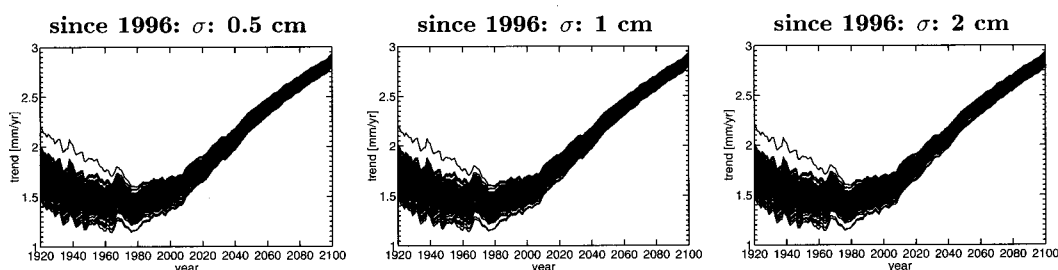


Fig. 6.40 Estimated trend versus date up to which observations have been used. Past height connection: *historical*, *optimistic* noise level. Future height connection: *annual*; 3 noise levels. First, trend of 1.5 mm/yr; in 1991 abrupt change to 4.5 mm/yr. All time series contain the same periodic fluctuations.

relatively large standard deviations, their influence will be diminished if a sufficiently large number of years has been included.

In preceding sections, it has been shown that inconsistencies between time series due to height connection errors could sometimes be discerned from reconstructions based on singular values. From figure 6.41, the different frequencies of height connections before and after 1996 can clearly be seen. The pattern introduced by inconsistencies between the time series due to the four height differences determined up to 1996 are clearly visible. After 1996, reconstructions show a noise-like behaviour, corresponding to the random differences in annual mean values between the time series.

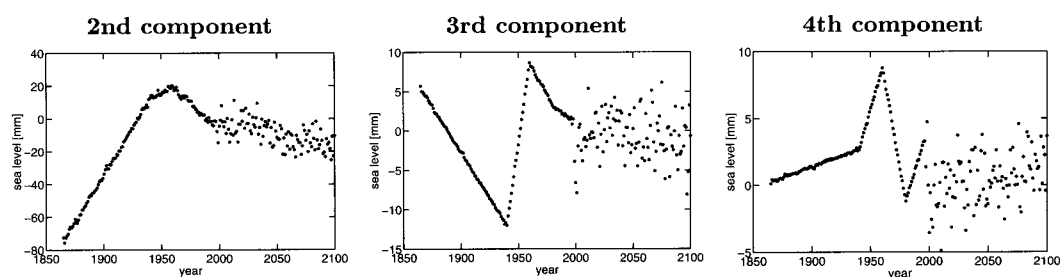


Fig. 6.41 Reconstructions (3rd station) based on specific principal components. Past height connection: *historical*, *pessimistic* noise level. Future height connection: *annual*; σ : 1 cm. All time series contain the same periodic fluctuations.

Periodic fluctuations based on different sea-level height time series

Trend estimates hardly change if time series contain different periodic fluctuations instead of the same periodic pattern. This is confirmed by the ranges of trend estimates as given in table C.10. Therefore, results for time series containing different periodic fluctuations will not be shown.

6.5.4 Future height connections once every 5 or 10 years

In the preceding section it has been shown that due to the long time interval between past height connections, precision of future height connections (on an annual basis) hardly influences the results. In this section, the effect of enlarging the period between future height connections will be examined.

For data up to 1996, same history of height connections is assumed as in the preceding section. Instead of yearly connections, after 1996 heights of tide gauge bench marks are determined every 5 or 10 years in specific measuring campaigns. Errors introduced by these connections are described by normally distributed random values using the same standard deviation for all stations.

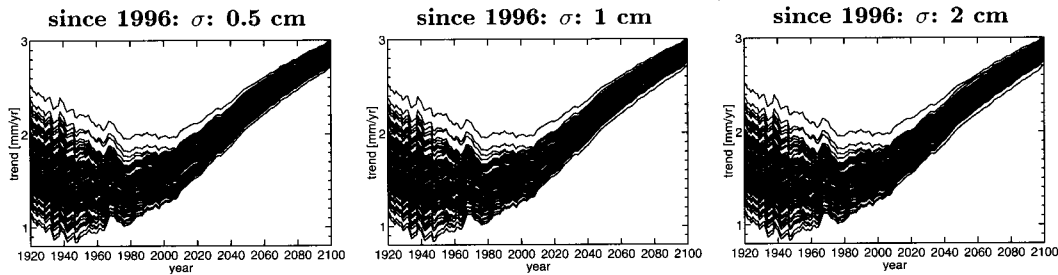


Fig. 6.42 Estimated trend versus date up to which observations have been used. Past height connection: *historical, pessimistic* noise level. Future height connection: *regular*; $N = 5$ years; 3 noise levels. First, trend of 1.5 mm/yr; in 1991 abrupt change to 4.5 mm/yr. All time series contain the same periodic fluctuations.

Figure 6.42 shows estimated trends, based on the *pessimistic* set of standard deviations for past height connections. Future connections are assumed every five years using three different noise levels. Comparison with results as presented in figure 6.38, shows that trend estimates are hardly influenced if height connections are performed every five years instead of at least once a year.

Analogous to results based on permanent monitoring of tide gauge bench marks, a large amount of observations might be required before sea-level rise acceleration can be discerned from trend estimates as given in figure 6.42. This is, again, due to the (assumed) low quality of historic height connections. If the *optimistic* set of standard deviations is used for height connections performed in the past, trend estimates are derived as shown in figure 6.43. From these graphs, the acceleration in sea-level rise is clearly visible after only a limited number of data has become available.

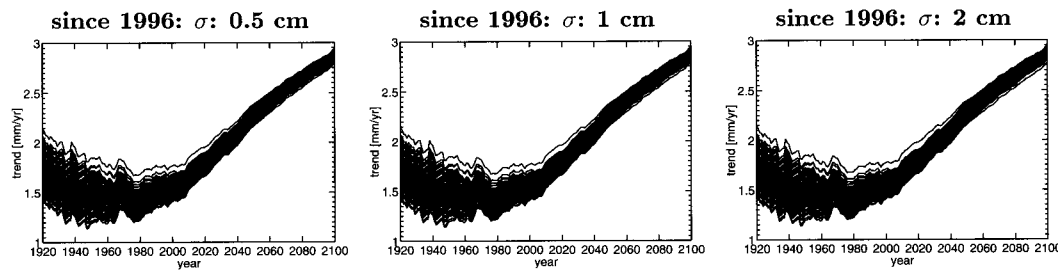


Fig. 6.43 Estimated trend versus date up to which observations have been used. Past height connection: *historical, optimistic* noise level. Future height connection: *regular*; $N = 5$ years; 3 noise levels. First, trend of 1.5 mm/yr; in 1991 abrupt change to 4.5 mm/yr. All time series contain the same periodic fluctuations.

Next, it is tried whether or not enlarging the period between future height connections from 5 to 10 years, will effect estimated trend values. Figures 6.44 and 6.45 show estimated trends based on resp. the *pessimistic* and *optimistic* set of standard deviations for historic height connections. Results as shown in these figures show a large similarity with results based on connections every 5 years (figures 6.42 and 6.43) and permanent monitoring of heights (figures 6.38 and 6.40). This is confirmed by ranges of trend estimates as given in tables C.10, C.11 and C.12, all in appendix C.2.

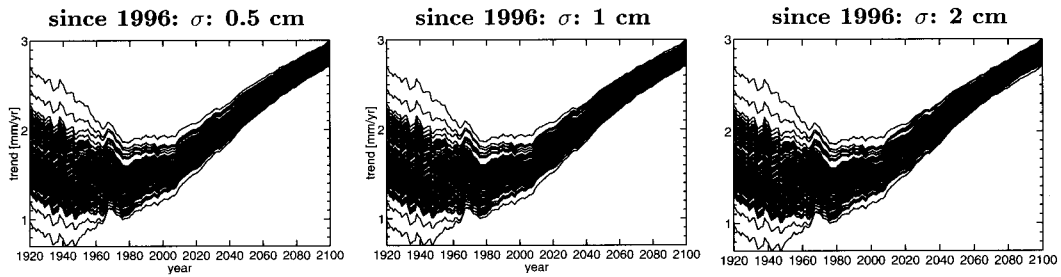


Fig. 6.44 Estimated trend versus date up to which observations have been used. Past height connection: *historical, pessimistic* noise level. Future height connection: *regular*; $N = 10$ years; 3 noise levels. First, trend of 1.5 mm/yr; in 1991 abrupt change to 4.5 mm/yr. All time series contain the same periodic fluctuations.

Estimated trends presented in this section show a large similarity with results based on permanent (future) monitoring of tide gauge bench marks. From these figures it is clear that spread in estimated trend values is only reduced if a better quality applies to past height connections. Increasing the noise level of future height connections (up to a maximum of 2 cm) or enlarging the period between measurements (up to 10 years) does not influence the results.

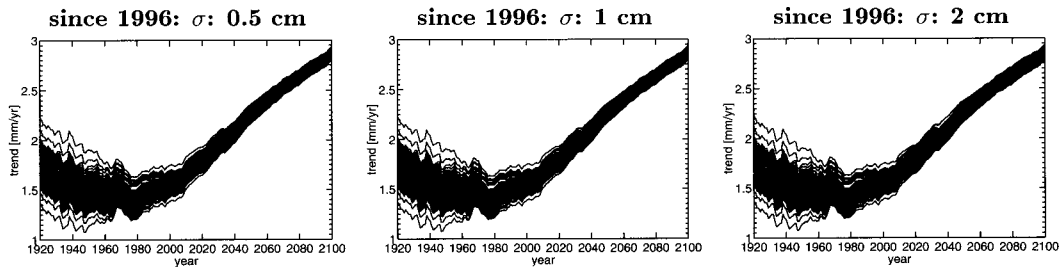


Fig. 6.45 Estimated trend versus date up to which observations have been used. Past height connection: *historical, optimistic* noise level. Future height connection: *regular*; $N = 10$ years; 3 noise levels. First, trend of 1.5 mm/yr; in 1991 abrupt change to 4.5 mm/yr. All time series contain the same periodic fluctuations.

Estimates based on data sets containing different periodic information are almost identical to those using time series with the same periodic pattern. Therefore, no results will be shown for data sets in which periodic fluctuations have been based on actual sea-level data for different tide gauges.

6.5.5 Conclusions and recommendations

Based on results with simulated data sets as presented in preceding sections, following conclusions and recommendations can be made.

Concerning the number of time series By adding more time series to a data set, effect of random errors (e.g., measuring errors) is reduced. However, the large amount of observations required for trend estimates to stabilise around their actual values is due to long periodic fluctuations in the time series and is not a result of measuring errors. Therefore,

- Adding more time series with the same long periodic fluctuations does not improve the detectability of a common sea-level variation pattern in the time series. If time series contain periodic information based on data collected by different tide gauges along the Dutch coast, having more time series gives a slight improvement.
- The above conclusion does not imply that one time series is enough to determine the sea-level variation curve in a specific region. If only one time series is used, erroneous information (both errors in sea-level measurements and distortion of the regional pattern by local circumstances) in this data set directly affect the estimated pattern.

- In addition, based on only one time series, it cannot be ascertained that a common curve suffices to describe sea-level variation in a specific region. Inspection of various sea-level height time series is required in order to establish that they follow a common curve.

Concerning height connections performed in the past How much variation is present between trend estimates based on different realizations of height connection noise depends both on the quality of the height measurements and the time span between the subsequent height connections. Based on different scenarios of possible height connections, the following conclusions can be made:

- A deterioration of the precision of the height measurements from 1 to 2 cm, leads to a significant increase in spread between trend estimates based on different realizations of connection noise.
- For higher noise levels, it is more pronounced that the larger the time span between subsequent connections, the larger the variation that can be present in trend estimates.
- However, even if height connections can be performed with a very good accuracy, long periods between height connections are not advisable. In order to correct for determined height differences, a model concerning the height changes (e.g., secular movements) has to be assumed. If this model is not correct, e.g., because one tide gauge has experienced an abrupt change in height, the longer the period between subsequent connections, the larger the error that can be introduced.

Concerning future height connections In order to predict future sea-level rise and detect accelerations in sea-level variation historical data has to be used as well. Consequently, detectability of greenhouse-gas induced sea-level rise is not only influenced by precision of future measurements, but largely determined by accuracy of measurements obtained in the past.

- If long periods have elapsed between subsequent historic height connections, increasing the standard deviation of future height connections from 2 cm to 5 mm, hardly influences the measuring time required to detect an acceleration in sea-level rise.
- In addition, permanent monitoring of tide gauge heights does not yield significantly better results as compared to height connections determined every 5 or 10 years in specific measuring campaigns.
- The above conclusion only applies if tide gauge bench marks experience secular movements. Permanent monitoring (or at least yearly measurements) of tide gauge heights minimises the influence of more abrupt movements of tide gauges.

Recapitulating it can be said that having more time series containing the same sea-level variations and short intervals between height connections will hardly improve the detectability of this variation pattern. However, more time series and a high frequency of height connections are required to improve the reliability of detected patterns.

Regional height datum connection

7.1 Introduction

In preceding chapters, it has been explained that tide gauges measure sea-level variations relative to a local tide gauge bench mark. In order to determine a (reliable) common sea-level variation pattern for a group of tide gauges, inconsistencies should be removed from the individual time series. Inconsistencies between the time series introduced by vertical movements of the tide gauge bench marks can be removed by connecting the tide gauges in height.

For historical tide gauge data, often no direct height measurements between the tide gauges are available. Usually, tide gauges have been connected to a local height reference system by means of spirit levelling. Consequently, orthometric heights (or normal heights, etc.; see chapter 5) and variations in these heights are, in principle, available for the various tide gauges. As a result, for a group of tide gauges, a common sea-level variation pattern, relative to the local height reference system, can be determined.

In theory, the reference surface should equal the geoid, but in practice some kind of approximation of the geoid has been introduced. Often, a reference surface for local orthometric height measurements is defined by averaging sea-level observations at one or more fundamental tide gauges, thereby creating a local vertical datum. Due to various processes, e.g., wind forcing, variations in salinity, etc., mean sea level is not an equipotential surface. Therefore, different vertical datums refer to different equipotential surfaces. As a result, off-sets exist between the different height datum zones. In addition, fundamental stations in the various datum zones, from which the local height systems originate, might experience vertical movements, e.g., as a result of post-glacial rebound.

In chapter 6, a common sea-level variation curve has been determined for a group of tide gauges along the Dutch coast. Of interest were sea-level variations relative to the Dutch height system (NAP). Therefore, height variations of the NAP system itself, have not been considered.

In chapter 8, patterns in sea-level variations will be examined for a group of tide gauges situated in the North Sea area. In this area, tide gauge heights have been determined relative to different vertical datums. Vertical movements of the fundamental stations in the different datum zones will have introduced inconsistencies between time series corresponding to tide gauges situated in different height datum zones. In order to remove these inconsistencies, the different vertical datums should be connected in height.

In this chapter, an indirect method for connecting vertical datums will be discussed, and the quality that might be expected from the datum connection will be investigated. The technique used in this chapter is based on the method of Rummel and Teunissen (1988), and can be explained with the following example.

Figure 7.1 shows two vertical datums (equipotential surface *A* and equipotential surface *B*) defined by a reference station, fundamental station *A* and fundamental station *B*, in the two datum zones. To determine the difference in height between the two equipotential surfaces, orthometric heights of both reference stations are needed. As can be seen from figure 7.1, the orthometric height of the fundamental station above the geoid can be derived if in the datum zone at least one station is available for which the geometric height above the selected reference surface is measured, the orthometric height relative to the fundamental station is determined based on e.g., levelling, and the corresponding geoid height is estimated through solving a geodetic boundary value problem.

In this example, the difference in orthometric height between the fundamental stations in the datum zones have been used to connect the two datums. Since orthometric heights are subject to assumptions concerning topography and crust density, in the following the potential difference (or to be more precise, dynamic heights) between the equipotential surfaces will be used for connecting vertical datums.

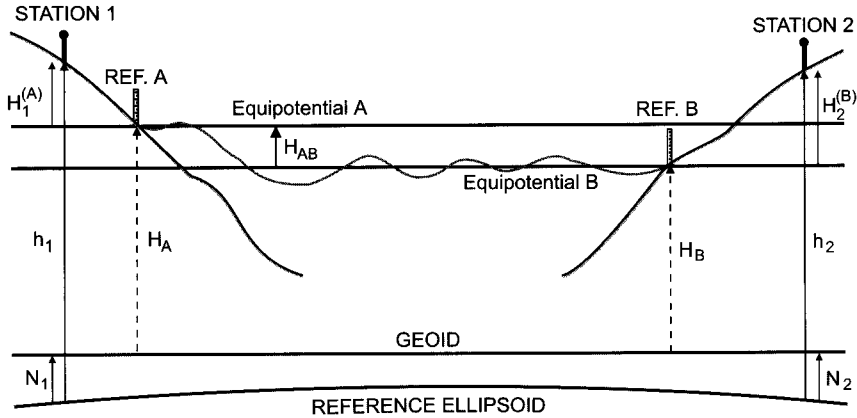


Fig. 7.1 Vertical datums A and B are connected by potential difference $C_{AB} = H_{AB} \cdot \gamma$, which can be determined from a combination of geometric, orthometric, and geoid heights.

7.2 Adding datum shifts to a geodetic boundary value problem

The example discussed in the preceding section demonstrates that only potential *differences* between datum zones can be determined using the proposed method. Consequently, to connect vertical datums, some kind of reference equipotential surface has to be selected. For connecting various datum zones only the potential differences between the datum zones themselves are important, not the potential differences between the datum zones and the adopted reference equipotential surface. As a result, the selection of the reference equipotential surface is not of major importance. Therefore, the equipotential surface defined by the fundamental station in an arbitrarily selected datum zone can be used.

If the potential of the reference equipotential surface is denoted by W_0 , the potential difference between this reference surface and any fundamental bench mark, P , is given by:

$$C_{P0} = W_0 - W(P) = W_0 - \frac{GM}{R} \sum_{l,m,\alpha} \left(\frac{R}{r_p}\right)^{l+1} C_{lm\alpha} Y_{lm\alpha}(P) - Z(P) \tag{7.1}$$

with $Z(P)$ the centrifugal potential.

Based on equation (7.1), Bruns' formula can be derived; see Rummel and Teunissen (1988) for more details.

$$N = \frac{T - \Delta W_0}{\gamma} \tag{7.2}$$

In this equation, ΔW_0 is the reference potential anomaly, and T the anomalous potential. Equation (7.2) yields "geoid heights" relative to the selected reference equipotential surface (W_0).

To illustrate the parameters that have to be solved for in a datum connection problem, figure 7.2 shows the separation between a selected reference equipotential, the adopted reference ellipsoid, and a number of other equipotential surfaces corresponding to local vertical datums. The separation between the reference equipotential and the geoid is given by Bruns' formula, i.e., equation (7.2). The separation between datum zone i and the reference zone is given by $\frac{C_{i0}}{\gamma}$. In order to solve the datum connection problem, these separations have to be determined.

Solution for one datum zone First, one unified global datum is assumed, i.e., ΔW_0 is constant. Substituting a representation for the disturbing potential (T) into Bruns' formula yields the solution for the geodetic boundary value problem based on one, uniform, datum. The geoid height for a point P can

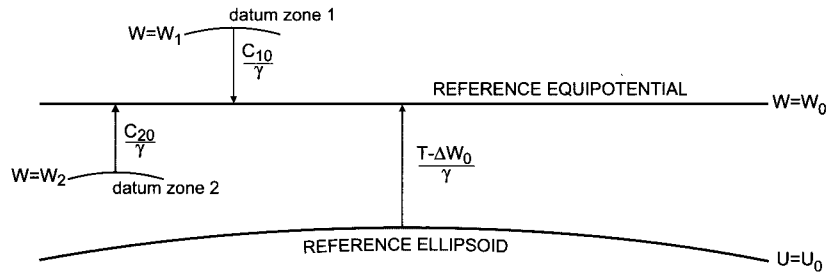


Fig. 7.2 Separation between reference ellipsoid, adopted reference equipotential surface and other equipotential surfaces as defined by local bench marks.

be determined from:

$$N(P) = N_0 + N_1 + \frac{GM}{r\gamma} \sum_{l=2}^{\infty} \left(\frac{R}{r}\right)^l \sum_{m=0}^l (\Delta C_{lm} \cos m\lambda + \Delta S_{lm} \sin m\lambda) P_{lm}(\cos \theta) \quad (7.3)$$

or, if all terrestrial gravity measurements have been reduced to the geoid (or to be more precise, to the unified global datum that is used as an approximation of the geoid), in spherical (constant radius) approximation as

$$N(P) = N_0 + N_1 + \frac{R}{4\pi\gamma} \int_{\sigma} St(\psi_{PQ}) \Delta g(Q) d\sigma_Q \quad (7.4)$$

In these equations σ is a unit sphere, $St(\psi_{PQ})$ is Stokes' integral function, N_1 is the first degree term, i.e., the deviation between the centre of mass of the reference ellipsoid and the centre of mass of the earth, and N_0 the zero-degree term, i.e.,

$$N_0 = -\frac{(W_0 - U_0)}{\gamma} + \frac{GM - GM_0}{r\gamma} = -\frac{\Delta W_0}{\gamma} + \frac{\delta(GM)}{R\gamma} \quad (7.5)$$

By solving the datum connection problem, the zero degree term is solved for as well. However, it is not possible to estimate $\frac{\Delta W_0}{\gamma}$ as a separate unknown. Only the combination of ΔW_0 and $\delta(GM)$ can be solved for. Fortunately, the geocentric gravitational constant of the reference ellipsoid, GM_0 can be determined rather accurately from satellite tracking measurements. Therefore, it is assumed that, with a high enough accuracy, $\delta(GM) = 0$, i.e., the "true" geocentric gravitational constant, GM , is equal to the geocentric gravitational constant of the reference ellipsoid.

In this thesis, the first degree term will be neglected as well, i.e, it is assumed that the centre of mass of the reference ellipsoid and the centre of mass of the earth coincide. Including the first degree term in the datum connection problem has been discussed by van Onselen (1998). For estimating the first degree term a global distribution of measurements is needed. Since, for this thesis only the North Sea area is considered, the first degree term will not be treated.

Solution for more datum zones Instead of one, unified, global datum it is assumed that there are $(I + 1)$ datum zones worldwide. One of these datum zones is used as reference equipotential surface. The potential differences between the fundamental station in the reference zone and the fundamental stations, Q_i , of all other datums zones are denoted $C_{Q_i,0}$.

For stations in the reference zone, the geoid height can still be determined from Bruns' formula. However, since N is the separation between the fundamental station and the reference ellipsoid, for other datum zones Bruns' formula has to be adapted, i.e.,

$$N^{(i)} = \frac{T - \Delta W_0 + C_{Q_i,0}}{\gamma} \quad (7.6)$$

The notation $N^{(i)}$ is used to indicate that although the term geoid height is used, actually the height of the equipotential surface through the fundamental station in zone i above the adopted reference ellipsoid is meant.

Based on the adapted version of Bruns' formula the geoid height for a point P situated in datum zone i can be determined. The actual solution for the geodetic boundary value problem depends on the nature of the available gravity information. In this chapter, only the combination of satellite derived potential coefficients with terrestrial gravity measurements will be considered. For a discussion of results based on either satellite derived potential coefficients or surface gravity data see van Onselen (1998).

If both potential coefficients and terrestrial gravity data in a spherical cap about the station of interest are available, the geoid height for a point P situated in datum zone i consists of three parts, i.e.,

$$N^{(i)}(P) = N_0^{(i)} + N_t + N_s \quad (7.7)$$

N_0 is the zero degree term, which is given by:

$$N_0^{(i)} = -\frac{\Delta W_0}{\gamma} + \frac{C_{Q,0}}{\gamma}$$

N_t is the contribution of the terrestrial gravity measurements in the spherical cap (ψ_c) around the station. It can be derived, see van Onselen (1998), that this contribution can be written as an adapted version of Stokes' integral, i.e.,

$$N_t = \frac{R}{4\pi\gamma} \int_{\psi=0}^{\psi_c} \int_{\alpha=0}^{2\pi} St(\psi_{PQ}) \left[\Delta g_t^{(j)} + \frac{2}{R} C_{Q_j,0} \right] \sin \psi d\psi d\alpha \quad (7.8)$$

in which $\Delta g_t^{(j)}$ are gravity anomalies reduced with respect to datum zone j . Since we have assumed $(I+1)$ datum zones, the index j runs from 1 to I , indicating that for gravity anomalies that have been reduced to datum (j) , the potential difference $C_{Q_j,0}$ has to be included.

N_s is the contribution of the potential coefficients, i.e.,

$$\begin{aligned} N_s &= \frac{R}{4\pi\gamma} \int_{\psi=\psi_c}^{\pi} \int_{\alpha=0}^{2\pi} St(\psi_{PQ}) \Delta g_s \sin \psi d\psi d\alpha = \frac{R}{2\gamma} \sum_{l=2}^{\infty} Q_l \Delta g_l(\theta, \lambda) \\ &= \frac{GM}{2\gamma r} \sum_{l=2}^{L_0} (l-1) \left(\frac{R}{r}\right)^l Q_l \sum_{m=0}^l (\Delta C_{lm} \cos m\lambda + \Delta S_{lm} \sin m\lambda) P_{lm}(\cos \theta) + \\ &\quad \frac{GM}{2\gamma r} \sum_{l=L_0+1}^{\infty} (l-1) \left(\frac{R}{r}\right)^l Q_l \sum_{m=0}^l (C_{lm} \cos m\lambda + S_{lm} \sin m\lambda) P_{lm}(\cos \theta) \end{aligned} \quad (7.9)$$

in which information above degree L_0 is either omitted or estimated based on some kind of model, and Δg_l is the l -th degree Laplace harmonic of $\Delta g(\theta, \lambda)$, and Q_l are truncation coefficients as given by Molodenskii *et al.* (1962).

Kernel modification In the preceding, "normal" Molodenskii truncation coefficients corresponding to Stokes' function have been used. In order to minimise omission errors, and/or the total error, Stokes' kernel can be modified, leading to different truncation coefficients. Modified truncation coefficients combine, for the area of the spherical cap, terrestrial gravity information with gravity information from the potential coefficients. Different authors prefer different types of kernel modifications; see e.g., Heck and Gruninger (1987). de Min (1996) claims that probably the best results are obtained using a combined Meissl/Wong&Gore modification.

Results for error propagation in vertical datum connections, as presented in the following sections, will all be based on the modified Meissl/Wong&Gore truncation coefficients. For more details on the inclusion of these truncation coefficients in the method of vertical datum connection, and comparisons of results based both on these modified coefficients and the Molodenskii truncation coefficients, see van Onselen (1998).

Comment For high quality connection of vertical datums, the solution of the geodetic boundary value problem should be based on a (scalar) Molodenskii approach. As an alternative, an approach based on gravity ratios and ratios of radial distances could be used; for more details see Baarda (1979) and Baarda (1995). However, in this chapter it is not tried to find an optimal method for connecting vertical datums in which all possible contributions are incorporated. The purpose of this chapter is to gain insight in the influence of the various geodetic measurements on the quality of the derived datum connection parameters. Consequently, model errors will not be considered and error propagation can be based on a more simple solution of the geodetic boundary value problem. Therefore, to investigate error propagation in vertical datum connections, the solution of the geodetic boundary value problem will be based on the Stokes approach.

7.3 Least-squares solution of vertical datum connection

To connect the vertical datums, the potential differences $C_{Q_i,0}$ between the I datum zones and the selected reference zone have to be determined. In addition, the potential value of the selected reference zone (or to be more precise the reference potential anomaly) ΔW_0 has to be estimated. These datum connection parameters can be determined as follows.

In every datum zone at least one station is assumed for which the geoid height can be determined by solving a scalar Stokes' boundary value problem. These geoid heights are related to the equipotential surface determined by the fundamental station in the datum zone in which the station under consideration is situated. Consequently, the solution for the geoid height of station P , situated in datum zone i , not only contains the unknown value of ΔW_0 but also the unknown value of $C_{Q_i,0}$.

For every station $P^{(i)}$ the geoid height cannot only be determined through a geodetic boundary value problem, but also from measurements of the geometric height of the station and the orthometric height of the station relative to the fundamental station in the datum zone in which $P^{(i)}$ is situated. From these two equations for every station the unknown datum connection parameters can be determined by means of a least-squares adjustment. The advantage of using a least-squares adjustment is that this method allows the verification of the precision of the derived datum connection parameters and the reliability of the measurements and datum connection parameters.

Observation equations For every station $P^{(i)}$ we have two equations to determine the geoid height of this station relative to the equipotential surface as defined by the fundamental station of the datum zone in which the station is situated. The geoid height can be determined from the geocentric height, h , and orthometric height, $H^{(i)}$ (with respect to the vertical datum zone i in which the station is situated), as:

$$N^{(i)}(P) = h(P) - H^{(i)}(P) \quad (7.10)$$

Besides, the geoid height of this station can be determined as a solution of a scalar Stokes' boundary value problem, i.e., by equation (7.7).

Comparing the two sets of equations for the geoid height for all stations allows, after some rearranging, the system of observation equations to be written in the form:

$$Y = AX + \varepsilon \quad (7.11)$$

in which Y is a vector containing for every station the observations, A is the design matrix, and X is the vector containing the unknown datum connection parameters.

It is assumed that the gravity anomalies in a cap centred around point P , all refer to the same vertical datum, i.e., the vertical datum i in which point P is situated. Consequently, there is only one vertical datum involved with the gravity anomalies. In this case:

- Y : the observation vector has elements $y_{P_k} = h - H^{(i)} - \frac{R}{\gamma} St^c(\Delta g_t^{(j)}) - N_{\text{sat}}^c - N_{\text{om}}^c$
- A : the design matrix has elements either 0, -1, or $(1 + 2IS_{P_k Q_i}^c)$
- X : the vector with unknowns has elements $\frac{\Delta W_0}{\gamma}, \frac{C_{Q_i,0}}{\gamma}, i = 1, 2, \dots, I$

in which the following abbreviations have been used:

$$\frac{R}{\gamma} St^c(\Delta g_t^{(j)}) = \frac{R}{4\pi\gamma} \int_{\psi=0}^{\psi_c} \int_{\alpha=0}^{2\pi} St^*(\psi) \Delta g_t^{(j)} d\sigma_j \quad (7.12)$$

$$N_{\text{sat}}^c = \frac{GM}{2\gamma r} \sum_{l=2}^{L_0} (l-1) \left(\frac{R}{r}\right)^l Q_l^* \sum_{m=0}^l (\Delta C_{lm} \cos m\lambda + \Delta S_{lm} \sin m\lambda) P_{lm}(\cos \theta) \quad (7.13)$$

$$N_{\text{Om}}^c = \frac{GM}{2\gamma r} \sum_{l=L_0+1}^{\infty} (l-1) \left(\frac{R}{r}\right)^l Q_l^* \sum_{m=0}^l (C_{lm} \cos m\lambda + S_{lm} \sin m\lambda) P_{lm}(\cos \theta) \quad (7.14)$$

$$IS_{P_k Q_i}^c = \frac{1}{4\pi} \int_{\psi=0}^{\psi_c} \int_{\alpha=0}^{2\pi} St^*(\psi) d\sigma_i \quad (7.15)$$

N_{Om}^c is not really an observation; this term is either neglected or approximated based on a model.

Precision To solve the datum connection parameters from the system of observation equations, i.e., equation (7.11), the a-priori variance-covariance matrix of the measurements is needed. Following Xu and Rummel (1991), if the observations of geometric, orthometric, and geoid height can be assumed uncorrelated, the variance-covariance matrix of the observations can be determined by:

$$\Sigma_y = \Sigma_h + \Sigma_H + \Sigma_N \quad (7.16)$$

in which Σ_h is the variance-covariance matrix for the observations of geometric height, Σ_H is for orthometric height measurements, and Σ_N is the variance-covariance matrix corresponding to geoid heights. How these a-priori variance-covariance matrices can be obtained will be derived in section 7.4.

The well-known solution for the unknown datum connection parameters, X , following from a least-squares adjustment of equation (7.11) is:

$$X = (A^T \Sigma_y^{-1} A)^{-1} A^T \Sigma_y^{-1} Y \quad (7.17)$$

The first part of equation (7.17) consists of the a-posteriori variance-covariance matrix of the datum connection parameters,

$$\Sigma_x = (A^T \Sigma_y^{-1} A)^{-1} \quad (7.18)$$

the diagonal elements of this matrix contain the variances for the estimated datum connection parameters, i.e., the variances for $\frac{\Delta W_0}{\gamma}$ and $\frac{C_{Q_j \sigma}}{\gamma}$. These variances indicate how well the unknown potential value of the reference surface, and the potential differences between the reference surface and the other datum surfaces can be determined. The variance of the potential difference between two arbitrary datum zones, C_{PQ} , can be estimated from the covariance matrix as given in equation (7.18) by:

$$\sigma_{C_{PQ}}^2 = \sigma_{C_{P_0}}^2 + \sigma_{C_{Q_0}}^2 - 2 \cdot \sigma_{C_{P_0} C_{Q_0}} \quad (7.19)$$

It should be noted that potential differences divided by γ are estimated in order to derive more convenient results in metres. However, for reasons of simplification, often only potential difference is written, whereas potential difference divided by γ is actually meant.

The relative effect of an error in resp. the geometric height, orthometric height, or geoid height on the precision of the derived datum connection parameters can be computed as:

$$\begin{aligned} \Sigma_{Xh} &= \Sigma_x A^T \Sigma_y^{-1} \Sigma_h \Sigma_y^{-1} A \Sigma_x \\ \Sigma_{XH} &= \Sigma_x A^T \Sigma_y^{-1} \Sigma_H \Sigma_y^{-1} A \Sigma_x \\ \Sigma_{XN} &= \Sigma_x A^T \Sigma_y^{-1} \Sigma_N \Sigma_y^{-1} A \Sigma_x \end{aligned} \quad (7.20)$$

These matrices give the precision of the derived datum connection parameters due to the uncertainty in the measurements of respectively geometric height, orthometric height, and geoid height.

Reliability The advantage of solving the datum connection problem by means of a least-squares adjustment is that not only the precision of the derived datum connection parameters can be estimated but their reliability and the reliability of the involved measurements can be verified as well.

A measure of the reliability of the measurements, often referred to as the internal reliability, is the minimal detectable bias, $\overline{\Delta y}_i$. This is a measure of the error in the measurements that can be detected with significant level α and power β . Following Baarda (1968), this minimal detectable bias can be calculated with the following equation:

$$\overline{\Delta y}_i = \sqrt{\frac{\lambda_0}{M_i}} \quad (7.21)$$

In this equation λ_0 is related to the test parameters α and β . For example, for $\alpha = 0.05$ and $\beta = 0.8$, $\sqrt{\lambda_0}$ has the value 2.8. The parameter M_i can be determined from:

$$M_i = c_i^T (\Sigma_y)^{-1} Q_\varepsilon (\Sigma_y)^{-1} c_i \quad (7.22)$$

If applied to data snooping, c_i is a vector consisting of zeros except for the i -th position corresponding to the measurement that is been tested, i.e., $c_i = (0, 0, \dots, 1, 0, \dots, 0)^T$. Q_ε is the variance-covariance matrix of the measurement errors, i.e., $Q_\varepsilon = \Sigma_y - A\Sigma_x A^T$.

The reliability of the derived datum connection parameters, often referred to as the external reliability, is the influence of a minimal detectable bias $\overline{\Delta y}_j$ on the estimated parameters. The influence of a minimal detectable bias on the i -th datum connection parameter is, according to Baarda (1968), given by

$$\overline{\Delta X}_i = \Sigma_x A^T \Sigma_y^{-1} \overline{\Delta Y}_j \quad (7.23)$$

If applied to data snooping, $\overline{\Delta Y}_j$ is a vector consisting of zeros except for the position corresponding to the influence of the measurement that is been tested, i.e., $\overline{\Delta Y}_j = (0, 0, \dots, \overline{\Delta y}_j, 0, \dots, 0)^T$.

7.4 A-priori covariance matrices

In order to determine the accuracy of datum connection parameters, the a-priori variance-covariance matrix of the measurements is needed. Assuming no correlation between the three types of observations, the a-priori covariance matrix of the measurements can be determined by simply adding the a-priori covariance matrices for the measurements of resp. geometric height, orthometric height, and geoid height.

7.4.1 A-priori variance-covariance matrix for orthometric heights

In order to determine the a-priori variance-covariance matrix for orthometric height measurements, it is assumed the the precision of orthometric heights is entirely determined by the precision of the levelling measurements (for a justification of this assumption see van Onselen (1998)). Consequently, the variance-covariance matrix for the orthometric heights can be derived from the variance-covariance matrices of existing levelling networks.

Since the area of interest is the North Sea region, variance-covariance matrices resulting from, e.g., the UELN-95 adjustment could be used. Although resulting in very realistic values for the precision of orthometric heights, this method has a number of disadvantages, among which:

- Using the full covariance matrices from the UELN-95 adjustment would involve a tremendous amount of data from which covariances for the stations under consideration have to be selected. Therefore, practically only variances of stations can be used.
- Not all stations under consideration are necessarily a part of the UELN network, sometimes points nearby have been used. Consequently, variances for these stations have to be estimated based on the results for nearby UELN-stations.
- Standard deviations are given relative to NAP. For the data configuration under consideration, standard deviations relative to other reference equipotentials are needed as well.

Therefore, for error propagation studies, the precision of the orthometric heights will be based on a general guideline describing levelling precision. In general, the standard deviation for levelling measurements can be written as

$$\sigma_{\Delta H}(mm) = \alpha\sqrt{S} \quad (7.24)$$

with S the levelling distance in km, and α the unit standard deviation. For first order levelling networks, e.g., in Europe, a standard deviation of $0.6 \text{ mm}/\sqrt{\text{km}}$, is feasible. Since the actual levelling distance between the stations and the corresponding fundamental station is hard to recover, horizontal distances between the stations have to be used with an adapted (larger) value for α .

For the following sections, a value $\alpha = 0.8$ will be used. This factor 0.8 is selected to give standard deviations that show, on average, a large similarity with standard deviations as presented by Lang and Sacher (1996a). Since the horizontal distance between stations is used instead of the actual levelling distance, stations like Brest (in the western corner of France) will get a slightly over-optimistic estimate of their standard deviation, whereas for stations in e.g., Italy, the estimate for the standard deviation based on the general guideline is slightly too pessimistic.

7.4.2 A-priori variance-covariance matrix for geometric heights

Most stations used in the following sections are IERS sites. Consequently, standard deviations for these stations as published by IERS can be used. Since, from general IERS publications (e.g., Boucher *et al.* (1992) or Boucher and Altamimi (1993)), no information about correlation between the stations is available, it is assumed that the geometric height measurements are uncorrelated.

For stations that are not part of a global “fundamental reference network” of VLBI, SLR, or GPS stations, relative geometric heights with respect to one or more of these “fundamental space stations” can be determined using differential GPS. According to Bock (1996), the variance of these relative measurements can be estimated as

$$\sigma^2(\text{mm}^2) = 9.0 + (0.006 \cdot s)^2 \quad (7.25)$$

in which s is the distance (in km) between the station under consideration and the “fundamental space station”. Table 7.1 shows standard deviations for the geometric heights of the 30 stations used in the following sections, based on the values for ITRF92 as published by Boucher and Altamimi (1993).

Station	st. dev.	Station	st. dev.	Station	st. dev.
Grasse	0.6	Kootwijk	0.6	Kirschberg	1.1
Toulouse	1.6	Westerbork	0.7	Tromso	0.6
Brest	1.2	Zimmerwald	0.7	Honefos	1.8
Graz	0.6	Monte Generoso	1.8	Trysil	0.9
Borowiec	3.3	Potsdam	1.5	Onsala	0.6
Bologna	0.7	Wetzell	0.6	Martsbo	0.7
Trieste	2.0	Hohenbunstorf	0.9	Metsahovi	0.7
Monte Venda	2.1	Effelsberg	0.8	Chilbolton	1.1
Madrid-Robledo	0.5	Hohenpeissenberg	1.7	Herstmonceux	0.6
Madrid-Facultad	0.6	Karlsburg	0.6	Carnutsy	1.7

Table 7.1 Stations and their standard deviations (in cm) for geometric heights, based on ITRF92

7.4.3 A-priori variance-covariance matrix for geoid heights

In order to derive a variance-covariance matrix for the combination of potential coefficients and surface gravity data, a procedure as described by Smeets (1992) is used. The geoid height can be determined as:

$$N = \frac{R}{4\pi\gamma} \int_{\sigma_c} St^*(\psi) \Delta g d\sigma + \frac{R}{4\pi\gamma} \int_{\sigma-\sigma_c} St^*(\psi) \Delta g d\sigma \quad (7.26)$$

in which St^* is used to indicate that instead of the “normal” Stokes function, modified kernel functions can be used as well.

Instead of the “true” gravity anomalies, in the first integral the mean terrestrial gravity anomalies, $\Delta\bar{g}_t$, are used and in the second integral the anomalies derived from the potential coefficients, Δg_s . The error caused by this substitution is given by

$$\delta N = \frac{R}{4\pi\gamma} \int_{\sigma_c} St^*(\psi) (\Delta\bar{g}_t - \Delta g) d\sigma + \frac{R}{4\pi\gamma} \int_{\sigma-\sigma_c} St^*(\psi) (\Delta g_s - \Delta g) d\sigma \quad (7.27)$$

This error can be rewritten as:

$$\begin{aligned} \delta N &= \frac{R}{2\gamma} \sum_{l=2}^{\infty} \left[\frac{2}{l-1} - Q_l^*(\psi_c) \right] (\varepsilon_t)_l \\ &- \frac{R}{2\gamma} \sum_{l=2}^{\infty} \left[\frac{2}{l-1} - Q_l^*(\psi_c) \right] [1 - \beta_l(\psi_\beta)] (\Delta g)_l \\ &+ \frac{R}{2\gamma} \sum_{l=2}^{L_0} Q_l^*(\psi_c) (\varepsilon_s)_l - \frac{R}{2\gamma} \sum_{l=L_0+1}^{\infty} Q_l^*(\psi_c) (\Delta g)_l \end{aligned} \quad (7.28)$$

in which $(\varepsilon_t)_l$ is the square root of the error degree variance of the terrestrial measurements, $(\Delta g)_l$ the square root of the degree variances of the gravity anomalies, $(\varepsilon_s)_l$ the square root of the error degree variance of the satellite derived gravity anomalies, β_l the so-called smoothing-coefficients and ψ_β the radius of the spherical cap over which the block mean values are determined.

Based on the four contributions to the error in geoid height as introduced in equation (7.28), the variance-covariance matrix for the geoid height can be written as

$$\Sigma_{N_P N_Q} = \Sigma_{N_P N_Q}^p + \Sigma_{N_P N_Q}^d + \Sigma_{N_P N_Q}^c + \Sigma_{N_P N_Q}^o \quad (7.29)$$

in which $\Sigma_{N_P N_Q}^p$ is the variance-covariance matrix due to the commission error in the terrestrial gravity measurements, referred to as propagated error, $\Sigma_{N_P N_Q}^d$ is due to the omission error in the terrestrial gravity measurements, referred to as discretization error, and $\Sigma_{N_P N_Q}^c$ and $\Sigma_{N_P N_Q}^o$ are the variance-covariance matrices due to resp. the commission and omission errors in the potential coefficients.

Variance-covariance matrix due to the propagated error The commission error in the terrestrial gravity measurements, i.e., inaccuracies in the measurements themselves, is referred to as propagated error to make the distinction with the commission error for the potential coefficients.

Inaccuracies in the terrestrial gravity measurements are assumed stochastic, no systematic effects are present. From equation (7.28) it can be derived that the variance-covariance matrix due to the propagated error in the gravity measurements can be estimated by:

$$\Sigma_{N_P N_Q}^p = \left(\frac{R}{2\gamma} \right)^2 \sum_{l=2}^{\infty} \left[\frac{2}{l-1} - Q_l^*(\psi_c) \right]^2 d_l P_l(\cos \psi_{PQ}) \quad (7.30)$$

in which d_l are the error degree variances of the gravity anomalies.

Using $C(\psi)$ for the covariance function of the gravity anomalies, the error degree variances of the gravity anomalies can be determined from:

$$d_l = \frac{2l+1}{2} \int_0^\pi C(\psi) P_l(\cos \psi) \sin \psi d\psi = C_0 (1-\mu) \mu^l \quad (7.31)$$

The covariance function of the terrestrial gravity anomalies can be computed as, see Sjöberg (1986),

$$C(\psi) = C_0 \left\{ \frac{1-\mu}{(1-2\mu \cos \psi + \mu^2)^{\frac{1}{2}}} - (1-\mu) - (1-\mu)\mu \cos \psi \right\} \quad (7.32)$$

Consequently, for a specific variance and correlation length of the gravity anomalies, the parameters C_0 and μ can be determined.

As an example, according to de Min (1996), for the second order gravity network in the Netherlands errors in terrestrial gravity measurements can be described by a combination of the following three effects:

- Errors in first order network. This effect will have a relatively long wavelength. To describe this error a standard deviation of 10 μgal and a correlation length of 0.5 degrees could be used.
- Connection of second order network. Described by a theoretical covariance function with a standard deviation of 50 μgal and a correlation length of 0.1 degrees.
- Measuring noise. This effect will have a very short wavelength. To estimate this noise a standard deviation of 200 μgal and a correlation length of 0.01 degrees could be used.

Assuming the three error sources mentioned above to be uncorrelated, these three effects can be added to model the propagated error.

Variance-covariance matrix due to the discretization error Discretization errors are associated with the gravity anomalies being given at discrete locations (or as mean values) instead of a continuous function. From equation (7.28), the variance-covariance matrix due to the discretization errors can be determined from

$$\begin{aligned}\Sigma_{N_P N_Q}^d &= \left(\frac{R}{2\gamma}\right)^2 \sum_{l=2}^{\infty} \left[\frac{2}{l-1} - Q_l^*(\psi_c) \right]^2 [1 - \beta_l(\psi_\beta)]^2 c_l \\ &+ 2 \left(\frac{R}{2\gamma}\right)^2 \sum_{l=L_0+1}^{\infty} Q_l^*(\psi_c) \left[\frac{2}{l-1} - Q_l^*(\psi_c) \right] [1 - \beta_l(\psi_\beta)] c_l\end{aligned}\quad (7.33)$$

in which c_l are the anomaly degree variances.

Discretization errors are a very local effect, consequently, anomaly degree variances are needed up to very high degree in order to calculate meaningful results. However, it could be argued that since terrestrial measurements are only used in a small area (e.g., $\psi_c = 2^\circ$) around a limited number of observation points, the discretization error can be made negligible small by adding enough terrestrial measurements. In the following it will be assumed that the effect of the discretization error on the geoid height can be reduced to a few millimetres, and is, therefore, neglected.

Variance-covariance matrix due to the commission error It can be derived, see van Onselen (1998) that the commission error (uncertainties in the potential coefficients), can be determined from:

$$\Sigma_{N_P N_Q}^c = F(P) \Sigma_{C_S}^s F^T(Q) \quad (7.34)$$

where $F(P)$ and $F(Q)$ are coefficient matrices that relate ΔC_{nm} and ΔS_{nm} to the geoid heights at points P and Q , respectively. $\Sigma_{C_S}^s$ is the variance-covariance matrix of the potential coefficients ΔC_{nm} and ΔS_{nm} for the area outside the spherical cap ψ_c . This variance-covariance matrix for the area outside the spherical cap can be determined by introducing additional eigenvalues $(\frac{l-1}{2} Q_l^*)^2$ in the calculations.

Presently, global geopotential models up to degree and order 360 are available; e.g., EGM96. However, these models are not only based on satellite measurements, but also on terrestrial gravity measurements. Since terrestrial gravity measurements have usually been reduced to some kind of equipotential surface based on orthometric height measurements, terrestrial gravity measurements in different height zones will have been reduced to different equipotential surfaces. As a result, these terrestrial measurements themselves and, consequently, the resulting potential coefficient models, are affected by discrepancies between vertical datums.

Another disadvantage of potential coefficient models based on terrestrial gravity measurements is that we do not want correlation between terrestrial measurements used to improve the quality of the datum connection, and the set of potential coefficients itself. Consequently, it seems more prudent to use potential coefficient models that are not based on terrestrial gravity measurements. Therefore, we the following two potential coefficient models will be used:

- JGM2s - the Joint Gravity Model, developed for the Topex/Poseidon mission and obtained from tracking to various satellites with various orbit characteristics. Presently (1997) this is the best satellite-only model available. A full variance-covariance matrix up to degree and order 70 will be used.
- GOCE - a new gravity model to be obtained from a scheduled Gravity Explorer Mission. To obtain this GOCE variance-covariance matrix a simulation has been performed for a 6 months gradiometry mission, with a sun-synchronous orbit with a height of 270 km, in combination with GPS-tracking. This resulted in a block-diagonal matrix, containing information up to degree and order 180.

Variance-covariance matrix due to the omission error Using equation 7.36 of Heiskanen and Moritz (1967), the variance-covariance matrix resulting from the omission error in the potential coefficients can be found as:

$$\Sigma_{N_P N_Q}^o = \frac{R^2}{4\gamma^2} \sum_{l=L_0+1}^{\infty} (Q_l^*)^2 c_l P_l(\cos \psi_{PQ}) \quad (7.35)$$

In which c_l are again anomaly degree variances and Q_l^* the truncation coefficients.

7.5 Datum connection in North-West Europe

In this section, quality of regional datum connection will be investigated through error propagation. The region considered is North-West Europe, in which three datum zones have been defined:

1. Western-Europe; with zero-point NAP; as fundamental station Amsterdam is used. Note that NAP is also the zero point for the United European Levelling Network (UELN).
2. Scandinavia; with fundamental station Helsingborg in Sweden.
A common height system for investigations in the Baltic area is the Nordic Height System 1960, as introduced by Ekman and Mäkinen (1991), but its zero point is NAP. Therefore, Helsingborg, which was the original basis of the Swedish height system and from where the Swedish levelling network is connected to NAP has been used as fundamental station for this region.
3. Great Britain; with fundamental station Newlyn. Newlyn mean sea level for 1915-21 defines "Ordnance Datum Newlyn", a reference for geodetic levelling in the U.K.

These three datum zones are all part of UELN and, consequently, heights (in geopotential units) for stations in all of these zones are available relative to NAP. However, there is only one single connection line between resp. Great Britain and Scandinavia and the continent of Europe; see Ehrnsperger *et al.* (1982) for a description of the UELN-73 network and e.g., Lang and Sacher (1996a) for the enlarged UELN-95 network. For a high quality datum connection one measurement between datum zones is insufficient. Therefore, in this studies, these areas are considered as separate height datum zones. Figure 7.3 shows the distribution of stations and datum zones under consideration. In total 30 IERS sites have been used.

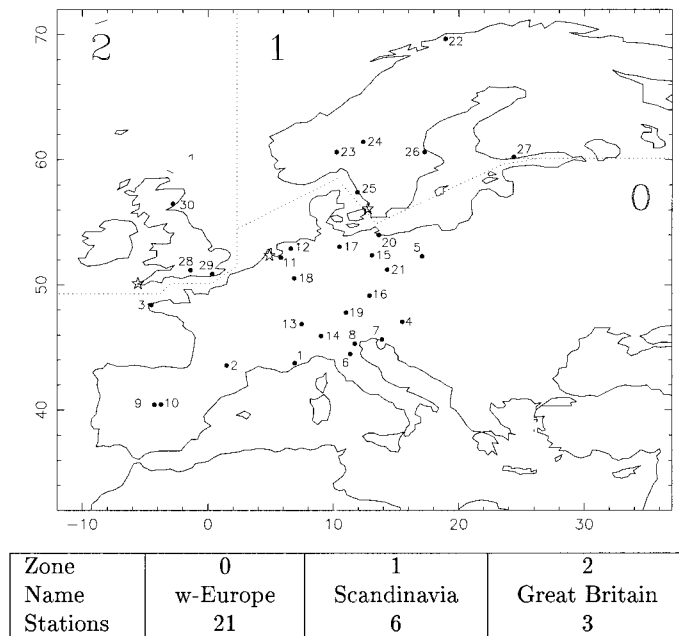


Fig. 7.3 Distribution of stations (●), fundamental stations (★) and datum zones.

While assessing the accuracies of the derived datum connection parameters as presented in the following sections it should be kept in mind that only the effect of the quality of the measurements, the station configuration, etc. has been considered. The effect of model errors (e.g., introduced by using a Stokes approach for solving the geodetic boundary value problem) on the quality of the datum connection parameters has been neglected.

Although actually $\frac{\Delta W_0}{\gamma}$ and $\frac{C_{ij}}{\gamma}$ are estimated, in the figures representing the results for the error propagation the notation ΔW_0 and C_{ij} will be used to simplify the captions. Furthermore, in the text often potential differences will be written while potential differences divided by normal gravity is meant.

Figure 7.4 shows standard deviations with which datum connection parameters can be determined for terrestrial gravity measurements in a spherical cap of two degrees around every station in combination with potential coefficients derived from resp. the JGM2 and GOCE potential coefficient model; modified Meissl/Wong&Gore truncation coefficients (MWG) have been used.

Based on the JGM2 model, standard deviations range between 13.5 and 21.9 cm. The largest values correspond to the connection with Great Britain (datum zone 2). This can be explained by the fact that the Great Britain datum zone contains only three stations. If the GOCE model becomes available these parameters could be determined with standard deviations ranging from 0.9 up to 1.4 cm, the larger values again applying to potential differences relative to the Great Britain height zone.

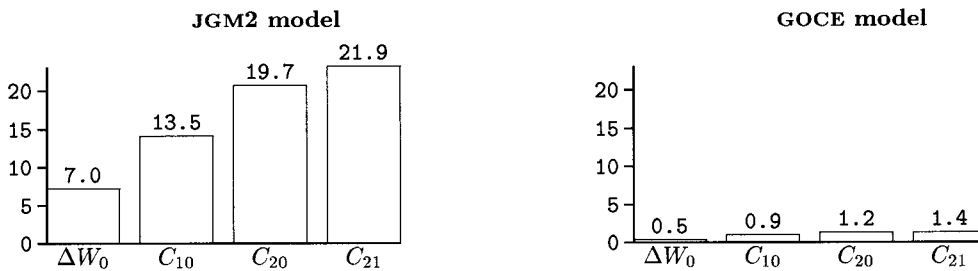


Fig. 7.4 Standard deviations of vertical datum connection parameters (in cm); $\psi_c = 2^\circ$.

From the relative effects of the various error sources, see figure 7.5, it is clear that if the JGM2 model is used the major part of the error is caused by the commission and omission error in the potential coefficients. Errors in orthometric height are the major limiting factor in case the GOCE model is used for solving the datum connection problem. Therefore, for this data configuration and these precisions for the other measurements, an improvement in the precision of geometric heights and terrestrial gravity information will not lead to a more precise datum connection. On the other hand, the precision with which the datum connection parameters can be determined could be improved by an increase in precision of the orthometric heights, i.e., an improvement in the precision of the levelling measurements.

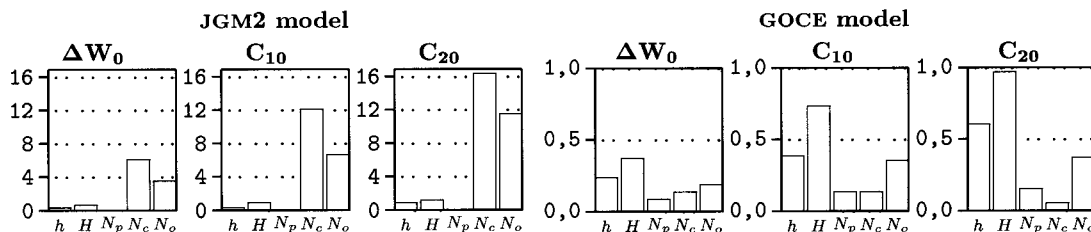


Fig. 7.5 Effect of contributing error sources on the precision of datum connection parameters (in cm). h : geometric heights, H : orthometric heights, N_p : propagated error, N_c : commission error, N_o : omission error.

Figure 7.6 shows the minimal detectable bias, $\overline{\Delta y_i}$, following from data snooping, for the 30 measurements. This figure shows that, with significance level $\alpha = 0.05$ and power $\beta = 0.8$, in case the JGM2 model is used errors ranging between 28 and 127 cm in measurements cannot be detected by testing. If the GOCE model is used, values for the minimal detectable bias range between 3.6 and 11.4 cm.

Figure 7.7 shows the external reliability based on data snooping, i.e., the influence of a model error $\overline{\Delta y_i}$ in one of the 30 measurements on the estimated parameters, i.e., on resp. $\frac{\Delta W_0}{\gamma}$, $\frac{C_{10}}{\gamma}$, and $\frac{C_{20}}{\gamma}$. The following conclusions can be made:

- The influence of a minimal detectable bias on the estimate of $\frac{\Delta W_0}{\gamma}$ is relatively small if the GOCE model is used, i.e., up to 0.7 cm. If the JGM2 model is used this effect can be up to 8.7 cm.
- If the JGM2 model is used, errors of up to 17.9 cm in $\frac{C_{10}}{\gamma}$ cannot be detected by testing. For the GOCE model, the maximum value for the external reliability of $\frac{C_{10}}{\gamma}$ is 1.8 cm.

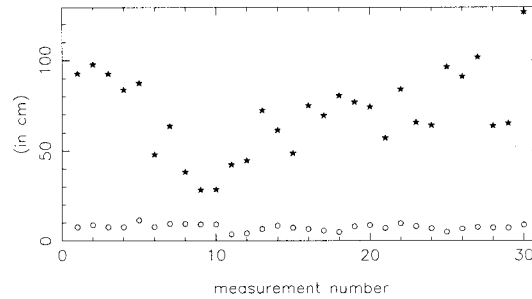


Fig. 7.6 Minimal detectable bias (in cm) for 30 measurements resulting from data snooping; based on JGM2 (\star), or GOCE model (\circ).

- For $\frac{C_{20}}{\gamma}$, a minimal detectable bias in one of the measurements can cause an error of up to 60 cm if the JGM2 model is used. Using the GOCE model instead, leads to a maximum value for the external reliability of almost 3 cm.
- The values for the JGM2 model show a lot more scatter than those corresponding to the GOCE model. This is due to the larger scatter in the values for the minimal detectable bias, which is again caused by the large inhomogeneity in the quality of the measurements if the commission error is based on the JGM2 model.

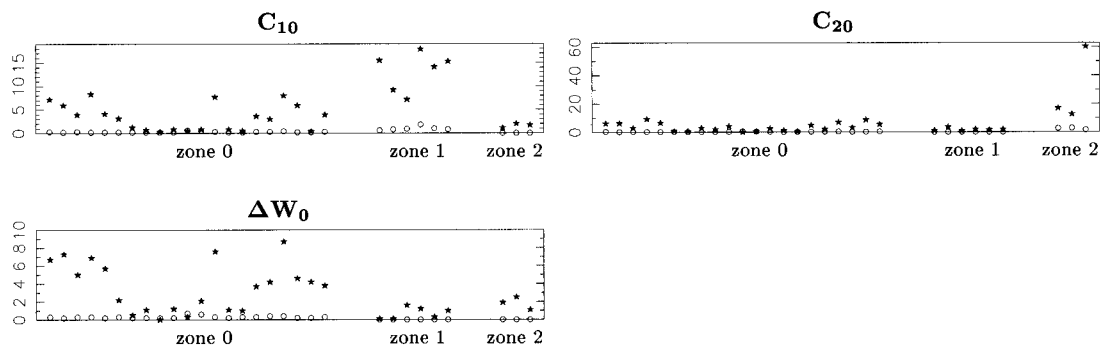


Fig. 7.7 External reliability for resp. ΔW_0 , C_{10} , C_{20} (in cm) due to a minimal detectable bias in one of the 30 measurements in one of the three datum zones; based on JGM2 (\star), or GOCE model (\circ).

The three datum zones used are all part of the UELN network. Therefore, results derived in figure 7.4 for the standard deviation of the potential differences between resp. the fundamental station in zone 1 (Helsingborg) and in zone 2 (Newlyn), and the fundamental station in the reference zone (Amsterdam) can be compared with the standard deviations of the corresponding heights (in gpu) resulting from the adjustment of the UELN-95/8 network. From figure 6 of Lang and Sacher (1996a) the standard deviation of the dynamic height between Helsingborg and Amsterdam can be estimated as around 15 mm and the standard deviation between Newlyn and Amsterdam as around 77 mm. It is clear that results derived using the JGM2 model are by far worse than these values.

If the GOCE model is used results are better, especially for the connection with zone 2 (Newlyn). Furthermore, in the UELN-95 network the reliability of the connection between Amsterdam and resp. Helsingborg and Newlyn is extremely low, since it consists of one single connection line. For the method under consideration, values for the external reliability range between 0.2 and 2.8 cm.

7.6 “Ideal” cap size for terrestrial gravity measurements

If the JGM2 gravity model has to be used, the commission and omission error in the potential coefficients are the major limiting factors in solving the datum connection problem. These errors can be reduced

by increasing the area in which terrestrial gravity measurements (of sufficient quality) are available. However, increasing the cap size not only reduces the commission and omission error in the potential coefficients, but also increases the terrestrial gravity error in the terrestrial gravity measurements (propagated error). Therefore, some kind of “ideal” cap size has to be found, based on the data configuration under consideration, which will give an optimal solution.

To demonstrate the effect of increasing the spherical cap in which high quality, high density terrestrial gravity information is assumed available, error propagation is performed for three additional cap sizes. Figure 7.8 shows standard deviations of estimated potential differences, based on the JGM2 potential coefficient model. Comparing these results with figure 7.4, shows a major increase in precision if the spherical cap is increased from two to five degrees. By increasing the size of the spherical cap to seven, or even ten degrees, standard deviations for the datum connection parameters decrease even further.

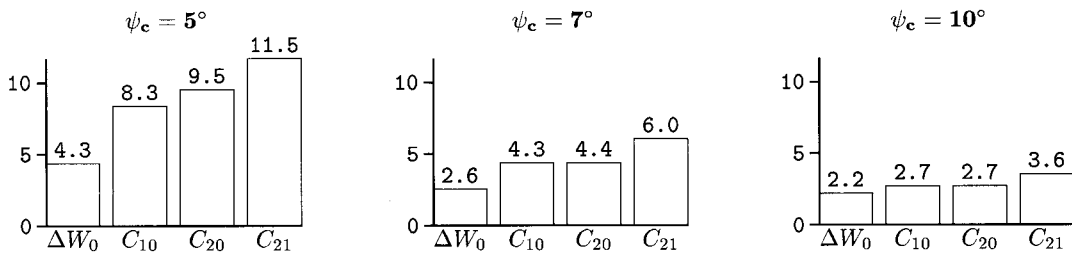


Fig. 7.8 Standard deviations of vertical datum connection parameters (in cm); JGM2 model; 3 cap sizes

Figure 7.9 shows, for these three cap sizes, the relative influences of the various error sources on the precision of both $\frac{C_{10}}{\gamma}$ and $\frac{C_{20}}{\gamma}$, again based on the JGM2 potential coefficient model. Comparing these results with those presented in figure 7.5, clearly shows that the further the cap size is increased, the further the relative influence of the commission and omission errors decreases. However, even for a cap size of ten degrees the commission error in the potential coefficients is still the limiting factor for solving the datum connection parameters.

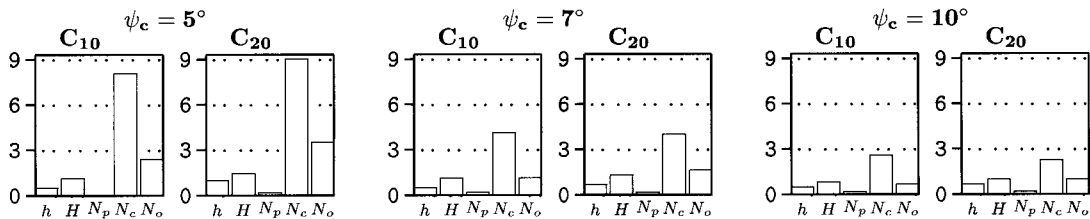


Fig. 7.9 Effect of contributing error sources on precision of vertical datum connection (in cm); JGM2 model; 3 different cap sizes.

Especially for a spherical cap of ten degrees, standard deviations of estimated datum connection parameters are rather good. Since, even for a cap size of ten degrees, the commission error in the potential coefficients of the JGM2 model is still the limiting factor for solving the datum connection parameters, it seems advantageous to even further increase the spherical cap size. Unfortunately large cap sizes yield all kind of other complications, for instance:

- Availability of high quality terrestrial gravity measurements around every station in large areas. To estimate the propagated error, quality estimates of the Dutch second order gravity network have been used. Since this is relatively very high quality gravity information, the assumption that gravity information of this quality is available over very large areas, e.g., cap size of 10 degrees, is rather unrealistic.
- High density of terrestrial measurements. It has been assumed that discretization errors in terrestrial gravity measurements could be neglected, assuming a high enough density of terrestrial measurements within the spherical caps.

- Terrestrial measurements refer to more than one datum zone.

It has been assumed that gravity anomalies in a cap centered around point P all refer to the vertical datum in which P is situated. For large spherical caps it is more likely that parts of the data set refer to neighbouring vertical datums. This makes the assumption of a uniform precision of gravity anomalies rather unrealistic. In addition, gravity measurements in the spherical cap have been reduced to different reference surfaces and additional datum shifts have to be included in the equations containing the gravity anomalies.

As a result, accuracies derived for datum connection parameters based on large spherical caps become rather unrealistic. To derive more realistic values, the above mentioned complications should be accounted for. These problems have been addressed by van Onselen (1998).

In the following section, for the JGM2 model a spherical cap size of only five degrees will be used, to prevent the above mentioned complications related to larger cap sizes. To compare results, figure 7.10 and figure 7.11 show respectively values for the minimal detectable bias and their influence on the estimated parameters; both based on data snooping.

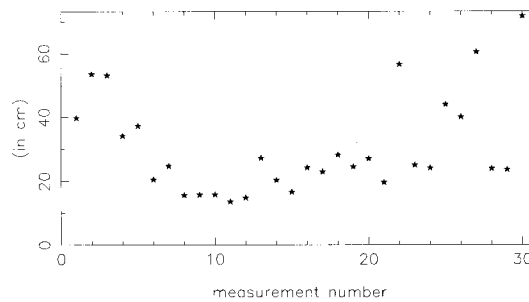


Fig. 7.10 Minimal detectable bias (in cm) for 30 measurements resulting from data snooping; based on JGM2 model; $\psi_c = 5^\circ$.

Comparing these values with those derived for a cap size of two degrees, as shown in figure 7.6 and figure 7.7, shows that, on average, values for the internal and external reliability decrease by a factor 2. Maximum value for the external reliability of $\frac{\Delta W_0}{\gamma}$ decreases from 9.1 to 7.0 cm, and for $\frac{C_{20}}{\gamma}$ from 17.9 to 11.9 cm. For $\frac{C_{20}}{\gamma}$ the improvement in external reliability is much more pronounced, i.e., the maximum error that cannot be detected by testing decreases from 60.3 to 27.7 cm.

It can be concluded that the improvement in external reliability depends on the number of stations in the datum zones. If one of the datum zones contains only a small number of stations, increasing the size of the spherical cap with terrestrial gravity measurements leads to an increase in external reliability. If the datum zones contain a larger amount of stations, the increase in external reliability is less profound. This can be explained as follows. If one of the datum zones contains only a small number of stations, only very large errors in the corresponding datum connection parameters can be detected by testing. If datum zones contain more stations (see next section), already smaller errors in the datum connection parameters can be detected. Therefore, reducing the commission error (the main error source if the JGM model is used), has a relatively smaller influence on the external reliability of datum connection parameters corresponding to datum zones containing a lot of stations.

7.7 Influence of the number of stations

In theory the method used for connecting vertical datums requires only one station in every height datum zone. In this section, it is tried to gain some insight in the number of stations needed in every datum zone to reach a certain precision and reliability for the derived potential differences between the datum zones. A first, simple, conclusion is that in order to detect outliers in measurements, more than one station is needed in every datum zone.

To gain more insight in the influence of the number of stations, a simple experiment is conducted. First, all a-priori covariance matrices for the different measurement types are assumed diagonal (uncorrelated

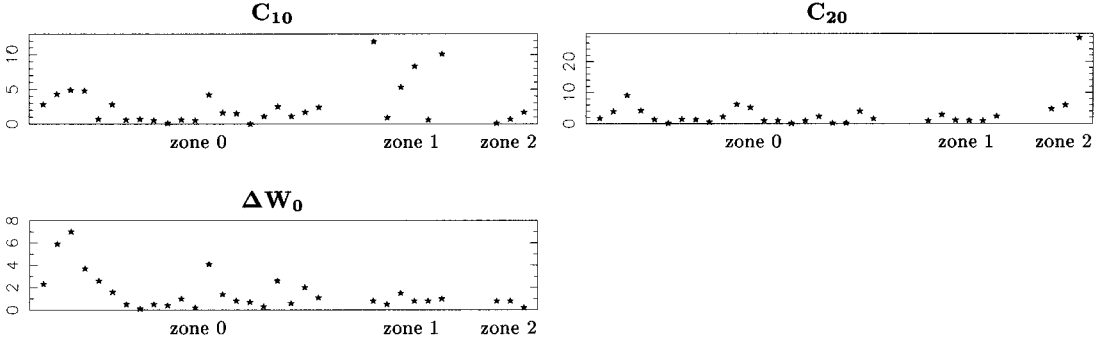


Fig. 7.11 External reliability for resp. ΔW_0 , C_{10} , C_{20} (in cm) due to a minimal detectable bias in one of the 30 measurements in one of the three datum zones; based on JGM2 model; $\psi_c = 5^\circ$.

measurements). In this case an analytical expression can be found for the a-posteriori weight matrix for the unknowns (normal matrix):

$$(\Sigma_x)^{-1} = A^T \Sigma_y^{-1} A = \begin{pmatrix} \sum_{j=1}^{J_{tot}} p_j & -\alpha \sum_{j=1}^{J_1} p_j & -\alpha \sum_{j=1}^{J_2} p_j \\ -\alpha \sum_{j=1}^{J_1} p_j & \alpha^2 \sum_{j=1}^{J_1} p_j & 0 \\ -\alpha \sum_{j=1}^{J_2} p_j & 0 & \alpha^2 \sum_{j=1}^{J_2} p_j \end{pmatrix} \quad (7.36)$$

in which J_0 is the number of stations in the reference zone, J_1 and J_2 resp. the number of stations in zone 1 and 2, J_{tot} is the total number of stations ($J_{tot} = J_0 + J_1 + J_2$), p_j are the weights of the observations, i.e., $p_j = (\sigma_j^2)^{-1}$, and $\alpha = (1 + 2IS_{PQ_i}^t)$. As an example, for measurements in a spherical cap of two degrees, $\alpha = 1.0756$.

Inverting this normal matrix yields the a-posteriori variance-covariance matrix for the unknowns. The diagonal elements of this matrix represent the variances for the datum connection parameters relative to the reference zone (zone 0), i.e.,

$$\begin{aligned} \sigma^2 \left(\frac{\Delta W_0}{\gamma} \right) &= \frac{1}{\sum_{j=1}^{J_0} p_j} & \forall_j: \underline{p_j} = p & \frac{1}{p \cdot J_0} \\ \sigma^2 \left(\frac{C_{Q_1 0}}{\gamma} \right) &= \frac{\sum_{j=1}^{J_0} p_j + \sum_{j=1}^{J_1} p_j}{\alpha^2 (\sum_{j=1}^{J_0} p_j \cdot \sum_{j=1}^{J_1} p_j)} & \forall_j: \underline{p_j} = p & \frac{J_0 + J_1}{\alpha^2 \cdot p \cdot J_0 \cdot J_1} \\ \sigma^2 \left(\frac{C_{Q_2 0}}{\gamma} \right) &= \frac{\sum_{j=1}^{J_0} p_j + \sum_{j=1}^{J_2} p_j}{\alpha^2 (\sum_{j=1}^{J_0} p_j \cdot \sum_{j=1}^{J_2} p_j)} & \forall_j: \underline{p_j} = p & \frac{J_0 + J_2}{\alpha^2 \cdot p \cdot J_0 \cdot J_2} \end{aligned} \quad (7.37)$$

The variance for the potential difference between zone 1 and zone 2 can be found as:

$$\sigma^2 \left(\frac{C_{Q_1 Q_2}}{\gamma} \right) = \frac{\sum_{j=1}^{J_1} p_j + \sum_{j=1}^{J_2} p_j}{\alpha^2 (\sum_{j=1}^{J_1} p_j \cdot \sum_{j=1}^{J_2} p_j)} \quad \forall_j: \underline{p_j} = p \quad \frac{J_1 + J_2}{\alpha^2 \cdot p \cdot J_1 \cdot J_2} \quad (7.38)$$

In this simplified approach of uncorrelated measurements it is clear that the precision with which the potential difference between two datum zones can be determined depends on the number of measurements in both datum zones and their variance. In an even further simplified example, i.e., assuming uniform precision for all combined height measurements, increasing the number of measurements, or decreasing the variance of the measurements by a factor two, both lead to an improvement in the precision for the potential difference of a factor two, see right-hand side of equations (7.37) and (7.38).

In reality measurements will not have uniform precision and the a-priori covariance matrix of the measurements will not be diagonal. However, variances of measurements are, in general, much larger than covariances between measurements. Therefore, equation (7.37) and (7.38) can give some insight in

the relation between the number of measurements and the precision of the derived datum connection parameters.

To verify the relation between the number of stations and the precision for the datum connection parameters, error propagation is performed using a data configuration with either two or three stations in every datum zone. Stations have been selected to minimise errors in geometric and orthometric height, i.e., stations with small standard deviations for the geometric height, see table 7.1, and close to the fundamental stations have been used. Figure 7.12 shows the distribution of stations and datum zones under consideration.

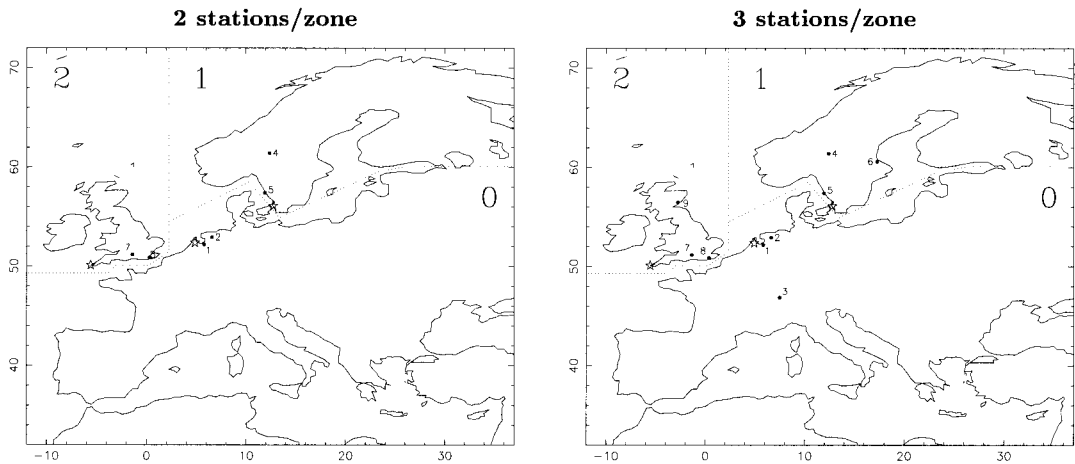


Fig. 7.12 Distribution of stations (•), fundamental stations (*) and datum zones.

Figure 7.13 shows standard deviations of datum connection parameters using the JGM2 model (cap size for terrestrial gravity measurements 5°). Compared to the results as shown in figure 7.8, standard deviations increase substantially. This decrease in precision is especially strong for the potential difference between zone 0 and zone 1. This is explained by the fact that these datum zones contained a relatively large number of stations in the original data configuration (see figure 7.3).

From equations (7.37) and (7.38) it can be derived that an increase in the number of measurements with a factor 1.5 leads to a decrease in variance with a factor 1.5. Applying this factor to the standard deviations as shown in the left-hand side of figure 7.13 (2 stations/zone), would yield for the standard deviations based on a data configuration with three stations/zone the following values: ΔW_0 15.3 cm, C_{10} 17.1 cm, C_{20} 16.7 cm, and C_{21} 15.9 cm. Comparing these values with those actually derived for this data configuration (see right-hand side of figure 7.13), shows a deviation of about 10%.

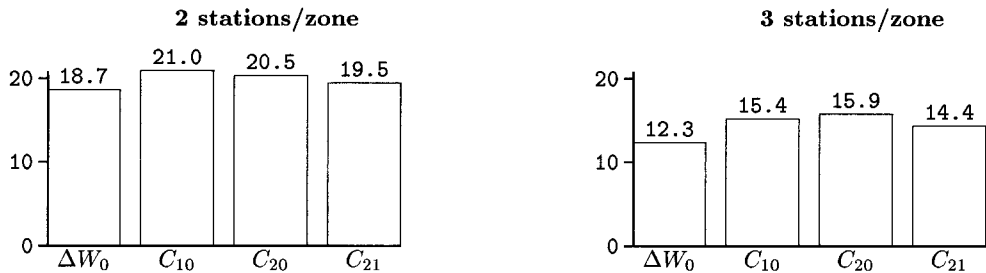


Fig. 7.13 Standard deviations of vertical datum connection parameters (in cm); JGM2 model, $\psi_c = 5^\circ$.

Figure 7.14 shows standard deviations for datum connection parameters, based on the GOCE potential coefficient model. Compared to the results as shown in figure 7.4 (original data configuration), standard deviations increase substantially if the number of stations in every datum zone is reduced. The larger the

number of stations in the original data configuration (see figure 7.3), the more pronounced the increase in standard deviation of the corresponding datum connection parameters.

If we decrease the variances derived for the data configuration with two stations/zone (see left-hand side of figure 7.14) by a factor 1.5, this would imply: ΔW_0 0.7 cm, C_{10} 1.1 cm, C_{20} 1.2 cm, and C_{21} 1.4 cm. Again, there is a strong resemblance with the values actually derived for the data configuration with three stations/zone (see right-hand side of figure 7.14). The deviation between the two sets of values is around 10%.

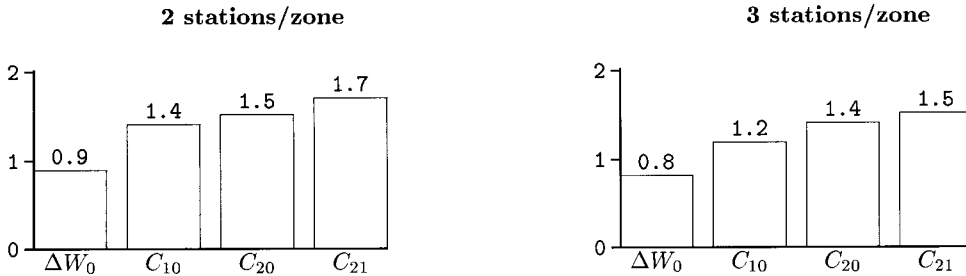


Fig. 7.14 Standard deviations of vertical datum connection parameters (in cm); GOCE model, $\psi_c = 2^\circ$.

In order to determine whether or not a certain amount of stations is sufficient to solve a specific datum connection problem, not only the precision of the derived datum connection parameters should be considered. The reliability of the measurements and the resulting reliability of the datum connection parameters should be taken into account as well.

Figure 7.15 shows values for the minimal detectable bias, $\overline{\Delta y_i}$, following from data snooping, for both data configurations. Comparison of the results based on the JGM2 model with those presented in figure 7.10 shows a substantial decrease in internal reliability for measurements in zones containing a relatively large number of stations in the full data configuration (measurements in zone 0 and 1). Minimal detectable bias for measurements in zone 2 increase by a much smaller amount.

Comparing the results for the GOCE model with those shown in figure 7.6 shows an increase in minimal detectable bias ranging between 0.5 and 2.4 cm for the data configuration with two stations/zone, and ranging between 0.2 and 1.2 cm for the data configuration with three stations/zone.

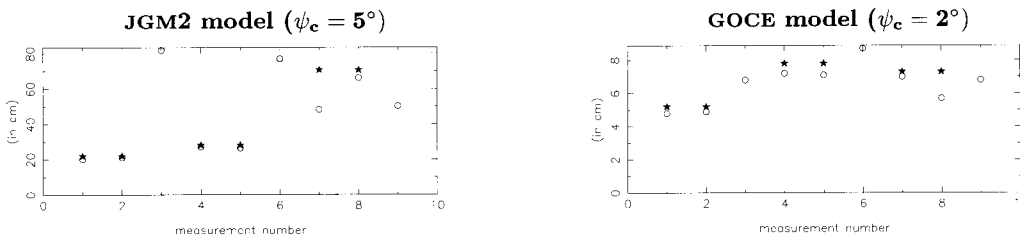


Fig. 7.15 Minimal detectable bias (in cm) resulting from data snooping; based on 2 stations/zone (*), or 3 stations/zone (o).

Figure 7.16 shows the external reliability based on the JGM2 potential coefficient model. Comparison with the results presented in figure 7.11 (based on the original data configuration; see figure 7.3), clearly shows that reducing the number of stations to only two or three stations/zone has an enormous impact on the reliability of the determined datum connection parameters. Furthermore it can be seen that:

- Errors in $\frac{\Delta W_0}{\gamma}$ ranging up to 16.7 cm (two stations/zone) or up to 37.6 cm (three stations/zone) cannot be detected by testing procedures. Note that the extremely large value for the data configuration with three stations/zone is caused by the large minimal detectable bias in measurement number three. This measurement has not been used in the data configuration with only two stations/zone.

- The maximum value for the external reliability of $\frac{C_{10}}{\gamma}$ was 11.9 cm for the original data configuration. For data configurations with resp. three or two stations/zone this maximum value is 36.8 cm and 37.4 cm.
- In the original data configuration the maximum value for the external reliability of $\frac{C_{20}}{\gamma}$ was found to be 27.7 cm. For the data configuration with two or three stations/zone this maximum value is 29.9 cm. Only a small deterioration in external reliability, since, in the original data configuration, zone 2 also contained only three stations.

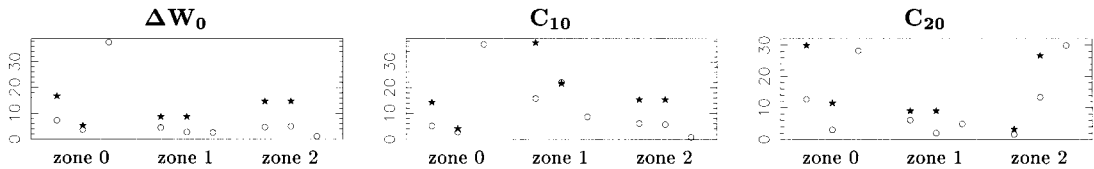


Fig. 7.16 External reliability for resp. ΔW_0 , C_{10} , C_{20} (in cm) due to a minimal detectable bias in one of the measurements; based on JGM2 model; $\psi_c = 5^\circ$; 2 stations/zone (*), or 3 stations/zone (o).

Figure 7.17 shows the external reliability for resp. $\frac{\Delta W_0}{\gamma}$, $\frac{C_{10}}{\gamma}$, and $\frac{C_{20}}{\gamma}$ due to a minimal detectable bias in one of the measurements, based on the GOCE potential coefficient model. Comparison with the results presented in figure 7.7 (based on the original data configuration), shows that the impact of reducing the number of stations to only two stations/zone on the reliability of the determined parameters is rather large. Depending on the number of stations in the original data configuration (see figure 7.3), maximum errors that cannot be detected by testing increase by a factor 1.3 (for $\frac{C_{20}}{\gamma}$), up to 4.3 (for $\frac{\Delta W_0}{\gamma}$). If the number of stations is reduced to three stations/zone, values for the external reliability of the derived parameters are significantly better than those based on only two stations/zone, but still much higher than those derived for the original data configuration.

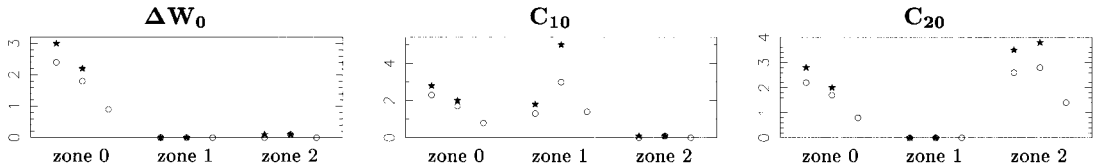


Fig. 7.17 External reliability for resp. ΔW_0 , C_{10} , C_{20} (in cm) due to a minimal detectable bias in one of the measurements; based on GOCE model; $\psi_c = 2^\circ$; 2 stations/zone (*), or 3 stations/zone (o).

It can be concluded that:

- If the GOCE model is used, reducing the number of stations to only three or two stations/zone still yields relative good results for the precision with which the datum connection parameters can be determined. However, the effect of reducing the number of measurements on the external reliability is much more pronounced.
- If the JGM2 model has to be used, reducing the number of measurements to only two or even three stations/zone leads to a substantial decrease in precision with which the datum connection parameters can be determined. The reliability of the measurements deteriorates even worse. Furthermore, a careful selection of stations is needed since some stations will yield measurements with relatively large minimal detectable bias, causing a relatively large value for the external reliability of the corresponding potential difference.

Stations have been selected in order to minimise errors in geometric and orthometric height. Since, if the JGM2 model is used, the commission error in the potential coefficients is the major limiting factor, stations should be selected that yield the smallest commission errors.

7.8 Conclusions and recommendations

In the preceding sections, error propagation has been performed for a number of data configurations. Only the effect of the quality of the measurements and the station configuration has been considered. The

effect of model errors, e.g., introduced by using a Stokes' approach for solving the geodetic boundary value problem, has been neglected. Based on the results presented in these sections, the following conclusions and recommendations can be made.

Comparison with UELN network Heights (in gpu) between fundamental stations as used in the datum connection scenarios have also been determined in European levelling networks. From figure 6 presented by Lang and Sacher (1996a), the standard deviation of the dynamic difference between Helsingborg and Amsterdam is estimated as around 15 mm, while the standard deviation between Newlyn and Amsterdam is of the order of 77 mm. Comparison with results derived in this chapter shows:

- In general, standard deviations derived for potential differences between datum zones based on the JGM2 coefficient model are much larger. Therefore, if only the JGM2 model is available, the proposed model of vertical datum connection does not improve on the precisions obtained by spirit levellings.
- However, the UELN-95 network consists of a single connection line between the continent of Europe and respectively Great Britain and Scandinavia. Therefore, errors in the derived height differences cannot be detected by testing.
- If around every station a relatively large spherical cap with high density, high quality terrestrial measurements is available, results derived using the JGM2 model are more comparable to those derived for UELN-95. Minimum required cap size to derive this precision is around 10 degrees.
- In general, using the GOCE potential coefficient model, standard deviations with which potential differences between datum zones can be derived are significantly better than those based on UELN-95, especially for the connection with Newlyn.

Concerning the influence of the different measurements The quality of datum connection parameters is determined by the quality of the geometric and orthometric height measurements, the quality of the surface gravity data, the quality of the satellite derived potential coefficients, and the degree and order up to which potential coefficients are available. For the precisions and data configurations under consideration it holds that:

- If the JGM2 is used, the quality of the datum connection parameters is limited by the quality of the potential coefficient model. Errors in the potential coefficients have the largest influence, followed by omission errors.
- If the GOCE model is used, largest errors in datum connection parameters result from uncertainties in orthometric heights.

Concerning the number of stations The accuracy of the derived potential difference between two datum zones highly depends on the number of stations available in these datum zones. The following remarks concerning the minimally required number of stations in every datum zone can be made:

- To detect (and remove) outliers in the measurements, at least two stations are needed in every datum zone.
- For the GOCE potential coefficient model, having only two stations in every datum zone yields relatively good results for the precision with which datum connection parameters can be determined.
- However, with only two stations in every datum zone, the reliability of the measurements is not very good. Therefore, at least three stations in every datum zone are needed.

Chapter 8

Sea-level variation patterns

8.1 Introduction

The main focus of this thesis is to determine how well patterns in sea-level variation can be detected, considering the fact that the required measurements are of limited quality. In chapter 4, sea-level variation curves in individual time series (relative to the local tide gauge bench mark) have been discussed. Of interest was, how well different curves could be distinguished and whether or not it was possible to determine the onset year of sea-level rise accelerations.

All time series used in chapter 6, contain long periodic fluctuations; either the same fluctuations for all tide gauges, or different time series contain different (but very similar) sets of long periodic fluctuations. For a group of six tide gauges, it has been examined how much the detectability of a common sea-level variation curve (relative to a local reference frame) is influenced by inconsistencies between the individual time series. These inconsistencies are introduced by inaccuracies in the height connections between the tide gauge bench marks and the national reference frame.

In this section, again (simulated) sea-level height data for a group of tide gauges will be used. Of interest is the influence of inconsistencies between the time series on the detectability of a spatial variation pattern in the North Sea area (relative to a regional height datum). These inconsistencies between the time series can be introduced by measuring noise of the tide gauge equipment and by inaccuracies in the height connections between the tide gauges.

Different strategies can be developed to examine the detectability of sea-level variation patterns. For example, analogous to preceding chapters, specific spatial patterns could be introduced into the time series. Next, it could be examined how well these patterns can be detected, given specific (height) measuring errors that are introduced into the time series. Furthermore, spatial patterns can be estimated for different attributes of the sea-level height series. This would result in a large number of scenarios that have to be examined in order to gain some insight into the influence of the height measurements on the detectability of spatial variation patterns. Therefore, a somewhat simpler approach will be used.

It will be assumed that no spatial variation pattern is present in the area. However, due to inconsistencies between time series (measuring noise, height connection errors, etc.), somewhat different trend values will be estimated for the various tide gauges. Using these trend values as input, spatial variation patterns in trend values can be determined. These erroneous patterns can be used as an indication of how much the estimation of actual patterns in the tide gauge data would be influenced by the inconsistencies between the time series.

In the following sections, erroneous spatial patterns introduced by different types of inconsistencies between the time series will be presented. Patterns shown in section 8.3 are based on time series that are equal except for normally distributed random errors added to the annual mean sea levels. Inconsistencies between the time series used in section 8.4, result from errors in the height connection between the tide gauge bench marks and the local reference frames. In section 8.5, inconsistencies between time series are introduced by linear movements of the vertical reference surfaces in relation to one another. Finally, in section 8.6, errors introduced by connecting the local reference frames will be added to the time series.

8.2 General structure of simulated data sets

All results shown in the following sections will be derived for a group of 18 tide gauges in the North Sea area; see chapter 3 for a description of these data sets. In reality, for some of these tide gauges data is only

available between 1898 and 1965. However, for most experiments it will be assumed that observations are available for the period 1865 up to 1996. The reason behind this decision is that we are interested in erroneous patterns introduced by the limited accuracy of measurements. By using time series with only 70 years of data, results will be too much influenced by the long periodic fluctuations in the data sets; see chapter 2.

Simulated time series are assumed to be constructed from (a number of) the following components: a sea-level variation curve, measuring noise, periodic fluctuations, local height connection noise, vertical movements of the local reference frames relative to one another, and vertical datum connection noise. As a result, using different scenarios to model these components, a huge number of data sets could be built. Based on experiences from preceding chapters, the following selections will be made.

Sea-level variation curves In principle, spatial variation of all kind of curves could be examined. For example, by applying SSA (with an appropriate window size) to the time series, it can be achieved that the first singular vector contains the common variation curve, and all other singular vectors contain only periodic fluctuations and noise (i.e., no remaining trend). Next, a spatial pattern can be derived for the elements of the V matrix relating the first singular vector to the various tide gauges.

Of interest is what kind of spatial patterns result from inconsistencies (e.g., introduced by height connections) between the time series. The actual pattern in the data set is of less importance. Therefore, it will be assumed that no spatial variation pattern is present in the area. For all time series a simple linear regression line, with the same slope value applying to all time series is used to model the sea-level variation curve. Analogous to preceding chapters, a trend of 1.5 mm/yr will be used.

Measuring noise With measuring noise, all errors are meant that lead to inconsistencies in the annual mean values. This can either be measurement errors introduced by the tide gauge equipment, or inaccuracies in height connections which yields errors in the annual mean sea-level values. It is assumed that these errors can be described by normally distributed random values with zero mean, i.e., no systematic errors are present. The same standard deviation is used throughout the time span under consideration, and for all time series.

Periodic fluctuations In chapter 6, experiments have been performed with a data set in which either all time series contained the same periodic fluctuations, or periodic fluctuations were based on actual tide gauge data for six stations along the Dutch coast. It was concluded that, since periodic fluctuations for these tide gauges are similar, results based on data set with different periodic fluctuations are not really different from those derived for the data set based on equal periodic fluctuations for all time series.

For a reliable detection of a trend in a time series containing long periodic fluctuations, of the order of 90 years of data is required (see chapter 4). However, for a large number of tide gauges in the North Sea area, such long time series are not available. Consequently, in order to simulate periodic fluctuations based on actual data for 18 tide gauges, full time series have to be reconstructed from only a limited number of observations. This will introduce unnecessary additional inconsistencies between the time series.

In chapter 3, it was found that there is a large similarity between the 18 stations in the North Sea area for which data is available between 1898 and 1965. Besides, for every individual time series, first a trend value will be estimated. Subsequently, these trend values are used as input for estimating the spatial patterns. As a result, variations in periodic fluctuations between the different time series are of much less importance than for estimating a common variation curve for a group of tide gauges. Therefore, all simulated time series used in this chapter will be based on the same set of periodic fluctuations, i.e., detrended data for tide gauge Den Helder (see figure 6.1).

Local height connection In chapter 6, it has been discussed that it is (almost) impossible to reconstruct the actual height-connection history for a group of tide gauges. To investigate the influence of inaccuracies in height measurements, a large number of local height connection scenarios have been introduced. In this chapter, only the following height connection scenarios will be used:

- Height connections have been performed every 10 years, with the same standard deviation applying to all connections and for all tide gauges.
- Height connections have been performed analogous to history of first-order levellings in the Netherlands, i.e., height connections in 1885, 1940, 1960, 1980, and 1996. Different standard deviations

apply to connections performed at different moments in time, but the same values applies to all tide gauges.

- Analogous to chapter 7, the North Sea area is divided into three regions (Western-Europe, Scandinavia, Great Britain). For each region, a separate set of standard deviations applies to the height connections.

It is assumed that inaccuracies in height measurements lead to fictitious height differences that can be represented by normally distributed random noise. In addition, tide gauges are assumed to follow secular movements, while determined height differences are distributed over the elapsed period between subsequent height connections; see section 6.2.4 for more details.

Vertical datum connection Prior to the space geodetic measuring techniques, height measurements were made relative to a local reference frame. The further back in time, the larger the number of different local reference systems that were in use. For reasons of simplicity, it is assumed that throughout the time span of the sea-level measurements, the same local height datums have been used as reference surfaces. Analogous to chapter 7, in the North Sea region, three height datum zones will be assumed: Western-Europe, Scandinavia, and Great Britain.

It is difficult to reconstruct the actual history of vertical datum connections in western Europe. A number of European levelling networks exist, e.g., UELN-55, UELN-73, and UELN-95, but it is difficult to determine when actual height connections have been performed. For example, the ending -73 only implies that in 1973 the first meeting of the sub-commission for a new UELN took place.

In addition, results for more than one adjustment of the same levelling network co-exist, in which different amounts of levelling data have been included. Consequently, different precisions have been derived. As an example, for the 1979 adjustment of UELN-73 (Kok *et al.*, 1980), the figure with isolines of precision gives a precision of approximately 30 mm for the north-eastern corner of Great Britain. For this same area, the 1986 adjustment of UELN-73 (Ehrensperger and Kok, 1986) predicts a precision of approximately 60 mm. Unfortunately, no explanation is given for this large decrease in precision.

Since the actual history of vertical datum connections is difficult to obtain, a number of connection scenarios will be examined. Two possibilities are assumed concerning the height differences between the three datum zones. The first option is that the offsets are constant in time, the second that the height datums experience linear movements relative to one another, e.g., as a result of post-glacial rebound. Two different models will be used to estimate vertical movements of the fundamental stations in the datum zones, resulting from post-glacial rebound. The first is presented by Emery and Aubrey (1991), and is based on least-squares regression analysis of data for 134 tide gauges. The second model is based on a visco-elastic Earth model (with 1066B elastic structure) as developed by Peltier (1990). From these two models, the following velocities for the height datums are estimated:

- Western-Europe, zero-point NAP (Amsterdam): -1 mm/yr (based on Emery and Aubrey (1991)) or -0.4 mm/yr (based on Peltier (1990))
- Scandinavia, zero-point Helsingborg in Sweden: +1 mm/yr (based on Emery and Aubrey (1991)) or +2 mm/yr (based on Peltier (1990))
- Great Britain, zero-point Newlyn: 0 mm/yr (based on Emery and Aubrey (1991)) or +0.2 mm/yr (based on Peltier (1990))

These possible height differences between the origins of the vertical datums, lead to the following datum connection scenarios:

1. Constant offsets are present; datum connection has been performed at most once.
Constant offsets do not influence the trend estimates, therefore, no additional error is introduced into the time series.
2. Constant offsets are present; datum connection has been performed at least twice.
Inaccuracies in the datum connections yield fictitious velocities between the datum points. This, in turn, results in inconsistencies between the time series belonging to different datums.
3. Height datums experience linear movements; datum connection has been performed at most once.
Height changes introduce inconsistencies between the time series belonging to different height zones.
4. Height datums experience linear movements; datum connection has been performed at least twice.
Inaccuracies in the datum connections yield fictitious velocities between the datums. This, in turn, results in inconsistencies between the time series belonging to different height zones.

8.3 Inconsistencies in annual mean values

As a first simple scenario, it is assumed that all 18 time series are equal, except for inconsistencies between the time series that can be described by normally distributed random values (with zero mean and a specific standard deviation) added to the annual mean sea levels. Although not a very realistic assumption, especially for historical data, this type of inconsistencies might occur if height connections between tide gauge bench marks have been performed at least once a year with space geodetic measurements.

Inconsistencies in annual mean values can also originate from measuring errors of the tide gauge equipment itself. Due to the inconsistencies added to the data sets, for every sea-level height series a trend value will be estimated that deviates somewhat from the actual value of 1.5 mm/yr. If spatial variation patterns are determined based on the trend values estimated for the individual tide gauges, erroneous patterns will result. These patterns can be interpreted as the influence of all random errors in annual mean sea levels on the estimation of a variation pattern for the North Sea region.

In chapter 3 it has been explained that, for this data set with 18 specific tide gauges, it seems only feasible to estimate spatial variation patterns with up to six parameters (a quadratic pattern). It was found that higher order models lead to unrealistic results, especially at the edges of the area considered. Therefore, only the following four spatial models have been applied: linear model, bi-linear model, quadratic model, and quadratic model without cross-term (xy). In chapter 3 it was found that the bi-linear model gives the best fit when applied to actual tide gauge data.

Analogous to chapter 3, trend values are determined for the 18 simulated sea-level height series and the four above mentioned spatial variation patterns of this trend value are estimated. Examples of resulting (erroneous) patterns are not shown since they are completely determined by the specific realisation of the measuring noise. A different realisation of noise will give a completely different pattern. Of interest is not one actual erroneous variation pattern, but insight in the range of deviations that can be expected as a result of the random differences between the data sets.

In order to show the range of errors that can result from the inconsistencies between the individual time series, the following method is used. One specific realisation of measuring errors is added to the data sets and trend values are estimated for the individual time series. Based on these trend values for the individual tide gauges, four different spatial variation patterns are estimated providing a relation between estimated trend value and longitude and latitude in the area enclosed by the tide gauges. This procedure is repeated for different realisations of measuring noise. This results in 100 (slightly) different realisations of the spatial variation patterns. Next, the area under consideration is divided into 100×100 cells. For every cell, the standard deviation of the trend values estimated for this cell based on the 100 realisations of measuring noise is determined. Twice these standard deviations (as determined for every individual cell) are used as an indication of the range of errors that can result from the inconsistencies between the time series.

Figure 8.1 shows ranges of errors (as a function of latitude and longitude) that can be expected if spatial patterns are estimated through trend values derived for 18 tide gauges in the North Sea area. The individual time series contain normally distributed random errors with zero mean and a standard deviation of 1 cm. From this figure it can be concluded that ranges of errors in trend estimates, resulting from the random differences between the time series, are within 0.1 mm/yr.

Figure 8.1 shows that the more complex the variation patterns, the larger the deviations in estimated trend values that might result from random differences between the time series. For all four variation patterns it holds that deviating values are larger near the boundaries of the area under consideration.

All results shown in figure 8.1 have been derived based on a standard deviation of 1 cm for the normally distributed random errors, added to the individual time series prior to regression. As can be seen from figure 8.2, resulting erroneous spatial variation pattern in trend estimates is (more or less) proportional to the standard deviation of the random errors.

All patterns estimated in the preceding have been based on time series containing 132 years of data. However, as has been discussed in chapter 3, in reality, for the 18 tide gauges under consideration, data is only available for the period 1898 up to 1965. If time series are shortened to contain only data for this period, a major increase in the range of erroneous trend values as a function of latitude and longitude is the result. This is demonstrated in figure 8.3 for two examples of spatial patterns. Compared to results shown in figure 8.1 (based on 132 years of data), ranges increase by approximately a factor three.

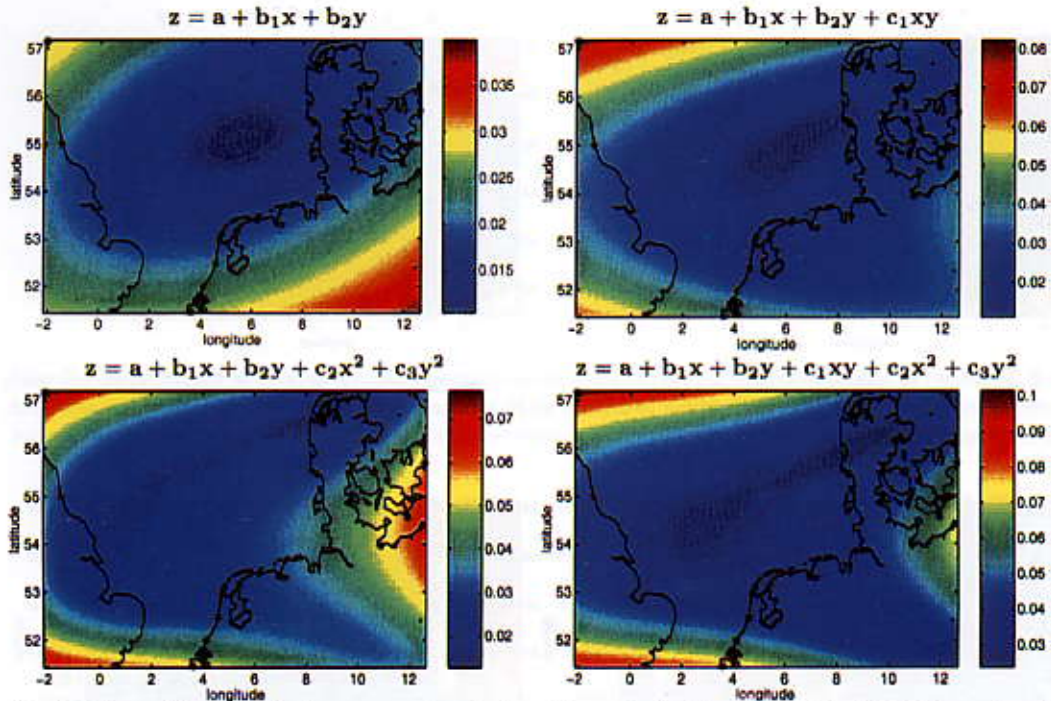


Fig. 8.1 Range (2σ value) of erroneous trend values (in mm/yr) estimated for the North Sea region based on 100 realisations of noise. Noise consists of normally distributed random values (σ : 1 cm) added to annual mean sea levels. Different spatial patterns estimated through trend values.

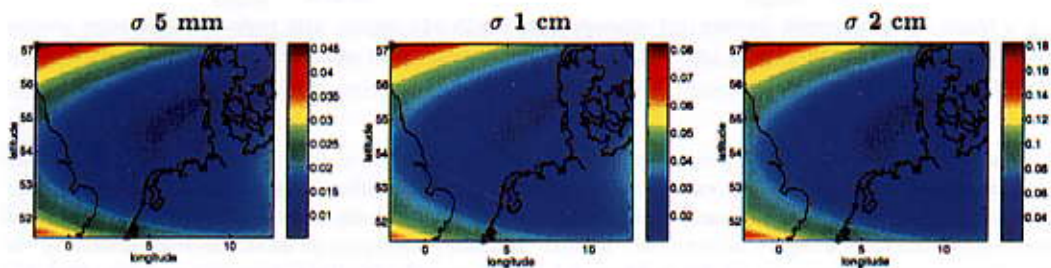


Fig. 8.2 Range (2σ value) of erroneous trend values (in mm/yr) for 100 realisations of noise. Noise: normally distributed random values added to annual mean sea levels. Estimated spatial pattern: bi-linear.

Not only the range of deviating trend values that might be expected increases if the length of the time series is reduced, the mean values of the trends are influenced as well. As indicated in chapter 4, for a reliable estimate of a trend value in a time series containing long periodic fluctuations, of the order of 100 years of data is required. Time series used to produce figure 8.3 contain only 68 years of observations. As a result, trends estimated for the individual time series might have been significantly affected.

In figure 8.4, mean values of trend estimates (based on a linear spatial pattern) are shown for 100 realisations of measuring noise. Both figures are based on 68 years of observations, but a different time window is used. This implies that a different part of the periodic fluctuation series has been used to simulate the time series. This figure clearly shows that both data sets result in deviating trend estimates. The actual trend value that should have been found is 1.5 mm/yr.

Due to the limited availability of tide gauges providing long time series of good quality (no long data gaps), in chapter 3 it has been decided to use only up to 18 tide gauges in the North Sea area. Results as shown in the preceding have been based on simulated data for these 18 tide gauge locations. To give some insight in the kind of results that could be derived if more stations with long records would be available, figure 8.5 shows results based on a larger area of the North Sea and using simulated data for

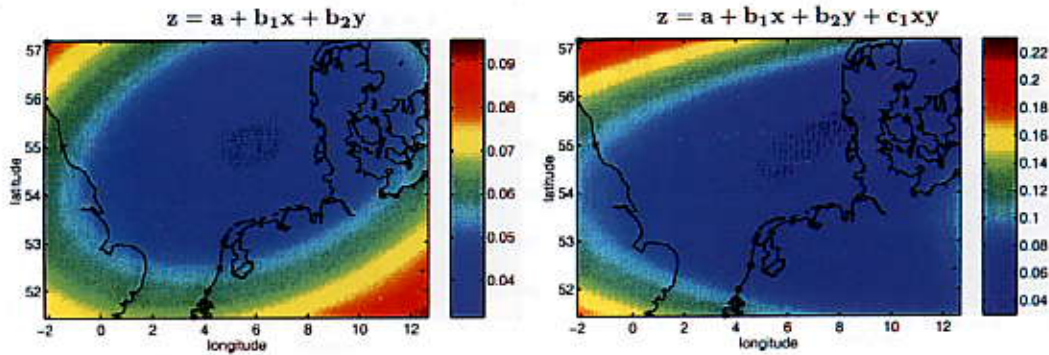


Fig. 8.3 Range (2σ value) of erroneous trend values (in mm/yr) for 100 realisations of noise. Noise: normally distributed random values (σ : 1 cm) added to annual mean sea levels. Based on data between 1898 and 1965. Estimated spatial pattern: linear.

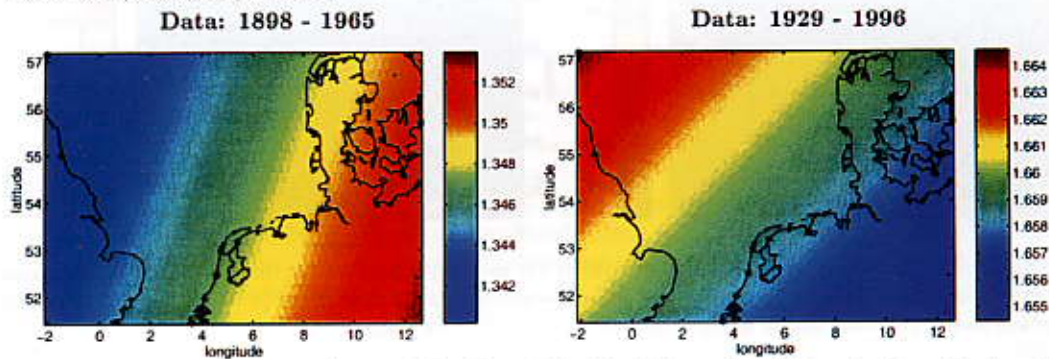


Fig. 8.4 Mean value of trends (in mm/yr) estimated for North Sea region; 100 realisations of noise. Noise: normally distributed random values (σ : 1 cm) added to annual mean sea levels. Only 68 years of data. Estimated spatial pattern: linear.

more locations. Analogous to the preceding, results shown are ranges of errors (as a function of latitude and longitude) in trend values that can be expected from inconsistencies between the time series.

The results shown in the left-hand side of figure 8.5, are based on a total of 113 stations, i.e., all stations in the North Sea region between 51° and 62° latitude, providing at least one year of data to the PSM SL. Compared to the results shown in figure 8.1 (based on only 18 tide gauges in a smaller area), the level of errors decreases significantly.

The results shown in the right-hand side of figure 8.5, are based on the 49 stations in the North Sea region for which the PSM SL data base contains at least 50 years of data (without any regard to data gaps and periods for which data is available). The range of erroneous trend values is equal to the range derived based on only 18 tide gauges; see figure 8.1. However, values given in figure 8.1 apply to a smaller area. Consequently, extrapolating the derived spatial variation pattern to the area covered in figure 8.5, would lead to larger errors in the region north of latitude 57° .

8.4 Inconsistencies introduced by local height connections

In this section, it is assumed that all 18 tide gauges contain a trend of 1.5 mm/yr plus periodic fluctuations based on tide gauge Den Helder; 132 years of data are available. Inconsistencies between the time series result from height connections between tide gauge bench marks and the local reference frames. It is assumed that no additional errors are introduced by connecting the vertical datums. For example, because constant offset exists between the different reference surfaces and no datum connection measurements have been performed.

First, a scenario will be used in which all tide gauge bench marks have been connected to the local reference frame at regular intervals of 10 years. It is assumed that for all tide gauges, connections have

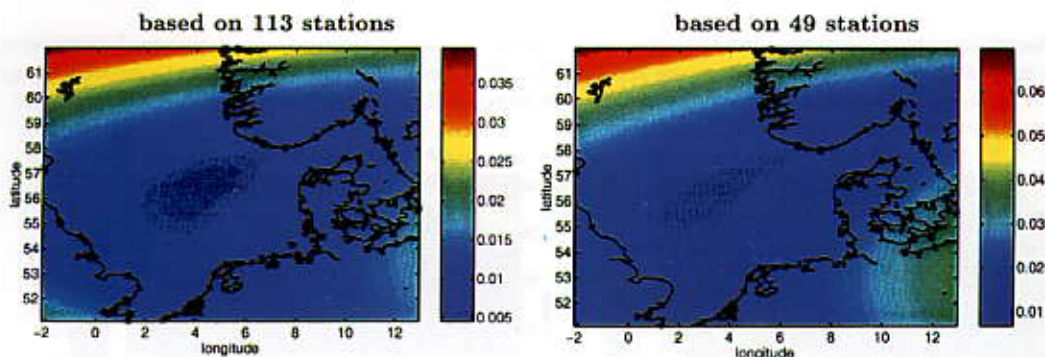


Fig. 8.5 Range (2σ value) of erroneous trend values (in mm/yr) estimated for (different parts of) the North Sea region based on 100 realisations of noise. Noise: normally distributed random values (σ : 1 cm) added to annual mean sea levels. Estimated spatial pattern: bi-linear.

been performed at the same epoch and with the same measuring precision. Inaccuracies resulting from height connections are described by normally distributed random values with zero mean and a specific standard deviation.

Analogous to the preceding section, figure 8.6 shows the range (twice the standard deviation) of deviating trend patterns that can result from the inaccuracies in the height connections. Compared to results based on random noise added to the annual mean sea levels (figure 8.1), values increase significantly, approximately by a factor three ($\sqrt{10}$ years). The pattern in the standard deviations of the trend values as a function of latitude and longitude does not really change.

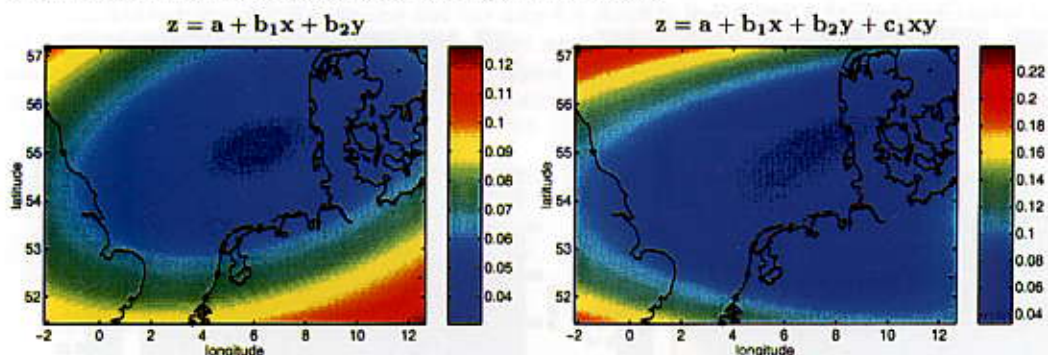


Fig. 8.6 Range (2σ value) of erroneous trend values (in mm/yr) for 100 realisations of height connection noise (σ : 1 cm). Height connections every 10 years. Estimated spatial pattern: linear or bi-linear.

Next, it is assumed that local height connections have been performed with varying time spans between the measurements. For all tide gauges, height connections are assumed at the same epochs, with the same set of standard deviations. This is not a very realistic assumption, but results can be interpreted as the best possible results obtainable with this kind of data. If, for different tide gauges, connections have been performed with different accuracies and at different epochs, inconsistencies between time series will be larger and, consequently, range of erroneous pattern will increase.

Analogous to chapter 6, height connections are assumed at time intervals corresponding to the Dutch history of first order levellings. One of the following sets of standard deviations will be used to represent the height connection errors:

- set 1 Height connection in 1885: $\sigma = 3$ cm, 1940: $\sigma = 2$ cm, 1960: $\sigma = 2$ cm, 1980: $\sigma = 1.5$ cm, 1996: $\sigma = 1.5$ cm. *Pessimistic.*
- set 2 Height connection in 1885: $\sigma = 2$ cm, 1940: $\sigma = 1.5$ cm, 1960: $\sigma = 1.5$ cm, 1980: $\sigma = 1$ cm, 1996: $\sigma = 1$ cm.
- set 3 Height connection in 1885: $\sigma = 1.5$ cm, 1940: $\sigma = 1$ cm, 1960: $\sigma = 1$ cm, 1980: $\sigma = 0.8$ cm, 1996: $\sigma = 0.8$ cm. *Optimistic.*

Resulting ranges (2 times standard deviation) based on the *pessimistic* set of standard deviations used to simulate height connection errors, are shown in figure 8.7. Compared to results based on regular height connections every 10 years (figure 8.6) ranges increase significantly; approximately by a factor 5.

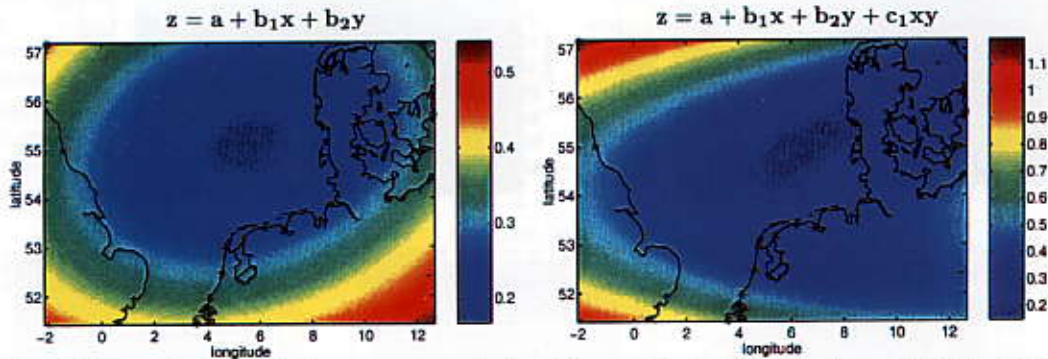


Fig. 8.7 Range (2σ value) of erroneous trend values (in mm/yr) for 100 realisations of height connection noise. Height connections in 1885 (σ : 3 cm), 1940 (σ : 2 cm), 1960 (σ : 2 cm), 1980 (σ : 1.5 cm), 1996 (σ : 1.5 cm). Estimated spatial pattern: linear or bi-linear.

If the *optimistic* set of standard deviations is assumed for the height connections, the range of erroneous trend values decreases by (approximately) a factor two as compared to the trend patterns based on the *pessimistic* set of standard deviations. This can easily be explained by the fact that standard deviations corresponding to the *pessimistic* scenario are roughly twice as large as those corresponding to the *optimistic* scenario. Comparison of figure 8.8 with the two preceding figures shows that, although the ranges of trend estimates may vary, the pattern in erroneous trends is (more or less) the same for all three height connection scenarios, i.e., regular height connection every 10 years, height connections following the history of Dutch first order levellings with a *pessimistic* or *optimistic* precision respectively.

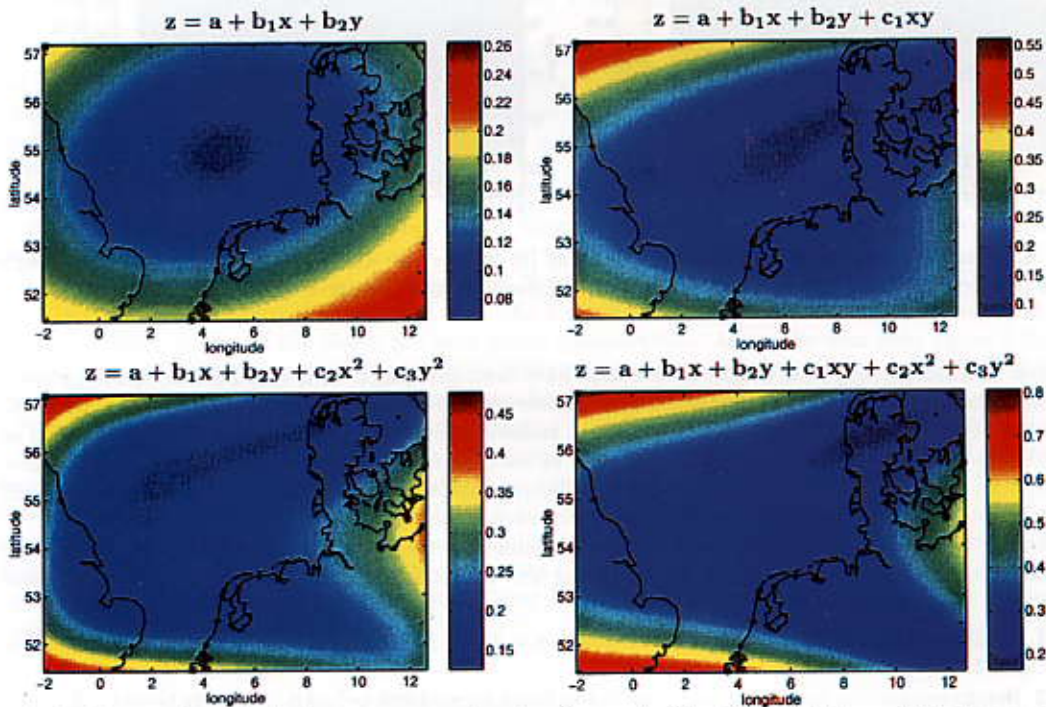


Fig. 8.8 Range (2σ value) of erroneous trend values (in mm/yr) for 100 realisations of height connection noise. Height connections in 1885 (σ : 1.5 cm), 1940 (σ : 1 cm), 1960 (σ : 1 cm), 1980 (σ : 0.8 cm), 1996 (σ : 0.8 cm). Different spatial patterns estimated through trend values.

All plots as presented up to now have been based on the same measuring precision for all height connections. It has been found that, with a change in this precision, the range of the erroneous trend patterns will vary, but the patterns themselves stay (more or less) the same. If, for different height datum zones, different precisions are assumed for the height connections, the resulting erroneous patterns change. Since precisions corresponding to the actual history of height connections in the region are difficult to obtain, two simple examples using an arbitrary selection of (sets of) standard deviations will be shown.

Erroneous patterns as shown in figure 8.9 are due to inconsistencies between time series resulting from height connection errors. For all tide gauges in Western-Europe (i.e., 15 tide gauges), the *optimistic* set of standard deviations are used to represent the height connection errors. Height connections in Scandinavia (1 tide gauge) are represented by the second set of precisions. Finally, for the two tide gauges in Great Britain the *pessimistic* set of standard deviations is used.

Comparison of figure 8.9 with figure 8.8 (all height connection errors based on the *optimistic* set of precisions) shows a general increase in the range of the erroneous trend values. In addition, patterns in erroneous trend values change. This is especially clear from comparing both lower-left graphs.

Next, for the height connection in Scandinavia the *pessimistic* set of height connection precisions is used, while height connection errors for the (two) tide gauges in Great Britain are based on the second set of precisions. Resulting erroneous patterns are shown in figure 8.10. Compared to figure 8.8 (all height connection errors based on the *optimistic* set of precisions), there is only a slight increase in the range of the erroneous trend values. However, a change in the pattern of the erroneous trend values is clearly visible from comparing the two upper-right graphs.

8.5 Height datums experience linear movements

In the preceding sections, it has been assumed that only constant offsets are present between the different height datums to which the tide gauge bench marks refer. However, as a result of post-glacial rebound (see, e.g., Peltier (1994)) zero-points of local height systems can experience vertical movements relative to one another. These vertical movements can (nowadays) be described by a linear trend with a slope value that is constant throughout the time of the sea-level measurements.

If tide gauges are connected in height to the local height datums, vertical movements of the zero-points of these datums are added to the sea-level data sets. As a result, inconsistencies are introduced between sea-level height series that are related to different height datums. Consequently, an erroneous sea-level variation pattern will be found, even if local height connections could be performed without introducing additional errors. The range and pattern in erroneous trend values depends on the vertical movements of the height datums relative to one another.

As explained in section 8.2, linear movements of the (assumed) zero-points of the three height regions as used in this chapter are based on two different post-glacial rebound models. The first model (based on Emery and Aubrey (1991)) gives a linear movement of -1 mm/yr for Amsterdam (zero-point of Western-Europe), an uplift of +1 mm/yr for Helsingborg (in Sweden, zero-point for Scandinavia), and no vertical movement for Newlyn (zero-point of Great Britain). Figure 8.11 shows the spatial patterns in trend values that result from these movements of the height datums relative to one another.

Erroneous patterns in figure 8.11 result from vertical movements (due to post-glacial rebound) of the zero-points of the three height datums only. No additional inconsistencies between the time series resulting from errors in the height connections to the local datums are added. Figure 8.11 clearly shows that spatial patterns estimated through the slope values derived for the various tide gauges show a large range in trend values.

Next, vertical movements of the height datums are based on the post-glacial rebound model given by Peltier (1990). This implies: Western-Europe (15 stations) -0.4 mm/yr, Scandinavia (1 tide gauges) +2 mm/yr, and Great Britain (2 tide gauges) +0.2 mm/yr. Resulting estimated patterns in trend values are shown in figure 8.12. The patterns in trend values are similar to those shown in figure 8.11. However, the range of trend values differs significantly. This is not surprisingly, since, if vertical movements are based on the model by Peltier (1990), the majority of the tide gauges (15, in Western-Europe) experience a much smaller subsidence compared to movements based on the model by Emery and Aubrey (1991).

In the above it has been shown that significant deviations in trend estimates between different time series can be introduced by vertical movements of the local height datums. One possibility to solve this problem is vertical datum connection, which will be discussed in the following section. As an alternative,

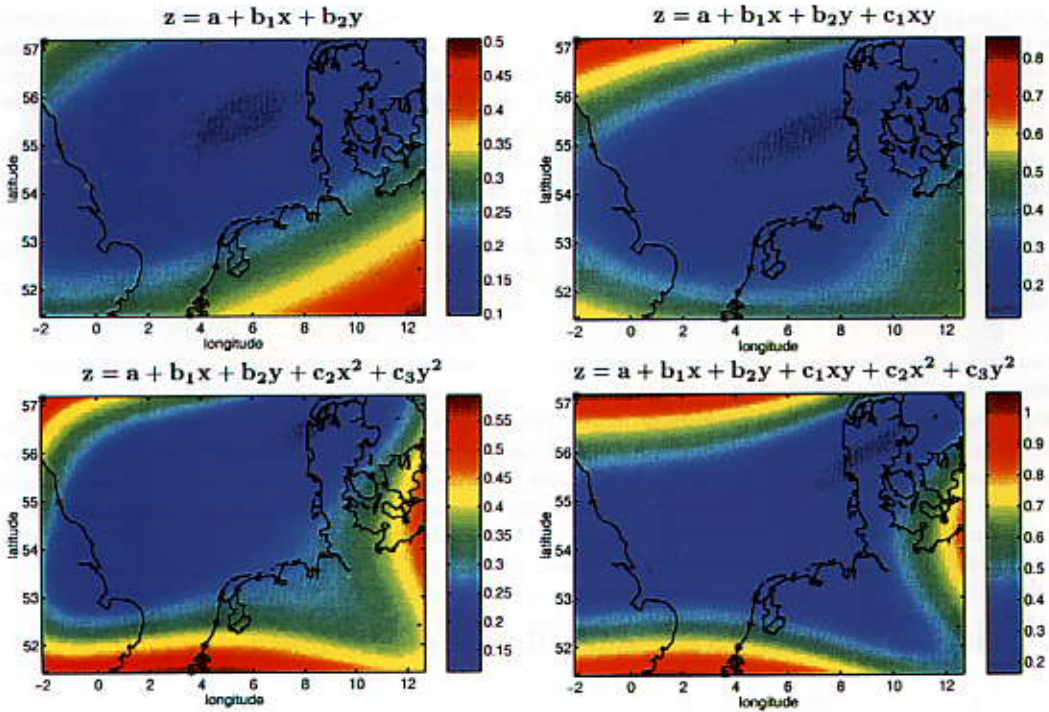


Fig. 8.9 Range (2σ value) of erroneous trend values (in mm/yr) for 100 realisations of height connection noise. Connections in Western-Europe (15 tide gauges) based on st. dev. from set 3, 1 connection in Scandinavia based on st. dev. from set 2, connections in Great Britain (2 tide gauges) based on st. dev. from set 1.

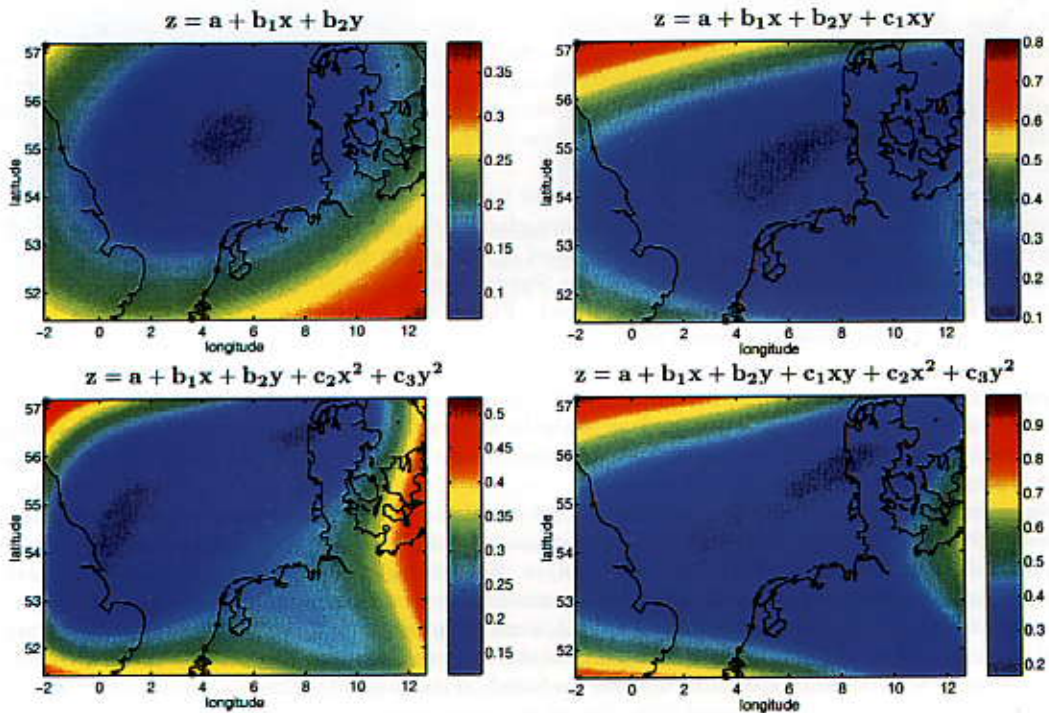


Fig. 8.10 Range (2σ value) of erroneous trend values (in mm/yr) for 100 realisations of height connection noise. Connections in Western-Europe (15 tide gauges) based on st. dev. from set 3, 1 connection in Scandinavia based on st. dev. from set 1, connections in Great Britain (2 tide gauges) based on st. dev. from set 2.

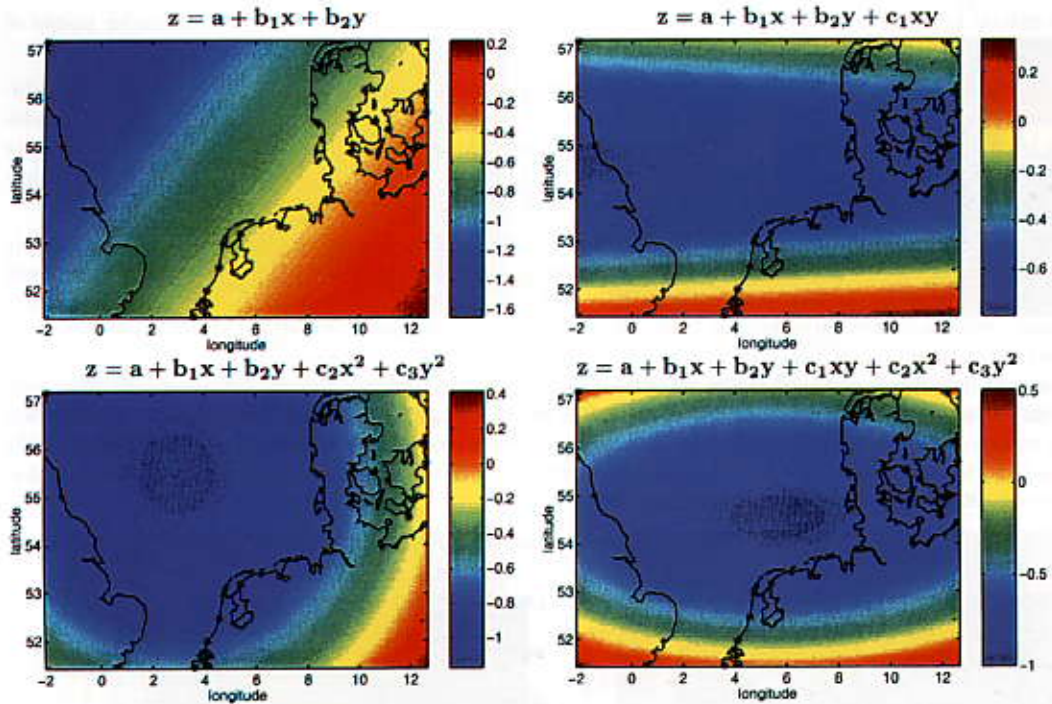


Fig. 8.11 Erroneous pattern (in mm/yr) introduced by vertical movements of local height datums. Western-Europe: -1 mm/yr, Scandinavia: $+1$ mm/yr, Great Britain: 0 mm/yr; based on post-glacial rebound model by Emery and Aubrey (1991).

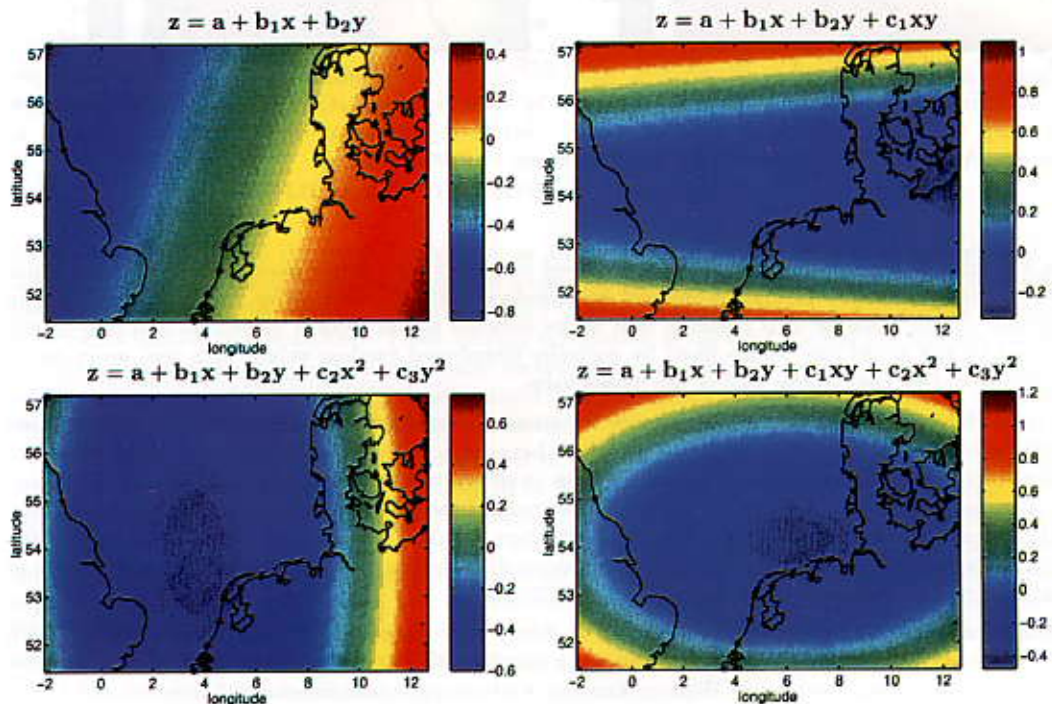


Fig. 8.12 Erroneous pattern (in mm/yr) introduced by vertical movements of local height datums. Western-Europe: -0.4 mm/yr, Scandinavia: $+2$ mm/yr, Great Britain: $+0.2$ mm/yr; based on post-glacial rebound model by Peltier (1990).

post-glacial rebound models can be used to estimate the vertical movements of the zero-order points of the different height datums.

Over the years, a number of different post-glacial rebound models have been developed, based on different principles and yielding different estimates for the resulting (present-day) velocities. Two examples have been used in this chapter, one based on tide gauge measurements (the model by Emery and Aubrey (1991)) and one based on a specific visco-elastic Earth model (by Peltier (1990)). There are significant differences between estimated vertical movements based on these two models.

Since the actual vertical movements are unknown, a specific post-glacial rebound model has simply to be chosen. Deviations between displacements estimated by the model and actual displacements will introduce erroneous slope values into the sea-level height data sets. A simple example, it is assumed that vertical movements are corrected for by using the post-glacial rebound model of Peltier (1990), while in reality tide gauges experience vertical movements following the model of Emery and Aubrey (1991). This introduces deviations in trend values between tide gauges situated in different datum zones. Resulting spatial patterns estimated through these (deviations in) trend values are shown in figure 8.13. Comparison with results shown in figures 8.11 and 8.12 shows that errors introduced by correcting vertical movements using the “wrong” model are less than errors which occur if vertical movements are not corrected for. However, deviating trend values can be significant.

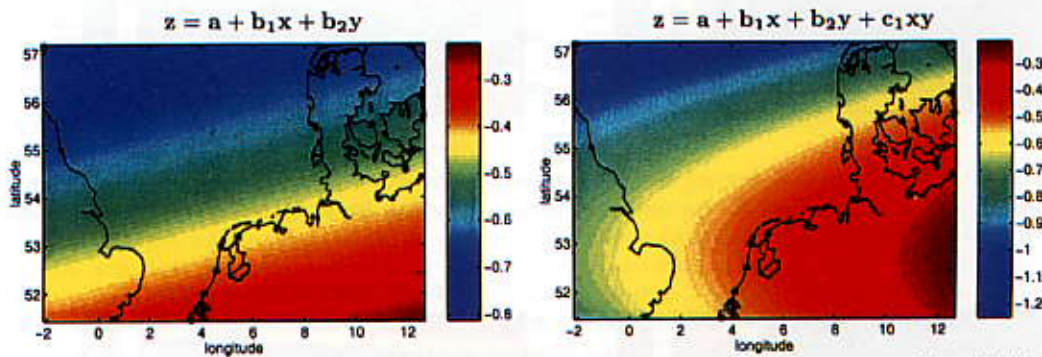


Fig. 8.13 Erroneous pattern (in mm/yr) introduced by correcting vertical movements of local height datums using the wrong post-glacial rebound model. Actual vertical movements are based on model by Emery and Aubrey (1991), corrections are based on model by Peltier (1990).

Even if a suitable post-glacial rebound model is used to correct for vertical movements of the zero-order points of the local height datums, errors will be introduced into the time series due to uncertainties in the model. As an example, it is assumed that errors between actual vertical movement and movements predicted by the model can be described by normally distributed random values with zero mean and a standard deviation that equals 10% of the model value.

Figures 8.14 and 8.15 show the range (twice the standard deviation) of deviating trend patterns based on 100 realisations of “model noise”, i.e. deviations between actual vertical movements and movements predicted by a post-glacial rebound model. Results as shown in figure 8.14 are based on “model noise” with standard deviations 10% of the vertical movements based on the model by Emery and Aubrey (1991), i.e. standard deviations of 0.1 mm/yr (Western-Europe), 0.1 mm/yr (Scandinavia), and 0.0 mm/yr (Great-Britain). Figure 8.14 shows that, depending on the type of pattern estimated, range of deviating trend estimates is of the order of 0.2 to 0.35 mm/yr.

Ranges of erroneous trend values as shown in figure 8.15 are estimated using “model noise” with standard deviations 10% of the vertical movements based on the model by Peltier (1990). This implies the following standard deviations: Western-Europe: 0.04 mm/yr, Scandinavia: 0.2 mm/yr, and Great Britain: 0.02 mm/yr. Comparison between figures 8.15 and 8.14 shows that not only the range of trend estimates is different, but pattern is erroneous trend values is completely different as well. This can easily be explained by the fact that results shown in figure 8.14 are based on a standard deviation of 0 mm/yr for the two tide gauges in Great Britain.

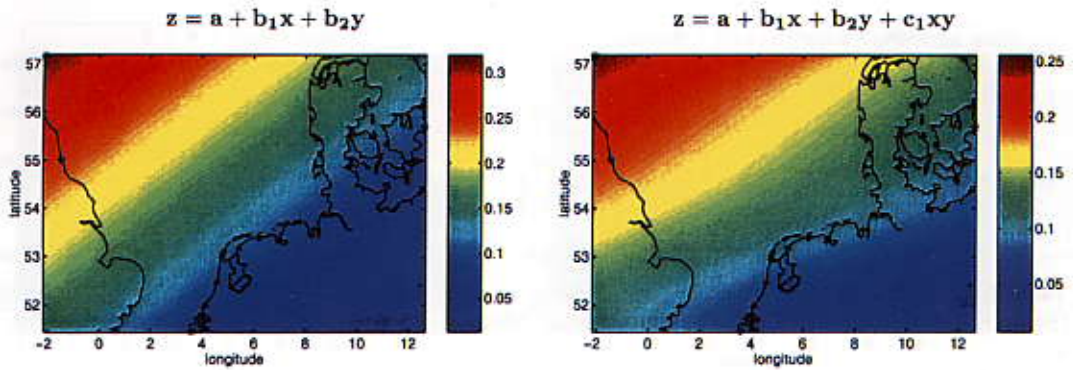


Fig. 8.14 Range (2σ value) of erroneous trend values (in mm/yr) for 100 realisations of errors in post-glacial rebound models. Standard deviations are 10% of the value predicted by the model; based on post-glacial rebound model by Emery and Aubrey (1991).

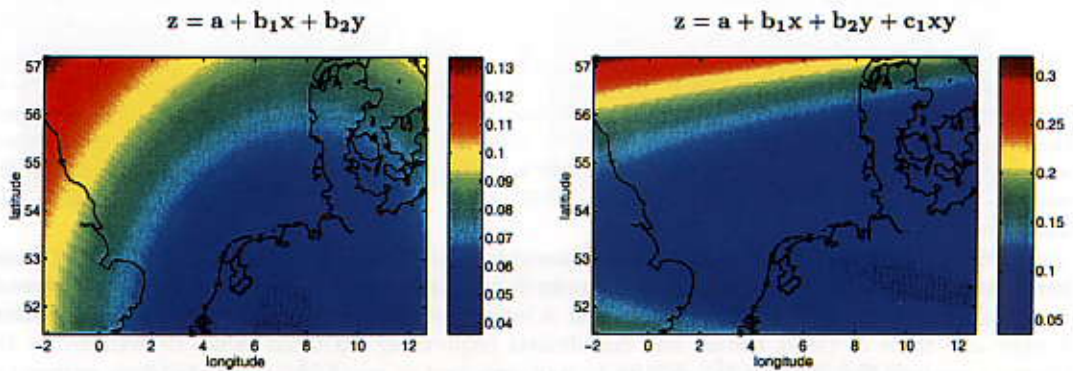


Fig. 8.15 Range (2σ value) of erroneous trend values (in mm/yr) for 100 realisations of errors in post-glacial rebound models. Standard deviations are 10% of the value predicted by the model; based on post-glacial rebound model by Peltier (1990).

8.6 Vertical datum connection

As has been described in the preceding section, as a result of (among others) post-glacial rebound, fundamental stations in the different height datum zones can experience uplift or subsidence. Consequently, the different local height systems, originating from these fundamental stations, can experience vertical movements relative to one another. These vertical movements of the fundamental stations are transferred into the heights of the tide gauge bench marks connected to the reference systems. As a result, inconsistencies are introduced between tide gauges situated in different datum zones. By connecting the different vertical datums, these inconsistencies can be removed.

As has been indicated in section 8.2, a number of (adjustments of) UELN exist, in which Scandinavia and Great Britain have been connected in height to Western-Europe by means of spirit levelling. For the various realisations of the European levelling networks, the precision of the height connections between the zero-order point in Western-Europe (NAP) and fundamental stations in Scandinavia (Helsingborg) and Great Britain (Newlyn) can be estimated from maps showing isolines of standard deviations of adjusted geopotential numbers. The first European levelling network (UELN-55) only presents results for Western-Europe. For (different realisations of) UELN-73 and UELN-95, estimated standard deviations for the height difference between NAP and Helsingborg and Newlyn respectively, are shown in table 8.1.

As has already been indicated in section 8.2, no explanation is given (it is not even mentioned) why the standard deviations of the adjusted geopotential numbers between Great Britain and NAP increase for later (adjustments of) European levelling networks. The improvement of the precision of the height difference with Helsingborg is due, e.g., to improved quality of the network blocks for Germany, the Netherlands, and Denmark. No specific referral is made to the levelling connection itself between Denmark and Sweden.

levelling network	adjustment	Helsingborg	Newlyn	reference
UELN-55		no information	no information	Alberda (1963)
UELN-73	adj. 1979	25 mm	35 mm	Kok <i>et al.</i> (1980)
	adj. 1981	25 mm	35 mm	Ehrnsperger <i>et al.</i> (1982)
	adj. 1986	25 mm	60 mm	Ehrnsperger and Kok (1986)
UELN-95	3	20 mm	77 mm	Lang and Sacher (1996b)
	8	15 mm	77 mm	Lang and Sacher (1996a)
	12	15 mm	77 mm	Sacher <i>et al.</i> (1999)

Table 8.1 Estimated standard deviations (in mm) of height difference between NAP and resp. Helsingborg (Scandinavia) and Newlyn (Great Britain). Based on different adjustments of European levelling networks.

Based on the various publications concerning the European levelling networks, an indication can be obtained from the precision between NAP and respectively Helsingborg (Scandinavia) and Newlyn (Great Britain), based on spirit levelling. However, it is very difficult to ascertain when the actual height connections with Scandinavia and Great Britain have been performed. In addition, even though newer adjustments sometimes provide different estimates for the precision of the height connections, this does not imply that they are actually based on new levelling connections to Great Britain and Scandinavia.

In order to simulate datum connection errors, it will simply be assumed that height connections between NAP and both Scandinavia and Great Britain have been performed in 1970 and 1992. Errors in the determined height differences are described by normally distributed random values with zero mean and specific standard deviations. Based on table 8.1, the following values are used for the standard deviations: connection to Helsingborg 25 mm (1970) or 15 mm (1992), height difference between NAP and Newlyn 60 mm (1970) and 77 mm (1992).

Due to the inaccuracies in the height connections, erroneous trend values are estimated for the (linear) movements of Helsingborg (fundamental station in Scandinavia) and Newlyn (Great Britain) relative to NAP. As a result, an erroneous linear movement is introduced between tide gauges situated in Western-Europe and those in Great Britain and Scandinavia respectively. If trend values determined for the resulting sea-level height series (all relative to NAP) are used as input for estimating linear patterns in trend values, results are derived as shown in figure 8.16. No additional errors resulting from local height connections (tide gauge bench marks to local reference frames) are added.

Figure 8.16 shows that if height connections between respectively Scandinavia and Great Britain and NAP are performed only twice, with standard deviations corresponding to UELN, erroneous trend estimates (as a function of latitude and longitude) can have ranges of up to 1 cm/yr. If a linear or a bi-linear variation pattern is estimated, the largest errors are estimated over land areas in the region. If a quadratic pattern (possibly without xy) is estimated, maximum ranges of erroneous trend values are derived for the southern part of the North Sea.

The major part of the errors shown in figure 8.16 is caused by the extremely low precision for the connection between NAP and Great Britain. As can be seen from figure 8.17, if for this height connection the same standard deviations are assumed as those applying to the connection with Scandinavia, the range of erroneous trend values decreases drastically. Unfortunately, still rather large errors (ranges up to 2.5 mm/yr) can occur for trends estimated in some parts of the North Sea.

In the preceding it has been assumed that, using spirit levelling, height connections to Great Britain and Scandinavia have been performed only twice (in 1970 and 1992). In chapter 7, an indirect method of connecting vertical datums, based on a combination of levelling, GPS and geoid information, has been introduced. The required geoid information was obtained from a global geopotential model in combination with local gravity measurements.

In chapter 7, it was found that, depending on the quality of the geopotential model and the number of stations in the datum zones, height differences could be determined with standard deviations of the order of 1 cm. It was also shown that a high quality vertical datum connection can only be obtained if a new geopotential model (GOCE) becomes available. The proposed launch for the GOCE mission is in 2004; see ESA (1999). Therefore, it is assumed that in the year 2004, a third connection in orthometric heights (or geopotential differences) is obtained. Based on results presented in section 7.5, the following standard deviations will be used: connection to Helsingborg 9 mm, height difference between Newlyn and NAP 12 mm.

Since three height connections are performed, two separate values could be derived for the velocities

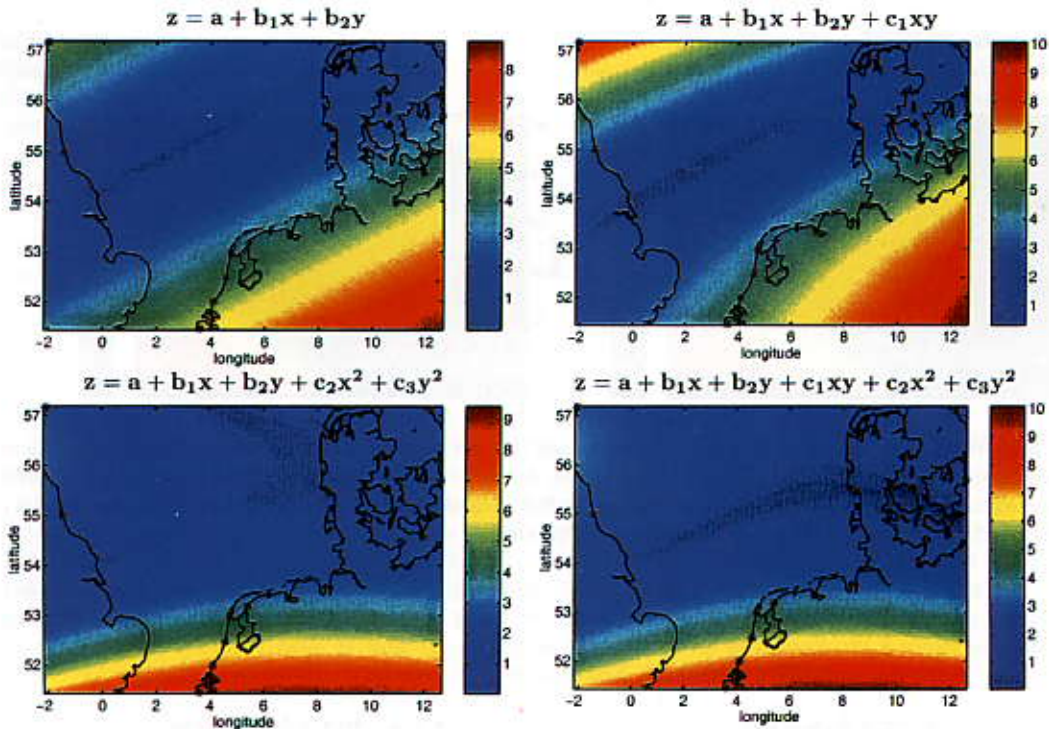


Fig. 8.16 Range (2σ value) of erroneous trend values (in mm/yr) for 100 realisations of errors in vertical datum connection. Standard deviations for connections between NAP and resp. Scandinavia (1970: 25 mm, 1992: 15 mm) and Great Britain (1970: 60 mm, 1992: 77 mm); based on UELN-73 and UELN-95.

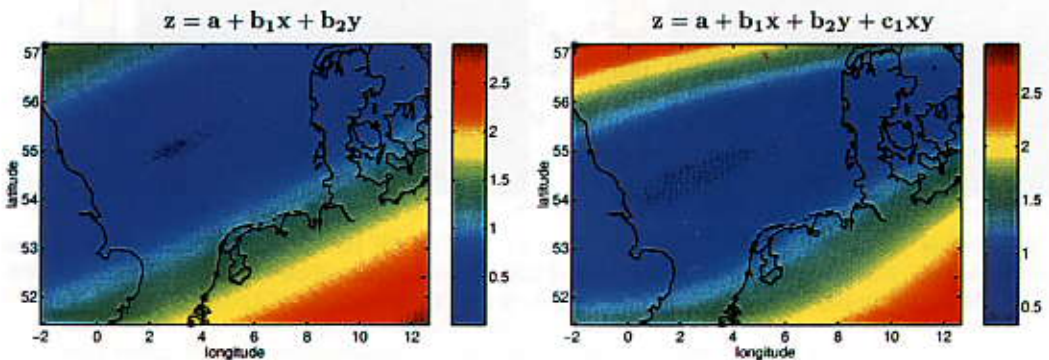


Fig. 8.17 Range (2σ value) of erroneous trend values (in mm/yr) for 100 realisations of errors in vertical datum connection. Standard deviations assumed for connections between NAP and resp. Scandinavia and Great Britain (1970: 25 mm, 1992: 15 mm).

between the fundamental stations. However, it is assumed that the vertical movements between the fundamental stations are solely caused by post-glacial rebound, which results (nowadays) in linear movements. Therefore, based on each set with three height differences, a linear height movement is determined between NAP and Helsingborg and Newlyn respectively. Due to inaccuracies in the height connections, erroneous slope values are estimated for the linear movements of the vertical datums relative to one another. These erroneous slope values are introduced into the sea-level height series for tide gauges situated in Scandinavia and Great Britain. Resulting erroneous spatial patterns in trend values are shown in figure 8.18.

Comparing results shown in figure 8.18 with those presented in figure 8.16 shows that by adding the third height connection (with a relatively good precision), ranges of erroneous trend values decrease significantly (approximately by a factor two). Unfortunately, errors which can occur in estimated trends

(for the major part of the North Sea) are still very large.

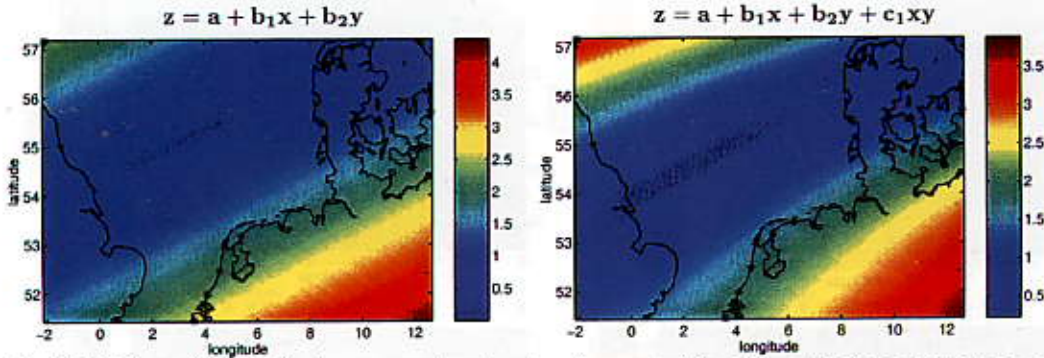


Fig. 8.18 Range (2σ value) of erroneous trend values (in mm/yr) for 100 realisations of errors in vertical datum connection. Linear vertical movements between datum zones are based on height connections in 1970 (Scandinavia, σ : 25 mm; Great Britain, σ : 60 mm), 1992 (Scandinavia, σ : 15 mm; Great Britain, σ : 77 mm) and 2004 (Scandinavia, σ : 9 mm; Great Britain, σ : 12 mm).

If all three height connections (in 1970, 1992, and 2004) could be performed with the standard deviations corresponding to vertical datum connection using the GOCE model, results could be derived as shown in figure 8.19. Ranges of errors in trend estimates are now at most 1 mm/yr. For the major part of the North Sea area these ranges are even smaller.

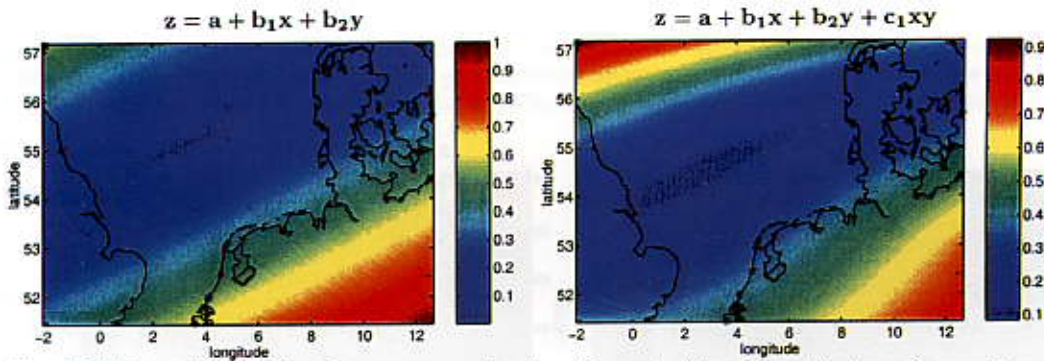


Fig. 8.19 Range (2σ value) of erroneous trend values (in mm/yr) for 100 realisations of errors in vertical datum connection. Linear vertical movements between datum zones are based on height connections in 1970, 1992, and 2004. For Scandinavia all connections have σ : 9 mm; Great Britain, σ : 12 mm.

In the preceding it has been shown that the quality of height datum connections (yielding potential differences) as performed up to now (or which might have been performed) is insufficient. Comparison with results presented in section 8.5, shows that errors introduced by inaccuracies in the height datum connections are much larger than vertical movements (resulting from post-glacial rebound) between the fundamental stations in the datum zones considered. Therefore, it might be concluded that, based on these accuracies of height connections, it is preferred not to correct sea-level height measurements for height movements of the datum zones relative to one another.

As an alternative for using height connections resulting from spirit levelling (as obtained from levelling campaigns performed in the last few decades), vertical movements of the local reference surfaces can be estimated by means of GPS measurements. It is assumed that the vertical movements of the fundamental stations in the datum zones can be adequately described, over the time span under consideration, by simple linear regression. Consequently, trend values can be estimated based on (permanent) GPS monitoring of the fundamental stations performed during only a limited number of years.

In order to translate recently obtained velocities between stations into a rate of orthometric height variation applying throughout the sea-level height time series, some assumptions concerning the geoid

heights have to be made. As indicated in chapter 5, the assumption of a stationary geoid (at the centimetre to sub-centimetre level), over time spans of the order of 100 years, is not valid. For example, post-glacial rebound not only influences geometric heights of stations, but geoid heights as well.

Ekman (1989) states that the maximum geoid rise (in the centre of the uplift area) is 0.7 mm/yr, while geoid rise in the outer zones of area affected by the post-glacial rebound is about half of this value. In a later publication (Ekman, 1993) he estimates a maximum geoid rise of only 0.4 mm/yr. Accurate estimates of variations in geoid height for the fundamental stations corresponding to determined variations in geometric height are difficult to obtain, since they require information about the accompanying mass changes as well. However, it seems reasonable to assume that the changes in geoid height can be described by a simple linear regression line as well. Consequently, the (unknown) trend in the geoid height variation can be considered an additional uncertainty, which has to be added to the trend in geometric height estimated using GPS.

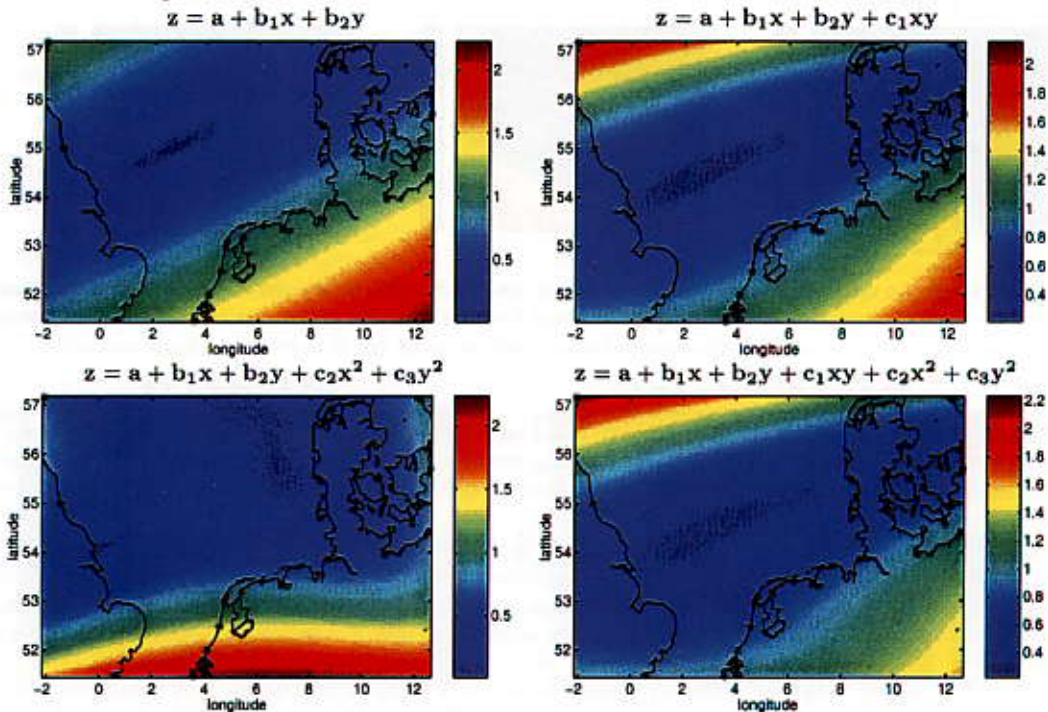


Fig. 8.20 Range (2σ value) of erroneous trend values (in mm/yr) for 100 realisations of errors in vertical datum connection. Zones Scandinavia (1 tide gauge) and Great Britain (2 tide gauges) connected to Western-Europe (15 tide gauges). Relative vertical movements between datum zones are determined with σ 1 mm/yr.

It is assumed that vertical movements of the reference surfaces (corresponding to the three datum zones) can be adequately described by linear trends relative to one another. Using the relative movements between the fundamental stations, all sea-level height series can be related to one (arbitrarily chosen) datum zone (e.g., NAP). For tide gauges not situated in the selected reference zone, inaccuracies in the slope values derived for the vertical movements between the datum zones are introduced into the sea-level heights relative to this selected reference datum.

As an example, vertical movements of fundamental stations Newlyn and Helsingborg are determined relative to NAP. It is assumed that the errors in estimated slope values are normally distributed with zero mean and a standard deviation of 1 mm/yr. Due to the inaccuracies in the slope values estimated for the vertical movements of the fundamental stations (Newlyn and Helsingborg), an erroneous trend value is introduced into the sea-level height series (relative to NAP) corresponding to these datum zones. Figure 8.20 shows ranges of erroneous spatial sea-level variations patterns based on the (erroneous) trend values estimated for the 18 tide gauges in the North Sea area.

Compared to ranges of trend estimates as shown in figures 8.16 and 8.18 (based on UELN networks, possibly in combination with a geopotential model), results show a major improvement. However, ranges

of erroneous trend values are still large as compared to the actual errors in trend introduced by post-glacial rebound movements of the fundamental stations (see figures 8.11 and 8.12).

Results as shown in figure 8.20 have been based on an assumed standard deviation of 1 mm/yr, with which vertical movements of fundamental stations relative to one another can be determined. This seems in correspondence with Zerbini *et al.* (1996), who state that (for the SELF project) vertical velocities between stations have been determined within 3 mm/yr. However, the actual value used for the standard deviation of estimated trend of the vertical movements between the fundamental stations is not of major importance. As can be seen from figure 8.21, if this standard deviation increases, the overall pattern in erroneous trend values hardly changes. The ranges of erroneous trend values are (more or less) proportional to the value used for the standard deviation of the linear height variation between the fundamental stations.

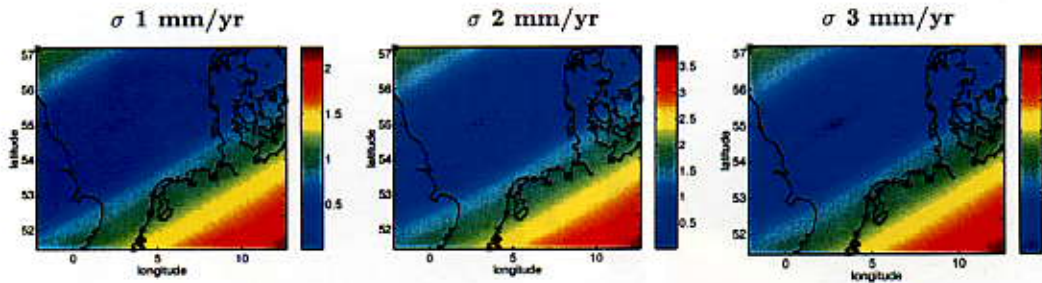


Fig. 8.21 Range (2σ value) of erroneous trend values (in mm/yr) for 100 realisations of errors in vertical datum connection. Zones Scandinavia (1 tide gauge) and Great Britain (2 tide gauges) connected to Western-Europe (15 tide gauges). Relative vertical movements between datum zones are determined with various values for σ . Estimated spatial pattern: linear.

Results as shown in figures 8.20 and 8.21 are based on height changes of fundamental stations Helsingborg and Newlyn, determined relative to NAP. Since datum zone Western-Europe contains the majority of the sea-level height series (for 15 tide gauges), only a small number of time series are influenced by errors in vertical datum connections.

Figures 8.20 and 8.21 are based on sea-level variation patterns estimated relative to NAP. If sea-level variation patterns relative to datum zone Scandinavia are required, vertical movements of NAP and Newlyn have to be determined relative to fundamental station Helsingborg in Scandinavia. As a result, inaccuracies due to vertical datum connections are introduced into a much larger number of sea-level height series.

Figure 8.22 shows ranges of erroneous trend values (as a function of latitude and longitude) that can result from inaccuracies in the connection of Western-Europe (15 tide gauges) and Great Britain (containing 2 tide gauges) to Scandinavia. Compared to results shown in figure 8.20 (patterns relative to NAP), ranges of erroneous trend values increase by 25 to 50%. However, not only the range of erroneous values increases, the pattern is changed as well. As a result, the maximum error ranges now occur in the south-western corner of the North Sea area under consideration. As can be seen from figure 8.20, if sea-level variation patterns are estimated relative to NAP, large error ranges occur mainly over land areas in the region under consideration, or in a much smaller area in the north-east.

If sea-level variation patterns are determined relative to datum zone Great Britain, vertical movements of NAP and Helsingborg have to be determined relative to Newlyn. Figure 8.23 shows results based on connection of Western-Europe (15 tide gauges) and Scandinavia (containing 1 tide gauge) to Great Britain. Ranges in erroneous trend values (as a function of latitude and longitude) are similar to those obtained for patterns relative to datum zone Scandinavia. However, even larger areas of the North Sea region are affected by relatively large error ranges. As can be seen from figure 8.23, if sea-level variation patterns are determined relative to datum zone Great Britain, small ranges of erroneous trend values are mainly found for land areas.

8.7 Conclusions and recommendations

In the preceding sections, spatial variation patterns in trend estimates for the North Sea area have been presented, based on a group of 18 tide gauges. The patterns shown are the results of inconsistencies in

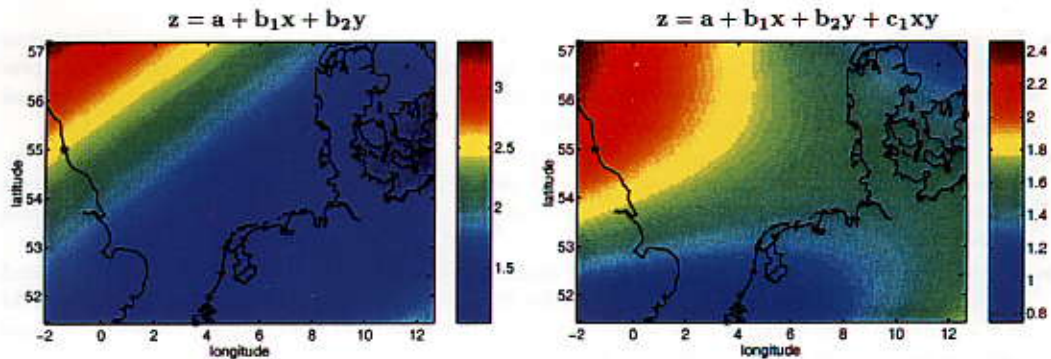


Fig. 8.22 Range (2σ value) of erroneous trend values (in mm/yr) for 100 realisations of errors in vertical datum connection. Zones Western-Europe (15 tide gauges) and Great Britain (2 tide gauges) connected to Scandinavia (1 tide gauge). Relative vertical movements between datum zones determined with σ 1 mm/yr.

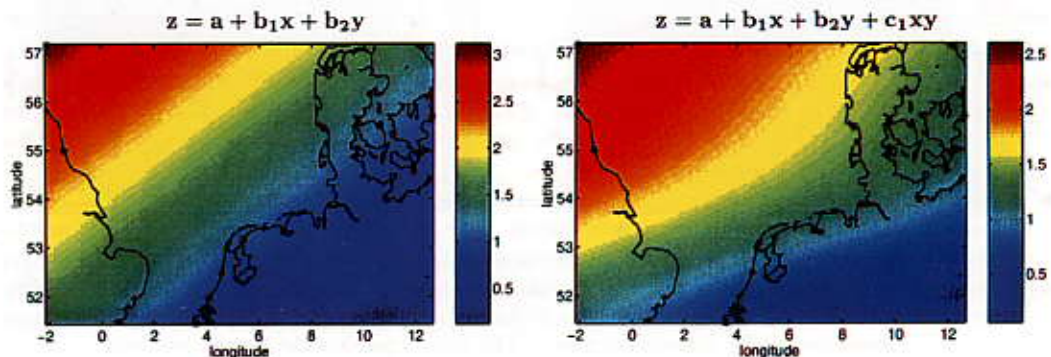


Fig. 8.23 Range (2σ value) of erroneous trend values (in mm/yr) for 100 realisations of errors in vertical datum connection. Zones Western-Europe (15 tide gauges) and Scandinavia (1 tide gauge) connected to Great Britain (2 tide gauges). Relative vertical movements between datum zones determined with σ 1 mm/yr.

the individual sea-level height series, resulting in erroneous trend estimates. Often, results shown are the ranges of erroneous trend estimates as a function of latitude and longitude.

Error ranges derived in the preceding sections are the result of one type of inconsistencies between the tide gauges only. If spatial variation patterns are determined for an actual group of tide gauges, these patterns will be influenced by a combination of the effects described. For example, if tide gauges have been connected in height to the local reference frames but no vertical datum connection has been performed, sea-level variation patterns are influenced by two error sources. First of all, erroneous patterns are introduced by inaccuracies in the local height connections. Secondly, systematic effects (as shown in section 8.5) are added due to relative vertical movements between the local reference frames used. If vertical datum connection has been performed, in addition to inconsistencies caused by local height connections, errors are introduced by inaccuracies in the vertical datum connection.

In the preceding sections, the effects of the different types of inconsistencies have not been added due to the following reasons. First of all, this would lead to a wide range of possible scenarios, of which only a few could be shown. Secondly, by showing the effects of the various error sources separately, more insight is gained in their individual contributions. Based on the experiments with simulated data, as shown in this chapter, the following conclusions and recommendations can be made.

Concerning the quality of the sea-level height measurements If sufficiently long time series are available (at least 100 years of data, see chapter 4), the occurrence of normally distributed random noise, e.g., resulting from inaccuracies in the sea-level height measurements themselves, introduces only small errors in trend estimates derived for the North Sea area.

- Erroneous trend values resulting from measurement errors are (more or less) proportional to the standard deviation of this measurement noise.

- The more complex the estimated spatial sea-level variation pattern, the larger the range of erroneous trend values that might be found. For example, for measurement noise with a standard deviation of 1 cm, ranges of erroneous trend values are up to 0.04 mm/yr if a linear pattern is estimated, and up to 1.1 mm/yr if a quadratic pattern applies.
- If only a limited number of yearly observations are available, range of erroneous trend values increases significantly. For example, using only 68 year of data, and estimating a linear pattern, this range is up to 0.9 mm/yr. Based on 132 year of data maximum range of erroneous trend estimates is 0.04 mm/yr.
- If only a limited number of observations are available, this also influences the mean value of trend estimates. Instead of the 1.5 mm/yr that applies throughout the area, values ranging between 1.34 and 1.35 mm/yr are found if data between 1898 and 1965 is used, and ranging between 1.65 and 1.66 mm/yr for data between 1929 and 1996.

Concerning the quality of height connections to local reference frames If tide gauges are connected in height to the local reference frames, inaccuracies in the height measurements lead to inconsistencies between the individual tide gauges. As a result, errors are introduced in the slope values estimated for the various tide gauges, resulting in erroneous spatial sea-level variation patterns.

- If the quality of the height connections is the same for all tide gauges, changes in this quality only influence the range of erroneous trend values. Changes in the standard deviation with which the height connection errors are described or in the time span between the height connections, do not influence the patterns in erroneous trend values.
- If height connections are performed every 10 years, ranges of errors in trend estimates (as a function of latitude and longitude) are approximately three times as large as results based on annual connection of heights; both for a standard deviation of the normally distributed errors of 1 cm.
- If an irregular height connection scenario applies (connections in 1885, 1940, 1960, 1980, 1996), range of erroneous trend values can become rather large, depending on the standard deviations used to represent the height connection noise. The more complex the spatial sea-level variation pattern estimated, the larger the range of erroneous trend values.

Concerning vertical movements of the local reference surfaces If fundamental stations in the datum zones experience vertical movements, these height changes are introduced into the sea-level height series for tide gauges connected in height to these fundamental stations. It is assumed that fundamental stations only experience movements resulting from post-glacial rebound, and movements can be described by linear regression lines.

- If vertical movements of fundamental stations are not corrected for, this will result in large errors in the trend values estimated as a function of latitude and longitude. The size of these errors depends on the type of spatial variation pattern determined and the differences in vertical movement of the fundamental stations relative to one another.
- Based on different post-glacial rebound models, different velocities are estimated for the fundamental stations. However, for the two models considered in this chapter, if one model is used to correct for the vertical movement of the fundamental stations, while in reality the other model applies, resulting errors in trend estimates are smaller than those caused by the post-glacial rebound itself (predicted by either of the two models).
- If inaccuracies in vertical datum connections are simulated based on quality information as published for UELN-73 and UELN-95, resulting erroneous trend estimates are much larger than those caused by the post-glacial rebound itself. Adding a third datum connection, using the method as described in chapter 7, does not sufficiently improve the results.
- Based on (permanent) GPS measurements, linear vertical movements between the fundamental stations can be derived as well. The ranges of erroneous trend values are (more or less) proportional to the value used for the standard deviation of the linear height variation between the fundamental stations (assuming the same standard deviation for the slope value derived between NAP and Helsingborg and Newlyn respectively).
- Even if slope values (for height variations between the fundamental stations) can be estimated with a standard deviation of 1 mm/yr, resulting erroneous trend values are larger than errors introduced by the post-glacial rebound itself.

Chapter 9

Conclusions and recommendations

9.1 Conclusions

The main objective of this thesis is to determine how well patterns in sea-level height variations can be detected, considering the fact that sea-level height time series are affected by inconsistencies. Different aspects of this objective have been discussed. Based on literature studied and numerous experiments performed with actual and simulated sea-level height data, the following conclusions have been derived.

Tide gauge measurements Depending on the tide gauge system used, e.g., tide pole, stilling-well tide gauge, or pressure tide gauge, different types of random and systematic errors can be introduced. Especially systems without automatic registration are prone to (e.g., reading) errors. Typical measuring precisions are: 3 mm for a 3 minutes average obtained by a reflection tide gauge, and 1 cm for hourly values using a stilling-well tide gauge.

When evaluating existing sea-level height time series with very long data spans, it is not realistic to assume a constant measuring accuracy, e.g., based on quality estimates for modern tide gauge operations. Differences in quality are not only the result of changes (improvements) in the tide gauge equipment used. The quality of annual mean sea levels is also influenced by the number of daily measurements contributing to these mean values. In general, it can be stated that the further back in time, the smaller the number of measurements that were registered on a daily basis.

Apart from changes in measuring precision, changes in tide gauge equipment might have been accompanied by a relocation of the tide gauge. Various tide gauges along the Dutch coast show a more or less abrupt change in sea-level height around 1880. For some tide gauges (Vlissingen and IJmuiden) this effect is clearly visible from plots of the sea-level height data itself. For other tide gauges (e.g., Delfzijl) these inconsistencies are more difficult to detect. If these discontinuities are not removed from the time series, they will lead to erroneous sea-level variation curves, e.g., wrong trend values, estimated from these data sets.

Long-periodic fluctuations Based on experiments with actual sea-level height data for an individual tide gauge, it was found that long-periodic fluctuations are the main factor in determining the amount of data that is required to detect a linear trend in a sea-level height time series. As an example, of the order of 90 years of data are required to determine a stable trend value for a data set containing a linear trend in combination with periodic fluctuations as found for tide gauge Den Helder. The influence random measuring errors is much smaller; e.g., if a noise level of 5 cm applies, around 35 years of data are required for a statistically significant trend estimate.

The occurrence of long-periodic fluctuations in a time series also hampers the distinction between different sea-level variation curves, e.g., between linear and quadratic rise. For data sets without long-periodic fluctuations, all combinations of regression lines tested for could be distinguished and the onset year of the acceleration could be estimated. If time series contain long-periodic fluctuations, it becomes difficult to detect some sea-level variation curves. For example, if (for a time series with 130 years of data) the first 30 years of data are based on a 0.8 mm/yr lower slope value, this change in trend can no longer be detected.

Different techniques can be used to smooth sea-level height time series. However, these techniques can only (realistically) be used to reduce the influence of short-periodic fluctuations. The longer the period of the fluctuations (in relation to the time span of the measurements), the harder they are to eliminate by means of smoothing. Consequently, smoothing of sea-level height data prior to regression will not significantly reduce the number of observations required for a stable trend estimate. However,

experiments with simulated data have shown that smoothing enhances the feasibility to determine the onset year of sea-level rise acceleration based on the statistical significance of the regression coefficients.

By adding more time series to a data set, only the influence of random errors is reduced, while more systematic effects remain. Analysis of data for 18 tide gauges in the North Sea area has revealed a large correlation between the different sea-level height time series. Consequently, compared to results based on a single time series, adding more data sets resulted in only a slight improvement in the number of observations required for a stable trend estimate.

Height connections For a group of tide gauges a *common* sea-level variation curve can be determined. Since averaging of time series reduces the influence of localised variations in sea level, the common sea-level variation curve is (ideally) more representative for the area under consideration than an arbitrary individual sea-level height series. Unfortunately, if relative height changes have occurred between the various tide gauges bench marks, this introduces apparent differences in the (relative) sea-level variation curves and hampers the detectability of a common curve.

As long as tide gauges experience only secular movements relative to one another, the common oscillation pattern can still be discerned by techniques like SVD, although the slope of the common curve might no longer be representative for the area under consideration. If tide gauges experience relative vertical movements which are not constant over time, the common oscillation patterns based on these data sets will be affected as well. By connecting the tide gauge bench marks in height (or to the local height datum), all individual sea-level height time series can be related to the same (local) reference height system. However, inaccuracies in the height connection measurements will again introduce inconsistencies between the individual time series.

In general it can be stated that the quality of the common variation curve depends not only on the quality of the height measurements, but also on the time span between subsequent height connections. If height connections have been performed every year, estimates of the common trend value stabilise within 10% of the actual trend value in the data, even if height connections have a rather large standard deviation of say 2 cm. For height connections performed on a regular basis (e.g., every 10, 20, or 30 years), it is found that the larger the time span between the height connections, the larger the spread between trend estimates based on different realisations of height connection noise. This effect is even more pronounced if larger levels of height connection noise apply.

Nowadays, it is often preferred to connect tide gauges in height by means of GPS observations. This allows for permanent monitoring of height changes with a good quality of measurements. Unfortunately, to predict future sea-level rise and detect accelerations in sea-level variation, e.g., resulting from greenhouse-gas induced warming, historical data has to be used as well. Experiments with simulated height connection scenarios shows that (for the time being) the quality of these historic height connections is the major limiting factor for the detectability of sea-level rise accelerations. The quality of the future height connections is of almost no influence. For example, if long periods have elapsed between subsequent historic height connections, increasing the standard deviation of future height connections from 2 cm to 5 mm, hardly influences the measuring time required to detect an acceleration in sea-level rise. In addition, permanent monitoring of tide gauge heights does not yield significantly better results as compared to height connections determined every 5 or 10 years in specific measuring campaigns.

Spatial variation patterns If more time series are available, a spatial pattern in sea-level height variations can be estimated. In this thesis, spatial variations in trend values are determined by regression of the trend values as determined for individual sea-level height series, against the latitude and longitude of the tide gauges. It is found that only models based on at most six regression parameters (quadratic model) yield realistic results for a spatial variation pattern in the North Sea area based on 18 tide gauges..

A spatial sea-level variation patterns should be based on "true" differences observed between the various locations, not on differences in trend values resulting from inconsistencies between the individual time series. These inconsistencies can be caused by measuring errors of the tide gauge equipment, by (uncorrected for) height changes between tide gauges bench marks, and by inaccuracies in height measurements used to connect the tide gauge bench marks in height. Based on experiments with simulated data, the influence of these error sources on the determined spatial variation patterns has been examined. It has been found that, if the time series contain enough observations (of the order of at least 90 years), sea-level measuring errors with standard deviations up to 2 cm yield only small differences in estimated spatial variation patterns.

In the past, tide gauge bench marks have often been connected to a local (national) reference frame. If height connections are performed every 10 years, ranges of errors in trend estimates (as a function of latitude and longitude) are approximately three times as large as results based on annual connection of heights. The more complex the spatial sea-level variation pattern estimated, the larger the range of erroneous trend values.

Due to, e.g., post-glacial rebound, local reference frames might experience vertical movements relative to one another. If these vertical movements are not corrected for, this will result in large apparent differences in the trend values estimated for tide gauges situated in different height datum zones. The size of the resulting errors in trend values as a function of latitude and longitude depends on the type of spatial variation pattern determined and the differences in vertical movements of the fundamental stations relative to one another. In principle, (part of) these movements could be corrected for using models describing vertical velocities resulting from post-glacial rebound. Unfortunately, based on different post-glacial rebound models, different velocities are estimated for the local reference frames.

In the past decades, Scandinavia and Great Britain have been connected in height to Western-Europe by means of spirit levelling. Unfortunately, if inaccuracies in vertical datum connections are simulated based on quality information as published for UELN-73 and UELN-95, resulting erroneous trend estimates are much larger than those caused by the post-glacial rebound itself. Based on (permanent) GPS measurements, linear vertical movements between the local reference frames can be derived as well. The ranges of erroneous trend values are (more or less) proportional to the value used for the standard deviation of these height connections. It is found that, even if slope values (for height variations between the datum zones) can be estimated with a standard deviation of 1 mm/yr, resulting erroneous trend values are larger than errors introduced by the post-glacial rebound itself.

9.2 General remarks concerning sea-level monitoring

In the preceding, it has often been concluded that more tide gauge stations and a higher frequency of height connections do not really improve the derived results. However, it should be noted that this only applies to the precision that can be achieved. In general it can be stated that in order to derive results that are reliable, several measurements are required. For example, it has been concluded that the detectability of a sea-level variation curve does not improve by adding more time series that contain similar long-periodic fluctuations. This does not imply that one time series is sufficient to determine a reliable sea-level variation curve for a specific area. If the selected time series contains erroneous information (gross measuring errors or distortions of the regional pattern by local circumstances), this will directly affect the estimated variation curve. In addition, only by comparing results for various tide gauges, it can be ascertained that a common variation curve applies in the region. It has also been concluded that having short intervals between future height connections does not reduce the number of observations required to detect sea-level rise accelerations. However, this conclusion only applies if tide gauge bench marks experience secular movements. Only by permanent monitoring (or at least yearly measurements) of tide gauge heights, the influence of more abrupt movements of tide gauges can be minimised.

How well a method works should not only be decided on the precision of the derived results, but on their reliability as well. As a simple example, without new global geopotential models, the precision that can be derived with the method for vertical datum connection as proposed in chapter 7, is much less than results derived in international levelling campaigns (e.g., UELN-95). However, the UELN-95 network consists of a single connection line between the continent of Europe and Great Britain. Therefore, gross errors in this height difference cannot be detected by testing. For the proposed method, an estimate can be made of the maximum values of errors that cannot be detected by testing. This value can be improved by adding more stations or changing the design of the network.

In this thesis, the term robustness is often applied as well. It is used to indicate whether or not results change significantly if the input conditions are (slightly) changed. Experiments with a wide range of methods that can be applied to forecast future sea-level heights, have shown that forecasted values are significantly influenced by the choice of the year in which the forecasting is started. It has been concluded that simple (linear) regression is one of the few methods that is robust against a small change in starting year for the forecasts.

It should be noted that the statistical significance of an estimated trend value is no guarantee that this value represents the “true” sea-level variation curve. For example, if a time series has zero mean and long-periodic fluctuations (e.g., with a period of 100 years), based on a time span of only 25 years of data

(and depending on the level of measuring noise), a trend value could be estimated that is statistically significant. However, this estimated trend value does not represent the true sea-level variation curve (in this case, no trend at all).

Tide gauges measure sea-level heights relative to the zero of the tide gauge system. In principle, these sea-level heights can be related to any required reference. It should be taken into account, however, that every step taken to relate sea-level heights to a different reference system, will introduce additional inconsistencies into the time series. This is especially true if the frequency of the measurements used for the transformation is not sufficient. For example, to relate sea-level heights to a local reference frame, permanent monitoring of height changes between the local tide gauge bench mark and the reference system should be available. If height measurements have only been obtained at specific epochs, assumptions have to be made concerning the vertical movements of the tide gauge bench mark. If it is assumed that the tide gauge bench mark has experienced a secular movement while in reality a more abrupt change in height has occurred, erroneous corrections have been applied to the data.

Since height transformations introduce inconsistencies in the data set, these transformations should only be applied if they are required to determine reliable results. For example, predictions of future sea levels for the harbour area near Den Helder should be based on measurements of this tide gauge relative to its tide gauge bench mark and not on sea-level variations relative to, e.g., ITRF92. On the other hand, if a sea-level variation pattern for the Dutch coast needs to be established, all sea-level height series should be related to one common reference height system. Otherwise, the resulting pattern will not only represent variations in sea level along the Dutch coast, but height variations between the tide gauge bench marks as well.

Corrections for determined height variations should not be applied thoughtlessly. Height corrections should only be applied if the expected vertical movements between the tide gauge bench marks are significant in relation to the precision of the height measurements. As an example, if (from external sources) it is known that fundamental stations in the datum zones experience secular movements relative to one another with velocities of the order of only 0.5 mm/yr, these height changes should not be corrected for as long as standard deviations for measured velocities are of the order of 1 mm/yr.

Nowadays, in the North Sea region, tide gauges are equipped with good quality measuring equipment, and all tide gauge bench marks could be connected in height by (permanent) GPS monitoring. Using these measurements, high quality variation patterns in sea-level heights can be determined over short (a few years or decades) time scales. However, to predict future sea-level heights and assess whether or not an acceleration in sea-level rise has occurred, long time series (of the order of 90 years of data) are required. Consequently, the quality of these sea-level variation patterns is (largely) determined by the quality (and frequency) of the measurements acquired in the past. This does not imply that future measurements should not be obtained with the best possible quality, otherwise, the present situation will never change. However, for the near future, the quality of historical data is the major limiting factor for the quality of estimated sea-level variation patterns on decadal time scales.

9.3 Recommendations for future research

Worldwide, a large number of people are working on issues related to monitoring sea-level height variations. It is often recognised that an effective approach requires an interdisciplinary effort. Consequently, for an individual researcher it is very difficult to have a good perception of all processes involved and aspects that (still) need further research. Therefore, except for the issues already mentioned in the preceding section, I will not try to give recommendations on how an “improved” sea-level observation system should be devised.

This thesis focuses on how well specific sea-level variation patterns can be detected, given the limited quality of the data available. Due to the limited time available for my research, for a number of aspects I have used “simple solutions”, while I think that further research might provide better (more realistic) results. On the other hand, there are probably many more factors limiting the quality of sea-level data (and required height connections) that I have not incorporated. Because of the interdisciplinary nature of sea-level research, the list of “things yet to research”, can become very long. Aspects I would have liked to research, and information that might improve the quality of derived sea-level variation curves are:

- Information on long-periodic fluctuations in sea-level heights

In literature, a large number of processes have been described that influence sea-level heights on shorter time scales (up to a few years). In the literature I have studied, no mention was made of processes having a (significant) influence on longer time scales. However, inspection of actual tide gauge data reveals very long-periodic (periods longer than 20 years) phenomena. In this thesis it was found that due to these long-periodic fluctuations, very long time series are required for a stable trend estimate. Consequently, external information (e.g. from oceanographic research) that can be used to eliminate (or at least reduce) these long-periodic fluctuations will improve the detectability of sea-level variation curves.

- Consistent models describing vertical movements in the North Sea region

If a “perfect” model would be available, all sea-level height series could be related to the same reference surface without requiring additional height measurements. With a good model, mean vertical movements of specific areas can be estimated. For example, vertical movements of fundamental stations on which local height datums are based (and which are hopefully located in relatively “stable” areas), can be estimated from post-glacial rebound models. Unfortunately, there are different post-glacial rebound models, based on different measurements and methods, and predicting different velocities. In this thesis, two models have simple been selected. Further research on these models might give insight in which is the best model to use for correcting vertical movements of the fundamental stations.

Of interest is also models that could give insight in vertical movements in the North Sea region over the past century. Nowadays, a lot of height measurements are performed. The further back in time, the scarcer this information. Therefore, based on existing height connection data, it is very difficult to correct older sea-level height data for height changes of the tide gauge bench marks. Consequently, common sea-level variation curves for a group of tide gauges are usually not based on time series that are all related to the same reference surface, but on data sets corresponding to local tide gauge bench marks. Any height variations between these tide gauge bench marks affect the quality of the common sea-level variation curve. With a reasonable model (i.e., errors are smaller than the variations described) of height movements in the North Sea region, at least a part of the inconsistencies between the individual time could be reduced.

- Research into the history of the tide gauges used

Some sea-level height series clearly show variations in relative sea level that cannot possibly be related to actual fluctuations in absolute sea level, but must be the result of changes in the tide gauge itself. For example, in case of tide gauge Vlissingen, sea-level heights decrease more or less abruptly by over 10 cm around the year 1885. If this type of deviations in the data sets are not detected (and corrected for, or the corresponding part of the data set is removed), sea-level variation curves based on these time series will be strongly affected. Studying the history of the tide gauges might give an indication of when troubles might be expected. For example, if a new tide gauge has been installed or major harbour reconstructions have taken place. Based on this knowledge, it can be decided whether or not it is safer to eliminate specific parts from a sea-level time series.

Research into the history of tide gauges might also reveal when tide gauge bench marks have been included in measuring campaigns. If information on height measurements can be found, this can be used to correct the sea-level heights. Of interest is also the quality of these height measurements.

- Application of wavelets

In this thesis, wavelets have only been used as a tool to smooth sea-level height time series. It was found that results were highly dependent on the choice of wavelet. Further research on wavelets might give an indication of which wavelet gives “optimal” results for processing sea-level height data.

To my opinion, it is not likely that the long-periodic fluctuations as seen in sea-level height data have fixed periods and amplitudes (e.g., if they are caused by atmospheric conditions). The use of wavelets in analysing the data might give more insight in when (how often) these phenomena occur and how their amplitudes change. This might help oceanographers in accounting for these oscillations.

- Influence of azimuthal asymmetries on GPS measurements

Some research has been conducted on the influence of azimuthal asymmetries on VLBI measurements, with the conclusion that measurements are especially influenced if they are obtained below 7° elevation. Therefore, some authors claim (e.g., MacMillan and Ma (1997)) that azimuthal asymmetries should not be a problem for GPS, since measurements are usually obtained with a 15° cutoff.

However, published results are for VLBI receivers situated well away from coastlines, while GPS receivers installed at (or close to) tide gauge bench marks, are placed near the coastline. As a result, part of the received signals have travelled over land, part over sea. The water vapour content over sea might differ significantly from that over land. Further research is needed to check whether or not applying the same mapping function for all measurements can introduce systematic errors into the derived height differences.

Appendix A

Information concerning tide gauge stations

For different experiments performed in chapter 3 (specific parts of) time series for a number of tide gauges have been used. In this appendix, some additional information concerning these data sets will be given.

Stations along the Dutch coast For 9 stations along the Dutch coast, the Permanent Service for Mean Sea Level (PSMSL) holds at least 100 years of data. However, three of these tide gauges (Hellevoetsluis, Maassluis, Zierikzee) are situated rather far inland. Therefore, these tide gauges are not included in the data analysis. Table A.1, lists for the six remaining stations the years for which sea-level heights are available. Since three stations (Delfzijl, IJmuiden, Vlissingen) show a deviating sea-level curve in the first part of the time series, often only data sets containing observations between 1886 and 1996 are used.

	tide gauge	data span	remarks
1	Delfzijl	1865 - 1996	relative to NAP
2	Harlingen	1865 - 1996	relative to NAP
3	Den Helder	1865 - 1996	relative to NAP
4	IJmuiden	1872 - 1996	relative to NAP
5	Hoek van Holland	1864 - 1996	relative to NAP
6	Vlissingen	1862 - 1996	relative to NAP

Table A.1 Availability of annual mean sea levels for six tide gauges along the Dutch coast.

16 stations in the North Sea area For a large number of stations in the North Sea area, the PSMSL holds annual mean sea-level values. However, the number of stations that can be used to estimate sea-level variation patterns for the North Sea region is very limited because:

- For some tide gauges, only short time series are available. Because of long-periodic fluctuations in the data (see chapter 4), in the order of 80 years of data should be available.
- Some stations are situated far inland (like Maassluis) or in an area far away from an open connection with the North Sea (e.g., Travemunde).
- Some stations cover a large time span, but also contain huge data gaps. For example, Sheerness has data available between 1832 and 1997. However, a number of data gaps occur, the largest with data missing between 1928 and 1950.
- For some tide gauges, long time series are available, but not over the period we are interested in. For example, for tide gauge Aberdeen 2, data is already available from 1862 onwards. However, this time series ends in 1965.

Due to the above limitations, it is not possible to have a group of tide gauges, well distributed over the North Sea area, with data available (without gaps), e.g., for the period 1900 to 1990. As an example, only the 6 stations along the Dutch coast (see table A.1) have time series available for this period without missing data and are located close to the North Sea itself. Therefore, in order to estimate sea-level patterns for the North Sea area, some compromises have to be made concerning the data. Possibilities are to allow small gaps in the data, use shorter time series, or change the time span for which data should be available. Based on the criteria used, different groups of tide gauges will result. As an example, allowing small data gaps, 16 tide gauges are available with annual mean sea levels for the period 1898 to 1981; see table A.2.

tide gauge	data span	missing observations	remarks
1 Aarhus	1889 - 1996	1956, 1963, 1969, 1970, 1982, 1984-88	RLR: 7012
2 Cuxhaven 2	1843 - 1986	-	relative to NN
3 Delfzijl	1865 - 1996	-	relative to NAP
4 Den Helder	1865 - 1996	-	relative to NAP
5 Esbjerg	1890 - 1996	1982, 1984, 1990	RLR: 6912
6 Fredericia	1890 - 1996	1981, 1982, 1991	RLR: 6978
7 Gedser	1898 - 1996	1972, 1985	RLR: 6888
8 Harlingen	1865 - 1996	-	relative to NAP
9 Hoek van Holland	1864 - 1996	-	relative to NAP
10 Hornbaek	1898 - 1996	1958, 1973, 1980, 1984, 1985, 1991	RLR: 7002
11 Kobenhavn	1889 - 1996	1983, 1991	RLR: 6948
12 Korsor	1897 - 1996	1977, 1979, 1982, 1984, 1986, 1991	RLR: 6957
13 Travemunde	1856 - 1984	-	relative to NN - 5000 mm
14 Varberg	1887 - 1981	-	RLR: 11726 (1887 - 1936) RLR: 4899 (1937 - 1981)
15 Vlissingen	1862 - 1996	-	relative to NAP
16 IJmuiden	1872 - 1996	-	relative to NAP

Table A.2 Tide gauges in the North Sea area containing data for the period 1898 - 1981. RLR is the RLR factor (in mm) as provided by the PSMSL that has to be added to the sea-level values. NN is Normal Null.

18 stations in the North Sea area The stations presented in table A.2 have been selected based on their data quality (length of time series, occurrence of data gaps) and a specific period for which data is required. Unfortunately, this data set does not contain sea-level heights for tide gauges in the United Kingdom. If we want to include stations from the U.K., some further reduction of the data span is required. The resulting data set contains sea-level observations between 1898 and 1965. Specifics for the two tide gauges added, are given in table A.3.

tide gauge	data span	missing observations	remarks
17 Aberdeen II	1862 - 1965	1915	RLR: 2186 (1862 - 1930) RLR: 4014 (1931 - 1963)
18 North Shields	1895 - 1997	1895, 1904, 1905, 1975, 1976, 1977 1978, 1979, 1980, 1983, 1993	RLR: 2186 (1964 - 1965) RLR: 4557 (1895 - 1957) RLR: 4575 (1958 - 1973) RLR: 4054 (1974, 1978 - 1997)

Table A.3 Tide gauges in the North Sea area containing data for the period 1898 - 1965. RLR is the RLR factor (in mm) as provided by the PSMSL that has to be added to the sea-level values.

Appendix B

Derivations

B.1 Variance of quadratic regression term

If the relation between sea-level height and time is quadratic, the system of linear equations relating the sea-level heights (y) to the years of observation (x) is given by:

$$Y = Au \iff \begin{pmatrix} y_1 \\ y_2 \\ \vdots \\ y_N \end{pmatrix} = \begin{pmatrix} 1 & x_1 & (x_1)^2 \\ 1 & x_2 & (x_2)^2 \\ \vdots & \vdots & \vdots \\ 1 & x_N & (x_N)^2 \end{pmatrix} \begin{pmatrix} a \\ b \\ c \end{pmatrix} \quad (\text{B.1})$$

From this equation, the covariance matrix of the regression coefficients a , b , and c can be found as:

$$\sigma_u^2 (A^T A)^{-1} \quad (\text{B.2})$$

in which σ_u is the standard deviation of regression. Assuming normally distributed measurement errors with zero mean and standard deviation σ_ϵ , this standard deviation of regression can be written as:

$$\sigma_u = \sqrt{\sum_{i=1}^N \frac{\epsilon_i^2}{N-2}} = \sigma_\epsilon \sqrt{\frac{N}{N-2}} \quad (\text{B.3})$$

in which N is the total number of measurements and ϵ are the measurement errors.

After some derivation, the third diagonal element of the matrix $(A^T A)^{-1}$, corresponding to the variance for the quadratic regression term c is found to be:

$$\frac{N \sum (x_i)^2 - (\sum x_i)^2}{N \sum (x_i)^2 \sum (x_i)^4 - N (\sum (x_i)^3)^2 - (\sum x_i)^2 \sum (x_i)^4 + 2 \sum x_i \sum (x_i)^2 \sum (x_i)^3 - (\sum (x_i)^2)^3} \quad (\text{B.4})$$

in which \sum has been written instead of $\sum_{i=1}^N$.

Using $x_i = (X+i)$ in which X is a constant representing the year prior to the first year of observation, the following relations can be derived.

$$\begin{aligned} \sum_{i=1}^N x_i &= X \cdot N + \frac{N(N+1)}{2} \\ \sum_{i=1}^N (x_i)^2 &= X^2 \cdot N + X \cdot N(N+1) + \frac{N(N+1)(2N+1)}{6} \\ \sum_{i=1}^N (x_i)^3 &= X^3 \cdot N + 3X^2 \cdot \frac{N(N+1)}{2} + 3X \cdot \frac{N(N+1)(2N+1)}{6} + \left(\frac{N(N+1)}{2}\right)^2 \\ \sum_{i=1}^N (x_i)^4 &= X^4 \cdot N + 4X^3 \cdot \frac{N(N+1)}{2} + 6X^2 \cdot \frac{N(N+1)(2N+1)}{6} + 4X \cdot \left(\frac{N(N+1)}{2}\right)^2 + \\ &\quad \frac{N(N+1)(2N+1)(3N^2+3N-1)}{30} \end{aligned} \quad (\text{B.5})$$

Substituting the above relations and equations (B.4) and (B.3) in equation (B.2) yields the required expression for the standard deviation of the quadratic regression coefficient c as:

$$\sigma_c = \sigma_\varepsilon \cdot \sqrt{\frac{180}{(N-2)(N^4 - 5N^2 + 4)}} \quad (\text{B.6})$$

B.2 Influence of jump in sea-level height on trend estimates

If a time series consists solely of a linear trend in combination with random measuring noise, for every sample i the following relation exists between sea-level height (y) and year of observation (x):

$$y_i = a + bx_i + \varepsilon_i \quad (\text{B.7})$$

in which ε is the measuring noise. The regression coefficients a (intercept) and b (slope) can be determined by means of least-squares adjustment. Equations B.7 are rewritten in matrix form as:

$$Y = Au \quad (\text{B.8})$$

in which Y is the vector containing the observations, A is the design matrix, and u contains the unknown regression coefficients a and b . Since normally distributed random measuring noise has been assumed, the solution of the least-squares adjustment can be written in matrix form as:

$$A^T Au = A^T Y \quad (\text{B.9})$$

After substitution of the elements this can be written as:

$$\begin{pmatrix} N & \sum x_i \\ \sum x_i & \sum (x_i)^2 \end{pmatrix} \begin{pmatrix} a \\ b \end{pmatrix} = \begin{pmatrix} \sum y_i \\ \sum x_i y_i \end{pmatrix} \quad (\text{B.10})$$

in which N is the total number of observations used and \sum is written instead of $\sum_{i=1}^N$. From the above equation, the parameter of interest (the slope b) can be estimated as:

$$b = \frac{N \sum x_i y_i - \sum x_i \sum y_i}{N \sum (x_i)^2 - (\sum x_i)^2} \quad (\text{B.11})$$

Next it is assumed that, due to relocation of the tide gauge, the first n observations contain a deviating sea-level height $y_i + \Delta\text{sl}$. Based on equation (B.11) the resulting deviating slope b' can be estimated as:

$$b' = b + \Delta b = \frac{N \Delta\text{sl} \sum_{i=1}^n x_i - n \Delta\text{sl} \sum_{i=1}^N x_i + N \sum_{i=1}^N x_i y_i - \sum_{i=1}^N x_i \sum_{i=1}^N y_i}{N \sum (x_i)^2 - (\sum x_i)^2} \quad (\text{B.12})$$

Consequently, the variation in trend due to a number of observations containing a jump in sea level, Δb , is given by:

$$\Delta b = \frac{N \Delta\text{sl} \sum_{i=1}^n x_i - n \Delta\text{sl} \sum_{i=1}^N x_i}{N \sum (x_i)^2 - (\sum x_i)^2} \quad (\text{B.13})$$

Next we use the fact that for subsequent years x_i the sum $\sum_{i=1}^n x_i$ can be written as:

$$\sum_{i=1}^n x_i = \sum_{i=1}^n (X + i) = n \cdot X + \sum_{i=1}^n i = n \cdot X + \frac{n(n+1)}{2} \quad (\text{B.14})$$

in which X is a constant representing the year prior to the first year of observation. As a result, the numerator of equation (B.13) can be simplified to:

$$N \Delta\text{sl} \sum_{i=1}^n x_i - n \Delta\text{sl} \sum_{i=1}^N x_i = n N \Delta\text{sl} \left(\frac{n-N}{2} \right) \quad (\text{B.15})$$

For the denominator in equation (B.13) it holds that

$$N \sum (x_i)^2 - \left(\sum x_i \right)^2 = N \sum_{i=1}^N (x_i - \bar{x})^2 \quad (\text{B.16})$$

with \bar{x} the mean value of the years under consideration. For subsequent years it can be derived that:

$$\sum_{i=1}^N (x_i - \bar{x})^2 = \frac{N(N^2 - 1)}{12}. \quad (\text{B.17})$$

Substitution of equations (B.15), (B.16) and (B.17) in equation (B.13) gives the relation between variation in trend Δb on the one hand and total number of observations (N), number of deviating observations (n), and jump in sea-level height (Δsl) as:

$$\Delta b = 6\Delta \text{sl} \frac{n(n - N)}{N(N^2 - 1)} \quad (\text{B.18})$$

B.3 Influence of an increase in slope on overall trend estimate

For the first n samples a linear trend b_1 applies, whereas the remainder of the time series contains a (higher) linear trend b_2 . If the complete data set is used to determine one value for the trend (b), this value will be smaller than the trend value that applies to only the last part of the data set, i.e., $b < b_2$. In this section, a relation will be derived between the increase in trend ($\bar{b} = b_2 - b_1$), the number of deviating samples (n), the total number of samples (N) on the one hand, and the decrease in estimated trend (Δb) on the other hand.

Due to the lower trend value, for the first n years, sea-level heights were determined by

$$y'_i = a_1 + b_1 x_i + \varepsilon_i = y_{n+1} + b_1(x_i - x_{n+1}) + \varepsilon_i \quad (\text{B.19})$$

If the “normal” trend b_2 is applied, sea-level heights would be:

$$y_i = a_2 + b_2 x_i + \varepsilon_i = y_{n+1} + b_2(x_i - x_{n+1}) + \varepsilon_i \quad (\text{B.20})$$

As a result, (using $\bar{b} = b_2 - b_1$) the relation between lower sea-level heights (y') and “normal” heights (y) is:

$$y'_i = y_i + \bar{b}(x_{n+1} - x_i) \quad (\text{B.21})$$

Due to these first n samples based on a lower trend, a deviating (lower) value for the overall trend ($b' = b_2 + \Delta b$) will be found if linear regression is applied to the complete data set. If in equation (B.11), for the first n samples y'_i is used instead of y_i , the deviating trend b' is determined as:

$$b' = b_2 + \Delta b = \frac{N \sum_{i=1}^n x_i y'_i + N \sum_{i=n+1}^N x_i y_i - \sum_{i=1}^n x_i \sum_{i=1}^n y'_i - \sum_{i=1}^N x_i \sum_{i=n+1}^N y_i}{N \sum (x_i)^2 - \left(\sum x_i \right)^2} \quad (\text{B.22})$$

Next, relation B.21 is substituted in the above equation. Furthermore, we use $x_{n+1} = X + n + 1$, in which X is a constant representing the year prior to the first observation. This leads to the following expression for the deviation in trend Δb :

$$\Delta b = \frac{N\bar{b}(X + n + 1) \sum_{i=1}^n x_i - N\bar{b} \sum_{i=1}^n (x_i)^2 - n\bar{b}(X + n + 1) \sum_{i=1}^N x_i + \bar{b} \sum_{i=1}^N x_i \sum_{i=1}^n x_i}{N \sum (x_i)^2 - \left(\sum x_i \right)^2} \quad (\text{B.23})$$

This equation can be simplified by using the relation:

$$\sum_{i=1}^n (x_i)^2 = \sum_{i=1}^n (X + i)^2 = n \cdot X^2 + 2X \frac{n(n + 1)}{2} + \frac{n(n + 1)(2n + 1)}{6} \quad (\text{B.24})$$

and substituting equation (B.14) and equations (B.16) and (B.17). After some derivation this yields the following relation:

$$\Delta b = \frac{n\bar{b}}{N(N^2 - 1)} (2n^2 + 9n - 9N - 3nN + 1) \quad (\text{B.25})$$

between the deviation in trend (Δb) on the one hand and the number of deviating samples (n), the total number of samples (N), and the difference in trend ($\bar{b} = b_2 - b_1$) on the other hand.

B.4 Test statistic for quadratic versus linear rise

It is assumed that over a time span of Δx years, an increase in sea-level height of Δsl has occurred. This increase in sea-level height is either caused by a linear sea-level rise, i.e.,

$$\Delta \text{sl} = b_l \Delta x \quad (\text{B.26})$$

or it has followed a quadratic increase:

$$\Delta \text{sl} = b_q \Delta x + c(\Delta x)^2 \quad (\text{B.27})$$

From the two above equations it follows that the quadratic regression term can be written as:

$$c = \frac{b_l - b_q}{\Delta x} \quad (\text{B.28})$$

After a period of X_r years (with $X_r > \Delta x$) will have passed by, sea level will have increased with

$$\Delta \text{sl}_l = b_l X_r \quad (\text{B.29})$$

if a linear pattern is followed. If sea-level increase follows a quadratic pattern the increase in sea-level height will be

$$\Delta \text{sl}_q = b_q X_r + c X_r^2 \quad (\text{B.30})$$

Assuming that after a period of X_r years, the increase in sea-level height due to the quadratic curve is β times the increase due to linear sea-level rise, i.e., $\Delta \text{sl}_q = \beta \Delta \text{sl}_l$, the following relation is found for the quadratic regression coefficient:

$$c = \frac{\beta b_l - b_q}{X_r} \quad (\text{B.31})$$

This equation in combination with equation (B.28) yields for the trend value in the quadratic regression, b_q :

$$b_q = b_l \frac{X_r - \beta N}{X_r - N} \quad (\text{B.32})$$

in which N , the required number of (yearly) observations, has been used instead of the required observation time (Δx).

Substituting this relation for b_q in equation (B.28) yields for the quadratic regression coefficient:

$$c = b_l \frac{\beta - 1}{X_r - N} \quad (\text{B.33})$$

The difference between linear and quadratic sea-level increase is significant if

$$\frac{\hat{c}}{\hat{\sigma}_{\hat{c}}} \geq t_{\alpha}(N - 2) \quad (\text{B.34})$$

where $t_{\alpha}(N - 2)$ represents a Student's distribution with $N - 2$ degrees of freedom and $\hat{\sigma}_{\hat{c}}$ is the a-posteriori standard deviation for the estimate of the quadratic regression coefficient (\hat{c}). As derived in appendix B.1, this standard deviation can be written as:

$$\hat{\sigma}_{\hat{c}} = \hat{\sigma}_{\varepsilon} \cdot \sqrt{\frac{180}{(N - 2)(N^4 - 5N^2 + 4)}} \quad (\text{B.35})$$

in which $\hat{\sigma}_\varepsilon$ is the a-posteriori standard deviation of the measurement errors.

Consequently, the test statistic for distinguishing between linear and quadratic sea-level rise is given by:

$$\frac{\hat{c}}{\hat{\sigma}_\varepsilon} = \frac{\beta - 1}{X_r - N} \frac{b_l}{\hat{\sigma}_\varepsilon} \sqrt{\frac{(N - 2)(N^4 - 5N^2 + 4)}{180}} \quad (\text{B.36})$$

Based on equation (B.36) it can be determined how many years of observations are required to detect (with a certain probability), a quadratic sea-level increase that would yield, e.g., after 50 years, an increase that would be 1.5 times as large as that based on the linear increase (with slope value b_l) over the observation period.

Appendix C

Additional information concerning common variation curves

C.1 Ratio between singular values

If all time series in a data set contain the same signal, singular value decomposition yields a very large first singular value while all other singular values are zero. If differences between time series in a data set are small, ratio between first and second singular value is still large. This implies that the majority of the signal (that part of the signal common to all time series) can be represented by the first singular vector. The other singular vectors contain that part of the signals that differs between the time series. Consequently, the ratio between first and second singular vector can be used as a measure of similarity between time series.

$\frac{\lambda_1}{\lambda_2}$	standard deviation noise					
	1 mm	5 mm	1 cm	2 cm	5 cm	10 cm
same fluctuations	276.0	55.3	27.7	13.9	5.6	2.9
same long periodic fluctuations	17.3	16.6	15.1	11.7	6.0	3.2
different fluctuations	8.8	8.6	8.2	7.2	4.7	2.9

Table C.1 Ratio between first and second singular value. To annual mean sea levels normally distributed random noise has been added based on various standard deviations.

height connection	same fluctuations			same long periodic			different fluctuations		
	1 cm	2 cm	5 cm	1 cm	2 cm	5 cm	1 cm	2 cm	5 cm
10 years	25.8	12.8	5.1	16.6	12.9	5.5	8.8	8.5	5.0
20 years	38.3	19.7	8.6	17.2	15.3	8.8	9.1	8.1	6.2
30 years	24.4	12.2	4.9	15.8	11.6	5.3	8.8	7.5	4.2
40 years	24.2	12.8	4.3	16.4	12.8	4.9	8.6	8.7	4.0
4 differences	21.8	10.8	4.3	14.9	10.2	4.6	8.8	7.6	4.0

Table C.2 Ratio between first and second singular value. Height connections every 10, 20, 30, or 40 years, or in 1885, 1940, 1960, 1980, 1996. Height connection errors are represented by normally distributed random noise with same st. dev. for all tide gauges. All connections have the same st. dev.: 1 cm, 2 cm, or 5 cm.

C.2 Mean value and range of estimated trends

In the following tables, mean values and ranges of trend estimates are given for 100 different realizations of height connection errors. Results are determined for full data sets, i.e., 132 years of observations obtained between 1865 and 1996. Estimates for future height connections use data from 1865 up to the year 2050 or 2100.

st. dev.	same fluctuations		same long periodic		different fluctuations	
	mean	range	mean	range	mean	range
1 mm	1.50	1.50 - 1.50	1.58	1.58 - 1.58	1.51	1.51 - 1.51
5 mm	1.50	1.49 - 1.51	1.58	1.57 - 1.59	1.51	1.50 - 1.52
1 cm	1.50	1.48 - 1.52	1.58	1.56 - 1.58	1.51	1.49 - 1.54
2 cm	1.50	1.45 - 1.55	1.58	1.54 - 1.62	1.51	1.48 - 1.56
5 cm	1.50	1.38 - 1.62	1.58	1.49 - 1.68	1.51	1.42 - 1.64
10 cm	1.50	1.25 - 1.74	1.57	1.39 - 1.78	1.51	1.34 - 1.76

Table C.3 Mean value and range of trend estimates based on full data sets (1865-1996). To annual mean sea levels normally distributed random noise has been added based on various standard deviations.

height connection		same fluctuations		same short periodic		different fluctuations	
period	st. dev.	mean	range	mean	range	mean	range
10 years	1 cm	1.50	1.42 - 1.56	1.58	1.50 - 1.64	1.51	1.43 - 1.57
	2 cm	1.49	1.34 - 1.63	1.57	1.42 - 1.71	1.51	1.35 - 1.64
	5 cm	1.49	1.10 - 1.81	1.57	1.19 - 1.90	1.50	1.12 - 1.83
20 years	1 cm	1.50	1.39 - 1.58	1.58	1.47 - 1.66	1.51	1.40 - 1.59
	2 cm	1.49	1.28 - 1.66	1.58	1.36 - 1.74	1.51	1.29 - 1.67
	5 cm	1.49	0.95 - 1.90	1.57	1.04 - 1.98	1.50	0.97 - 1.91
30 years	1 cm	1.50	1.41 - 1.60	1.58	1.49 - 1.68	1.51	1.42 - 1.61
	2 cm	1.50	1.32 - 1.69	1.58	1.40 - 1.78	1.51	1.33 - 1.71
	5 cm	1.50	1.04 - 1.99	1.58	1.12 - 2.07	1.51	1.05 - 2.00
40 years	1 cm	1.51	1.41 - 1.62	1.59	1.49 - 1.70	1.52	1.42 - 1.63
	2 cm	1.52	1.33 - 1.73	1.61	1.41 - 1.81	1.54	1.34 - 1.74
	5 cm	1.56	1.06 - 2.08	1.64	1.14 - 2.16	1.57	1.08 - 2.09
4 differences	1 cm	1.50	1.32 - 1.60	1.58	1.40 - 1.68	1.51	1.33 - 1.61
	2 cm	1.51	1.15 - 1.71	1.59	1.23 - 1.79	1.52	1.16 - 1.72
	5 cm	1.52	0.61 - 2.01	1.60	0.70 - 2.09	1.53	0.63 - 2.03
4 differences	3, 2, 2, 1.5, 1.5 cm	1.50	1.12 - 1.74	1.58	1.20 - 1.83	1.51	1.13 - 1.76
	2, 1.5, 1.5, 1, 1 cm	1.50	1.25 - 1.67	1.58	1.33 - 1.75	1.51	1.26 - 1.68
	1.5, 1, 1, 0.8, 0.8 cm	1.50	1.31 - 1.62	1.58	1.39 - 1.70	1.51	1.32 - 1.63

Table C.4 Mean value and range of trend estimates based on full data sets (1865-1996). Height connections every 10, 20, 30, or 40 years, or in 1885, 1940, 1960, 1980, 1996 (4 height differences). Height connection errors are represented by normally distributed random noise with same st. dev. for all tide gauges. Different connections either have the same precision (1, 2, or 5 cm), or later connections have better precisions (1885: 3, 2 or 1.5 cm, 1940: 2, 1.5 or 1 cm, 1960: 2, 1.5 or 1 cm, 1980: 1.5, 1 or 0.8 cm, 1996: 1.5, 1 or 0.5 cm).

height connection	same fluctuations		same long periodic		different fluctuations	
	mean	range	mean	range	mean	range
1885: 3 cm, 1940: 2 cm, 1960: 2 cm, 1980: 1.5 cm, 1996: 1.5 cm	1.50	1.07 - 1.89	1.58	1.15 - 1.97	1.51	1.09 - 1.90
	1.51	1.09 - 1.88	1.59	1.17 - 1.96	1.53	1.10 - 1.89
1885: 2 cm, 1940: 1.5 cm, 1960: 1.5 cm, 1980: 1 cm, 1996: 1 cm	1.50	1.19 - 1.78	1.58	1.27 - 1.86	1.51	1.20 - 1.79
	1.51	1.19 - 1.78	1.59	1.27 - 1.86	1.52	1.20 - 1.79
1885: 1.5 cm, 1940: 1 cm, 1960: 1 cm, 1980: 0.8 cm, 1996: 0.8 cm	1.50	1.29 - 1.70	1.59	1.37 - 1.78	1.52	1.30 - 1.71
	1.51	1.30 - 1.69	1.59	1.38 - 1.77	1.52	1.31 - 1.70

Table C.5 Mean value and range of trend estimates based on full data sets (1865-1996). Height connections in 1885, 1940, 1960, 1980, 1996. Height differences have been applied intermittently. Height connection errors are represented by normally distributed random noise with same st. dev. for all tide gauges. Subsequent connections have better precision. Tide gauge bench marks show secular movements with either small differences in velocities (first lines of values) or relatively large differences in velocities (second lines of values).

abrupt change year	size	same fluctuations		same short periodic		different fluctuations	
		mean	range	mean	range	mean	range
1865	5 cm	1.49	1.37 - 1.62	1.57	1.46 - 1.70	1.50	1.39 - 1.63
1870	5 cm	1.51	1.39 - 1.63	1.59	1.47 - 1.71	1.52	1.40 - 1.64
1880	5 cm	1.53	1.41 - 1.65	1.61	1.49 - 1.73	1.54	1.42 - 1.66
1890	1 cm	1.49	1.38 - 1.61	1.57	1.46 - 1.69	1.50	1.39 - 1.62
1890	5 cm	1.48	1.32 - 1.59	1.56	1.40 - 1.67	1.49	1.33 - 1.60
1890	10 cm	1.41	1.30 - 1.53	1.49	1.38 - 1.61	1.42	1.31 - 1.54
1912	5 cm	1.51	1.35 - 1.62	1.59	1.43 - 1.70	1.52	1.36 - 1.63
1935	5 cm	1.52	1.36 - 1.63	1.60	1.44 - 1.71	1.53	1.37 - 1.64
1945	5 cm	1.51	1.37 - 1.61	1.59	1.45 - 1.69	1.52	1.38 - 1.62
1950	5 cm	1.50	1.36 - 1.60	1.58	1.44 - 1.68	1.52	1.37 - 1.61
1955	5 cm	1.50	1.36 - 1.60	1.58	1.44 - 1.68	1.51	1.37 - 1.61
1965	5 cm	1.51	1.39 - 1.65	1.59	1.47 - 1.73	1.52	1.40 - 1.66
1970	5 cm	1.51	1.39 - 1.65	1.59	1.47 - 1.73	1.52	1.40 - 1.66
1975	5 cm	1.50	1.38 - 1.64	1.58	1.46 - 1.72	1.51	1.40 - 1.65
1985	5 cm	1.50	1.37 - 1.62	1.58	1.45 - 1.70	1.51	1.38 - 1.63
1988	5 cm	1.50	1.37 - 1.62	1.58	1.45 - 1.70	1.51	1.38 - 1.63
1991	5 cm	1.49	1.36 - 1.62	1.57	1.44 - 1.70	1.50	1.37 - 1.62

Table C.6 Mean value and range of trend estimates based on full data sets (1865-1996). Height connections in 1885, 1940, 1960, 1980, 1996; standard deviation 1 cm. Height differences have been divided over measurements obtained during the elapsed period between height connections. First time series has experienced an abrupt change in height.

height connection period	α	same fluctuations		same short periodic		different fluctuations	
		mean	range	mean	range	mean	range
10 years	0.5	1.50	1.46 - 1.53	1.58	1.54 - 1.61	1.51	1.47 - 1.54
	1	1.50	1.43 - 1.55	1.58	1.51 - 1.63	1.51	1.44 - 1.56
	2	1.49	1.35 - 1.60	1.57	1.43 - 1.68	1.50	1.36 - 1.62
20 years	0.5	1.50	1.46 - 1.53	1.58	1.54 - 1.61	1.51	1.47 - 1.55
	1	1.50	1.42 - 1.57	1.58	1.50 - 1.65	1.51	1.43 - 1.58
	2	1.50	1.35 - 1.64	1.58	1.43 - 1.72	1.51	1.36 - 1.65
30 years	0.5	1.50	1.44 - 1.55	1.58	1.52 - 1.63	1.51	1.46 - 1.56
	1	1.50	1.39 - 1.60	1.58	1.47 - 1.68	1.51	1.40 - 1.61
	2	1.50	1.28 - 1.70	1.58	1.36 - 1.78	1.51	1.29 - 1.71
40 years	0.5	1.50	1.44 - 1.55	1.58	1.52 - 1.64	1.51	1.45 - 1.57
	1	1.50	1.39 - 1.61	1.58	1.47 - 1.69	1.51	1.40 - 1.62
	2	1.50	1.27 - 1.72	1.58	1.35 - 1.80	1.51	1.28 - 1.73
4 differences	0.5	1.50	1.44 - 1.57	1.59	1.52 - 1.65	1.52	1.45 - 1.58
	1	1.51	1.38 - 1.64	1.59	1.46 - 1.72	1.52	1.39 - 1.65
	2	1.52	1.25 - 1.78	1.60	1.33 - 1.86	1.53	1.26 - 1.79
4 differences	3, 2, 1.5, 1, 0.8	1.50	1.14 - 1.78	1.58	1.22 - 1.86	1.51	1.15 - 1.80
	3, 1.5, 1, 0.8, 0.5	1.50	1.13 - 1.79	1.58	1.21 - 1.87	1.51	1.14 - 1.80
	2, 1.5, 1, 0.8, 0.5	1.51	1.25 - 1.69	1.58	1.33 - 1.77	1.51	1.26 - 1.70

Table C.7 Mean value and range of trend estimates based on full data sets (1865-1996). Height connections every 10, 20, 30, or 40 years, or in 1885, 1940, 1960, 1980, 1996 (4 height differences). Height connection errors are represented by normally distributed random noise with distance dependent standard deviations. Different connections either have the same precision ($\alpha = 0.5, 1, \text{ or } 2$), or later connections have better precisions (1885: $\alpha = 3 \text{ or } 2$, 1940: $\alpha = 2 \text{ or } 1.5$, 1960: $\alpha = 1.5 \text{ or } 1$, 1980: $\alpha = 1 \text{ or } 0.8$, 1996: $\alpha = 0.8 \text{ or } 0.5$).

st. dev.	same fluctuations		different fluctuations	
	up to 2050	up to 2100	up to 2050	up to 2100
5 mm	1.59 - 1.60	1.64 - 1.65	1.58 - 1.59	1.65 - 1.66
1 cm	1.58 - 1.61	1.64 - 1.66	1.57 - 1.60	1.64 - 1.66
2 cm	1.56 - 1.62	1.63 - 1.67	1.55 - 1.61	1.63 - 1.68
5 cm	1.51 - 1.66	1.60 - 1.70	1.50 - 1.65	1.61 - 1.71

Table C.8 Range of trend estimates resulting from 100 realizations of normally distributed random values added to annual mean sea level-heights; various standard deviations. Data sets contain measurements from 1865 up to either 2050 or 2100. Time series start with trend of 1.5 mm/yr, which (abruptly) increases in 1991 to 1.8 mm/yr.

st. dev.	same fluctuations		different fluctuations	
	up to 2050	up to 2100	up to 2050	up to 2100
5 mm	2.26 - 2.27	2.86 - 2.87	2.25 - 2.27	2.87 - 2.88
1 cm	2.25 - 2.28	2.86 - 2.88	2.25 - 2.27	2.86 - 2.89
2 cm	2.24 - 2.29	2.85 - 2.89	2.23 - 2.28	2.85 - 2.90
5 cm	2.18 - 2.33	2.82 - 2.92	2.17 - 2.32	2.83 - 2.93

Table C.9 Range of trend estimates resulting from 100 realizations of normally distributed random values added to annual mean sea-level heights; various standard deviations. Data sets contain measurements from 1865 up to either 2050 or 2100. Time series start with trend of 1.5 mm/yr, which (abruptly) increases in 1991 to 4.5 mm/yr.

standard deviations		same fluctuations		different fluctuations	
		up to 2050	up to 2100	up to 2050	up to 2100
3, 2, 2, 1.5, 1.5 cm	5 mm	2.06 - 2.45	2.73 - 2.99	2.05 - 2.44	2.74 - 3.00
3, 2, 2, 1.5, 1.5 cm	1 cm	2.06 - 2.45	2.72 - 2.99	2.05 - 2.44	2.73 - 2.99
3, 2, 2, 1.5, 1.5 cm	2 cm	2.07 - 2.44	2.73 - 2.98	2.06 - 2.43	2.73 - 2.99
2, 1.5, 1.5, 1, 1 cm	5 mm	2.13 - 2.39	2.77 - 2.95	2.12 - 2.37	2.78 - 2.96
2, 1.5, 1.5, 1, 1 cm	1 cm	2.12 - 2.38	2.77 - 2.94	2.11 - 2.37	2.77 - 2.95
2, 1.5, 1.5, 1, 1 cm	2 cm	2.13 - 2.38	2.77 - 2.95	2.12 - 2.37	2.78 - 2.95
1.5, 1, 1, 0.8, 0.8 cm	5 mm	2.17 - 2.36	2.80 - 2.93	2.16 - 2.35	2.80 - 2.93
1.5, 1, 1, 0.8, 0.8 cm	1 cm	2.17 - 2.36	2.79 - 2.93	2.16 - 2.35	2.80 - 2.94
1.5, 1, 1, 0.8, 0.8 cm	2 cm	2.17 - 2.36	2.79 - 2.93	2.16 - 2.35	2.80 - 2.94

Table C.10 Range of trend estimates resulting from 100 realizations of normally distributed random errors. Time series start with trend of 1.5 mm/yr, which (abruptly) increases in 1991 to 4.5 mm/yr. Height connections in 1885 (σ : 3, 2 or 1.5 cm), 1940 (σ : 2, 1.5 or 3 cm), 1960 (σ : 2, 1.5 or 1 cm), 1980 (σ : 1.5, 1 or 0.8 cm), and 1996 (σ : 1.5, 1 or 0.8 cm); height differences have been divided over measurements obtained during the elapsed period between connections. After 1996, connections on (at least) yearly basis with various standard deviations. Data sets contain measurements from 1865 up to either 2050 or 2100.

standard deviations		same fluctuations		different fluctuations	
		up to 2050	up to 2100	up to 2050	up to 2100
3, 2, 2, 1.5, 1.5 cm	5 mm	2.07 - 2.50	2.72 - 3.01	2.06 - 2.49	2.73 - 3.01
3, 2, 2, 1.5, 1.5 cm	1 cm	2.06 - 2.50	2.72 - 3.01	2.05 - 2.49	2.72 - 3.02
3, 2, 2, 1.5, 1.5 cm	2 cm	2.06 - 2.50	2.71 - 3.01	2.05 - 2.49	2.71 - 3.02
2, 1.5, 1.5, 1, 1 cm	5 mm	2.13 - 2.42	2.77 - 2.96	2.12 - 2.41	2.78 - 2.97
2, 1.5, 1.5, 1, 1 cm	1 cm	2.13 - 2.42	2.76 - 2.96	2.12 - 2.41	2.77 - 2.97
2, 1.5, 1.5, 1, 1 cm	2 cm	2.12 - 2.43	2.75 - 2.96	2.11 - 2.42	2.76 - 2.97
1.5, 1, 1, 0.8, 0.8 cm	5 mm	2.17 - 2.38	2.79 - 2.94	2.16 - 2.37	2.80 - 2.94
1.5, 1, 1, 0.8, 0.8 cm	1 cm	2.16 - 2.39	2.79 - 2.94	2.15 - 2.38	2.79 - 2.95
1.5, 1, 1, 0.8, 0.8 cm	2 cm	2.15 - 2.39	2.77 - 2.94	2.14 - 2.38	2.78 - 2.95

Table C.11 Range of trend estimates resulting from 100 realizations of normally distributed random errors. Time series start with trend of 1.5 mm/yr, which (abruptly) increases in 1991 to 4.5 mm/yr. Height connections in 1885 (σ : 3, 2 or 1.5 cm), 1940 (σ : 2, 1.5 or 3 cm), 1960 (σ : 2, 1.5 or 1 cm), 1980 (σ : 1.5, 1 or 0.8 cm), and 1996 (σ : 1.5, 1 or 0.8 cm); height differences have been divided over measurements obtained during the elapsed period between connections. After 1996, connections every 5 years with various standard deviations. Data sets contain measurements from 1865 up to either 2050 or 2100.

standard deviations		same fluctuations		different fluctuations	
		up to 2050	up to 2100	up to 2050	up to 2100
3, 2, 2, 1.5, 1.5 cm	5 mm	2.07 - 2.46	2.73 - 2.99	2.06 - 2.45	2.74 - 3.00
3, 2, 2, 1.5, 1.5 cm	1 cm	2.07 - 2.45	2.72 - 2.99	2.06 - 2.44	2.73 - 3.00
3, 2, 2, 1.5, 1.5 cm	2 cm	2.07 - 2.45	2.71 - 3.00	2.06 - 2.44	2.72 - 3.00
2, 1.5, 1.5, 1, 1 cm	5 mm	2.14 - 2.39	2.77 - 2.95	2.13 - 2.38	2.78 - 2.96
2, 1.5, 1.5, 1, 1 cm	1 cm	2.14 - 2.39	2.77 - 2.95	2.13 - 2.37	2.77 - 2.96
2, 1.5, 1.5, 1, 1 cm	2 cm	2.14 - 2.40	2.75 - 2.95	2.13 - 2.39	2.76 - 2.96
1.5, 1, 1, 0.8, 0.8 cm	5 mm	2.17 - 2.36	2.80 - 2.93	2.16 - 2.35	2.80 - 2.94
1.5, 1, 1, 0.8, 0.8 cm	1 cm	2.17 - 2.36	2.79 - 2.93	2.16 - 2.35	2.80 - 2.94
1.5, 1, 1, 0.8, 0.8 cm	2 cm	2.17 - 2.38	2.78 - 2.93	2.16 - 2.37	2.79 - 2.94

Table C.12 Range of trend estimates resulting from 100 realizations of normally distributed random errors. Time series start with trend of 1.5 mm/yr, which (abruptly) increases in 1991 to 4.5 mm/yr. Height connections in 1885 (σ : 3, 2 or 1.5 cm), 1940 (σ : 2, 1.5 or 3 cm), 1960 (σ : 2, 1.5 or 1 cm), 1980 (σ : 1.5, 1 or 0.8 cm), and 1996 (σ : 1.5, 1 or 0.8 cm); height differences have been divided over measurements obtained during the elapsed period between connections. After 1996, connections every 10 years with various standard deviations. Data sets contain measurements from 1865 up to either 2050 or 2100.

References

- Alberda, J. (1963). Report on the adjustment of the United European Levelling Net and related computations. Technical Report 2, Netherlands Geodetic Commission.
- Ashkenazi, V., Basker, G., Davison, M., Dodson, A., Hipkin, R., Stewart, M., Baker, T., Woodworth, P., Bordley, R., and Christie, R. (1990). Dynamic sea level and the geoid by gravimetric and GPS measurements. Technical report, University of Nottingham. NERC/SERC grant ref no. gst/02/142.
- Ashkenazi, V., Bingley, R., Whitmore, G., and Baker, T. (1993). Monitoring changes in mean sea-level to millimeters using GPS. *Geophysical Research Letters*, **20**(18), 1951–1954.
- Augath, W. (1991). Subcommittee United European Levelling Network (UELN). In *National report of the Federal Republic of Germany on the geodetic activities in the years 1987-1991. XX. General Assembly of the Int. Union for Geodesy and Geophysics 1991 at Vienna/Austria*, Deutsche Geodatische Kommission. Reihe B. Angewandte Geodasie Heft Nr. 294. Beck.
- Baarda, W. (1968). A testing procedure for use in geodetic networks. Technical Report 5, Netherlands Geodetic Commission.
- Baarda, W. (1979). A connection between geometric and gravimetric geodesy; a first sketch. Technical Report 4, Netherlands Geodetic Commission.
- Baarda, W. (1995). Linking up spatial models in geodesy; extended S-transformations. Technical Report 41, Netherlands Geodetic Commission.
- Baker, T., Curtis, D., and Dodson, A. (1995). Ocean tide loading and GPS. *GPS World*, **6**(3).
- Banaszek, A. (1985). Procedures and problems associated with the calibration and use of pressure sensors for sea level measurements. In *Evaluation, comparison and calibration of oceanographic instruments*, volume 4 of *Advances in underwater technology and offshore engineering*. Graham and Trotman, London.
- Barbarella, M. and Radicioni, F. (1990). Kalman filtering in levelling: an application. In P. Vyskocil, P. Cross, and C. Reigber, editors, *Global and regional geodynamics*, number 101 in International Association of Geodesy symposia. Springer-Verlag.
- Blewitt, G. (1994). The global positioning system. In W. Carter, editor, *Report of the Surrey workshop of the IAPSO tide gauge bench mark fixing committee*, pages 17–26, Surrey, United Kingdom. Institute of Oceanographic Sciences.
- Bock, Y. (1996). Reference systems. In A. Kleusberg and P. Teunissen, editors, *GPS for Geodesy*, number 60 in Lecture notes in earth sciences, pages 3–36. Springer.
- Bosworth, J. (1994). Global networks. In W. Carter, editor, *Report of the Surrey workshop of the IAPSO tide gauge bench mark fixing committee*, pages 41–66, Surrey, United Kingdom. Institute of Oceanographic Sciences.
- Boucher, C. and Altamimi, Z. (1993). ITRF 92 and its associated velocity field. Technical Report IERS technical note 15, IERS.
- Boucher, C., Altamimi, Z., and Duhem, L. (1992). ITRF 91 and its associated velocity field. Technical Report IERS technical note 12, IERS.
- Box, G. and Jenkins, G. (1976). *Time series analysis; forecasting and control*. Prentice Hall.
- Brand, G. (2000). 5e NWP - definitieve berekening waterpassen. This document will be published in 2001.

- Carrera, G., Tessier, B., and O'Reilly, C. (1996). Statistical behavior of digital pressure water level gauges. *Marine Geodesy*, **19**, 137–163.
- Carter, W., editor (1994). *Report of the Surrey workshop of the IAPSO tide gauge bench mark fixing committee*, Surrey, United Kingdom. Institute of Oceanographic Sciences.
- Carter, W., Aubrey, D., Baker, T., Boucher, C., LeProvost, C., Pugh, D., Peltier, W., Zumberge, M., Emery, K., and Enfield, D. (1989). Geodetic fixing of tide gauge bench marks. Technical Report WHOI-89-31, Woods Hole Oceanographic Institution, Woods Hole, Massachusetts 02543.
- Cartwright, D. (1983). On the smoothing of climatological time series, with application to sea-level at Newlyn. *Geophys. J. R. astr. Soc.*, **75**, 639–658.
- Chelton, D. and Enfield, D. (1986). Ocean signals in tide gauge records. *Journal of Geophysical Research*, **91**(B9), 9081–9098.
- Chen, G. and Herring, T. (1997). Effects of atmospheric azimuthal asymmetry on the analysis of space geodetic data. *Journal of Geophysical Research*, **102**(B9), 20489–20502.
- Chrzanowski, A., Chen, Y., and Leal, J. (1990). Modelling of ground subsidence from a combination of GPS and levelling surveys. In P. Vyskocil, P. Cross, and C. Reigber, editors, *Global and regional geodynamics*, number 101 in International Association of Geodesy symposia. Springer-Verlag.
- Cross, R. (1968). Tide gauge frequency response. *Journal of waterways and harbour division*, **94**(WW3). American Society of Civil Engineers.
- Cunietti, M., Facchinelli, F., Mozzi, G., Ricceri, G., Soranzo, M., and Vitelli, E. (1986). An experimental investigation on the stability of levelling bench mats into sedimentary soils. In A. Johnson, editor, *Land subsidence; 3rd international symposium*, number 151 in IAHS publication. IAHS.
- Daubechies, I. (1992). *Ten lectures on wavelets*, volume 61 of *CBMS-NSF regional conference series in applied mathematics*. SIAM.
- de Bruijne, A., Haagmans, R., and de Min, E. (1997). A preliminary north sea geoid model GEONZ97. Technical Report MDGAP-9735, Ministerie van Verkeer en Waterstaat, Directoraat-Generaal Rijkswaterstaat, Meetkundige dienst.
- de Min, E. (1996). *De geoid van Nederland*. Ph.D. thesis, Delft University of Technology. The geoid for the Netherlands; in Dutch.
- de Ronde, J. (1991). Rising waters. impacts of the greenhouse effect for the netherlands. Technical Report gwao 90.026, Ministry of transport and public works, tidal waters division.
- Diamante, J., Pyle, T., Carter, W., and Scherer, W. (1987). Global change and the measurement of absolute sea-level. *Progress in Oceanography*, **18**, 1–21.
- Dillingh, D. (1998). private communication.
- Ehrensperger, W. and Kok, J. (1986). Status and results of the 1986 adjustment of the United European Levelling Network - UELN-73. In *Proceedings on height determination and recent crustal movements in Western Europe*.
- Ehrensperger, W., Kok, J., and van Mierlo, J. (1982). Status and provisional results of the 1981 adjustment of the United European Levelling Network UELN-73. In R. Sigl, editor, *Proceedings of the international symposium on geodetic networks and computations of the International Association of Geodesy*, volume II, pages 25–50. Deutsche Geodätische Kommission, München.
- Ekman, M. (1989). Impacts of geodynamic phenomena on systems for height and gravity. *Bulletin Geodesique*, **63**, 281–296.
- Ekman, M. (1993). Postglacial rebound and sea level phenomena, with special reference to Fennoscandia and the Baltic Sea. Technical Report 115, the Finnish Geodetic Institute.

- Ekman, M. and Mäkinen, J. (1991). The deviation of mean sea level from the mean geoid in the Baltic Sea. *Bulletin Geodesique*, **65**, 83–91.
- Emery, K. and Aubrey, D. (1991). *Sea Levels, Land Levels, and Tide Gauges*. Springer-Verlag.
- ESA (1999). Gravity Field and Steady-State Ocean Circulation Mission. Reports for mission selection; the four candidate earth explorer core missions. ESA SP-1233(1).
- Fairbridge, R. and Jelgersma, S. (1990). Sea level. In R. Paepe, R. Fairbridge, and S. Jelgersma, editors, *Greenhouse effect, sea level and drought*, volume 325 of *NATO ASI Series, series C*. Kluwer Academic Publishers.
- Fisk, D. (1997). Climate change and its impacts - a global perspective. http://www.metu.gov.uk/sec5/CR_div/Brochure97/index-nf.html.
- Gommes, R. and du Guerne, J. (1998). Potential impacts of sea-level rise on populations and agriculture. <http://www.fao.org/sd/eidirect/EIre0045.htm>.
- Haagmans, R., de Bruijne, A., and de Min, E. (1998). A procedure for combining gravimetric geoid models and independent geoid data, with an example in the North Sea region. *DEOS Progress Letter*, **98.1**, 89–99.
- Hamon, B. and Godfrey, J. (1980). Mean sea level and its interpretation. *Marine Geodesy*, **4**(4), 315–329.
- Harnisch, G. (1993). Systematic errors affecting the accuracy of high precision gravity measurements. In H. Montag and C. Reigber, editors, *Geodesy and physics of the earth*, number 112 in International Association of Geodesy symposia. Springer-Verlag.
- Heck, B. (1990). An evaluation of some systematic error sources affecting terrestrial gravity anomalies. *Bulletin Geodesique*, **64**, 88–108.
- Heck, B. and Gruninger, W. (1987). Modifications of Stokes integral formula by combining two classical approaches. In *Proceedings of IAG XIX General Assembly, Vancouver*.
- Heinen, P. (1992). Singular spectrum analysis applied to time series. Technical Report DGW-92.031, Ministry of Transport, Public Works and Water Management, Directorate-General of Public Works and Water Management, Tidal Waters Division (RIKZ).
- Heinen, P. and Hoogkamer, M. (1993). Trends and meteorological influences in mean sea levels. Technical Report DGW-93.017, Ministry of Transport, Public Works and Water Management, Directorate-General of Public Works and Water Management, Tidal Waters Division (RIKZ).
- Heiskanen, W. and Moritz, H. (1967). *Physical geodesy*. W.H. Freeman and Co.
- Holdahl, S. (1978). Models for extracting vertical crustal movements from levelling data. In I. Mueller, editor, *Proc. of the 9th GEOP Conference, An International Symposium on the Applications of Geodesy to Geodynamics*, number 280 in Dept. of Geodetic Science Rept. The Ohio State University.
- IOC (1985). Manual on sea level measurement and interpretation. Technical Report 14, Intergovernmental Oceanographic Commission.
- IOC (1994). Manual on sea level measurement and interpretation. volume ii - emerging technologies. Technical Report 14, Intergovernmental Oceanographic Commission.
- Jachens, R. (1978). The gravity method and interpretive techniques for detecting vertical crustal movements. In I. Mueller, editor, *Proc. of the 9th GEOP Conference, An International Symposium on the Applications of Geodesy to Geodynamics*, number 280 in Dept. of Geodetic Science Rept. The Ohio State University.
- Kok, J., Ehrnsperger, W., and Rietveld, H. (1980). The 1979 adjustment of the United European Levelling Network (UENL) and its analysis of precision and reliability. In G. Lachapelle, editor, *Problems related to the redefinition of North American vertical geodetic networks; 2nd international symposium*, pages 455–483.

- Können, G. (1999). De toestand van het klimaat in Nederland 1999. <http://www.knmi.nl>.
- Kukkamäki, T. (1980). Errors affecting levelling. In G. Lachapelle, editor, *Problems related to the redefinition of North American vertical geodetic networks; 2nd international symposium*.
- Lambeck, K., Smither, C., and Johnston, P. (1998). Sea-level change, glacial rebound and mantle viscosity for northern Europe. *Geophysical Journal International*, **134**, 102–144.
- Lambert, A. (1994). Absolute gravity application to global sea level studies. In W. Carter, editor, *Report of the Surrey workshop of the IAPSO tide gauge bench mark fixing committee*, pages 33–40, Surrey, United Kingdom. Institute of Oceanographic Sciences.
- Lang, H. and Sacher, M. (1996a). Status and results of the adjustment and enlargement of the United European Levelling Network 1995 (UELN-95). In E. Gubler and H. Hornik, editors, *Report on the symposium of the IAG subcommission for the European Reference Frame, Ankara 1995*, number 54 in *Astronomisch-Geodatische Arbeiten*. Bayerischen Akademie der Wissenschaften.
- Lang, H. and Sacher, M. (1996b). Status and results of the adjustment and enlargement of the United European Levelling Network 1995 (UELN-95). In E. Gubler and H. Hornik, editors, *Report on the symposium of the IAG subcommission for the European Reference Frame (EUREF) held in Helsinki 1995*, number 56 in *Veröffentlichungen der Bayerischen Kommission für die Internationale Erdmessung*. Bayerischen Akademie der Wissenschaften.
- Langbein, J. and Johnson, H. (1997). Correlated errors in geodetic time series: implications for time-dependent deformation. *Journal of Geophysical Research*, **102**(B1), 591–603.
- Lennon, G. (1970). Sea level instrumentation, its limitations and the optimization of the performance of conventional gauges in Great Britain. In R. Sigl, editor, *Coastal Geodesy; symposium, Munich, July 1970*. z. uitg. International Union of Geodesy and Geophysics; Technical University Munich, Institute for Astronomical and Physical Geodesy.
- Lorenz, G., Groenewoud, W., and Schokking, F. (1991). Heden en verleden, Nederland naar beneden? interim-rapport over het onderzoek naar bodembeweging in Nederland. Technical Report ??, Ministerie van Verkeer en Waterstaat, Directoraat-Generaal Rijkswaterstaat, Meetkundige dienst.
- MacMillan, D. and Ma, C. (1997). Atmospheric gradients and the VLBI terrestrial and celestial reference frames. *Geophysical Research Letters*, **24**(4), 453–456.
- Makridakis, S. and Hibon, M. (1984). Accuracy of forecasting: an empirical investigation (with discussion). In S. Makridakis, A. Andersen, R. Carbone, R. Fildes, M. Hibon, R. Lewandowski, J. Newton, E. Parzen, and R. Winkler, editors, *The forecasting accuracy of major time series methods*, chapter 3. John Wiley & Sons.
- Makridakis, S. and Wheelwright, S. (1978). *Forecasting methods and applications*. John Wiley & Sons.
- Martin, D., Chapin, J., and Maul, G. (1996). State-of-the-art sea level monitoring. *Marine Geodesy*, **19**, 105–114.
- Mather, R. (1974). Geodetic coordinates in four dimensions. *The Canadian Surveyor*, **28**(5), 574–581.
- Mitchum, G. (1994). Report of oceanography working group. In W. Carter, editor, *Report of the Surrey workshop of the IAPSO tide gauge bench mark fixing committee*, pages 9–16, Surrey, United Kingdom. Institute of Oceanographic Sciences.
- Molodenskii, M., Eremeev, V., and Yurkina, M. (1962). Methods for study of the external gravitational field and figure of the earth. Israel program for scientific translations.
- Montag, H. (1970). On the accuracy of determination of secular variations of mean sea level at the Baltic Sea coast. In R. Sigl, editor, *Coastal Geodesy; symposium, Munich, July 1970*. z. uitg. International Union of Geodesy and Geophysics; Technical University Munich, Institute for Astronomical and Physical Geodesy.

- Mörner, N.-A. (1979). The Fennoscandian uplift and Late Cenozoic geodynamics - geological evidence. *GeoJournal*, **3.3**, 287–318.
- Murre, L. (1985). *Hervereffening van de tweede, derde en vierde nauwkeurigheidswaterpassing van Nederland en vergelijking van de resultaten*. Ph.D. thesis, Delft University of Technology. afstudeerscriptie.
- Nicholls, N., Gruza, G., Jouzel, J., Karl, T., Ogallo, L., and Parker, D. (1996). Observed climate variability and change. In J. Houghton, L. Meiza Filho, B. Callander, N. Harris, A. Kattenberg, and K. Maskell, editors, *Climate change 1995; the science of climate change; contributions of working group 1 to the second assessment report of the Intergovernmental Panel on Climate Change*, chapter 3, pages 133–192. Cambridge University Press.
- Oppenheim, A., Willsky, A., and Young, I. (1983). *Signals and Systems*. Prentice-Hall.
- Peltier, W. (1990). Glacial isostatic adjustment and relative sea level change. In *Sea-level change*. National Research Council, National Academy press.
- Peltier, W. (1994). Ice age paleotopography. *Science*, **265**, 195–201.
- Peltier, W. (1998). Postglacial variations in the level of the sea: implications for climate dynamics and solid-earth geophysics. *Reviews of Geophysics*, **36**, 603–689.
- Pirazzoli, P. (1990). Present and near-future sea-level changes: an assessment. In R. Paepe, R. Fairbridge, and S. Jelgersma, editors, *Greenhouse effect, sea level and drought*, volume 325 of *NATO ASI Series, series C*. Kluwer Academic Publishers.
- Pitman, W. (1979). The effect of eustatic sea level changes on stratigraphic sequences at atlantic margins. In J. Watkins, L. Montadert, and P. Dickerson, editors, *Geological and geophysical investigations of continental margins*, number 29 in *Memoir*, pages 453–460. American Association of Petroleum Geologists.
- Plag, H.-P. (1997). Chandler wobble and pole tide in relation to interannual atmosphere-ocean dynamics. In H. Wilhelm, W. Zürn, and H.-G. Wenzel, editors, *Tidal phenomena*, number 66 in *Lecture notes in earth sciences*. Springer.
- Plag, H.-P. (2000). personal communicationsbtex proefschrift1.
- Pöttgens, J. (1991). Land subsidence due to gas extraction in the northern part of the Netherlands. In A. Johnson, editor, *Land subsidence; proceedings of the fourth international symposium on land subsidence*, number 200 in IAHS publication. IAHS.
- Pugh, D. (1987). *Tides, surges and mean sea level, a handbook for engineers and scientists*. John Wiley & sons.
- Rae, J. (1976). The design of instrumentation for the measurement of tides offshore. In *The Hydrographic Society Symposium on tide recording, proceedings*, number 4 in special publication Hydrographic Society. Hydrographic Society.
- Rapp, R. and Balasubramania, N. (1992). A conceptual formulation of a world height system. Technical Report OSU 421, Department of Geodetic Science and Surveying, The Ohio State University.
- Richards, J. (1985). Minimizing systematic errors in levelling. In D. Zilkoski, editor, *Proceedings of the third international symposium on the North American vertical datum*. US Department of Commerce.
- Richter, B., Klopping, F., Peter, G., Bertis, K., Carter, W., and Goodkind, J. (1993). Detection of secular gravity variations; observations with superconducting gravimeters improve the accuracy of absolute gravity measurements. In H. Montag and C. Reigber, editors, *Geodesy and physics of the earth*, number 112 in *International Association of Geodesy symposia*. Springer-Verlag.
- Rietveld, H. (1986). Land subsidence in the Netherlands. In A. Johnson, L. Carbognin, and . Ubertini, editors, *Land subsidence; proceedings of the third international symposium on land subsidence held in Venice*, number 151 in IAHS publication. IAHS.

- Ronde, de, J., Dilingh, D., and Groenewoud, W. (1993). Past and future sea level rise in the Netherlands and its impacts; part of the EPOC project: climate change, sea level rise and associated impacts in Europe. Technical report, Ministry of Transport, Public works and Water Management.
- Rossiter, J. (1958). Note on methods of determining monthly and annual values of mean water level. *International Hydrographic Review*, **35**, 105–115.
- Rummel, R. and Teunissen, P. (1988). Height datum definition, height datum connection and the role of the geodetic boundary value problem. *Bulletin Geodesique*, **62**(4), 477–498.
- Sacher, M., Lang, H., and Ihde, J. (1999). Status and results of the adjustment and enlargement of the United European Levelling Network 1995 (UELN-95). In E. Gubler and H. Hornik, editors, *VEREF Publication no. 7/1*, number Band 6 in Mitteilungen des Bundesamtes für Kartographie und Geodäsie.
- Sager, G. and Matthäus, N. (1970). Theoretical and experimental investigations into the damping properties of tide gauges. In R. Sigl, editor, *Coastal Geodesy; symposium, Munich, July 1970*. z. uitg. International Union of Geodesy and Geophysics; Technical University Munich, Institute for Astronomical and Physical Geodesy.
- Scherneck, H.-G. (1986). *Tidal gravimetry, physical models and numerical methods for the reduction of environmental and instrumental problems in application to earth and ocean tide measurements*. Ph.D. thesis, Uppsalam University.
- Seeber, G. (1993). *Satellite Geodesy; Foundations, methods, and applications*. Walter de Gruyter.
- Sjöberg, L. (1986). Comparison of some methods of modifying Stokes' formula. In *Proceedings of the international symposium on the definition of the geoid*, volume II.
- Smeets, I. (1992). *Modellering en foutenanalyse van een precisiegeode op centimeter-niveau*. Ph.D. thesis, Katholieke Universiteit Leuven. Dutch.
- Smithson, M. (1997). Tide gauges. presented at the summerschool: sea level changes on micro to macro time scales: measurements, modelling, interpretation and application; Kos, Greece.
- Spencer, R. and Vassie, J. (1997). The evolution of deep ocean pressure measurements in the U.K. *Progress in Oceanography*, **40**, 423–435.
- Springer, T., Ambrosius, B., Noomen, R., and Herzberger, K. (1994). Results of the WEGENER/GPS-92 campaign. *Geophysical Research Letters*, **21**(16), 1711–1714.
- Strang, G. and Nguyen, T., editors (1996). *Wavelets and filter banks*. Wellesley-Cambridge Press.
- Strange, W. (1980). Errors affecting levelling. In G. Lachapelle, editor, *Problems related to the redefinition of North American vertical geodetic networks; 2nd international symposium*.
- Torge, W. (1989). *Gravimetry*. Walter de Gruyter.
- Van der Hoek Ostende, E. and Van Malde, J. (1989). De invloed van de bepalingwijze op de berekende gemiddelde zeestand. Technical report, Ministerie van verkeer en waterstaat, dienst getijdewateren. nota GWAO-89.006, in Dutch.
- Van der Made, J. (1987). *Analysis of some criteria for design and operation of surface water gauging networks*. Ph.D. thesis, Delft University of Technology. Van Gorcum, Assen.
- Van Malde, J. (1986). Relatieve rijzing van gemiddelde zeeniveaus. In *Zee-in-zicht, verslag symposium Gezelschap Praktische Studie, Delft*.
- van Onselen, K. (1998). Quality investigation of vertical datum connection. Technical Report 98.5, Delft Institute for Earth-Oriented Space Research.
- Vaniček, P. and Krakiwsky, E. (1986). *Geodesy: the concepts*. Elsevier Science Publishers. 2nd edition.
- Vaniček, P., Cross, P., Hannah, J., Hradilek, L., Kelm, R., Mäkinen, J., Merry, C., Sjöberg, L., Steeves, R., and Zilkoski, D. (1987). Four-dimensional geodetic positioning. *Manuscripta Geodetica*, **12**, 147–222. report of the IAG SSG 4.96.

- Varekamp, J. and Thomas, E. (1998). Climate change and the rise and fall of sea level over the millennium. *EOS, Transactions*, **79**(6).
- Virtanen, H. and Käariäinen, J. (1995). The installation of and first results from the superconducting gravimeter GWR20 at the Metsähovi station, Finland. Technical Report 95:1, the Finnish geodetic institute.
- Waalewijn, A. (1987). Drie eeuwen normaal amsterdams peil. Technical report, Rijkswaterstaat, Hoofd-directie van de Waterstaat. Rijkswaterstaat - serie 48.
- Warrick, R., Le Provost, C., Meier, M., Oerlemans, J., and Woodworth, P. (1996). Changes in sea level. In J. Houghton, L. Meiza Filho, B. Callander, N. Harris, A. Kattenberg, and K. Maskell, editors, *Climate change 1995; the science of climate change; contributions of working group 1 to the second assessment report of the Intergovernmental Panel on Climate Change*, chapter 7, pages 359–405. Cambridge University Press.
- Woodworth, P. (1999). High waters at Liverpool since 1768: the UK's longest sea level record. *Geophysical Research Letters*, **26**, 1589–1592.
- Woodworth, P. (2000). personal communications.
- Woodworth, P., Vassie, J., Spencer, R., and Smith, D. (1996). Precise datum control for pressure tide gauges. *Marine Geodesy*, **19**, 1–20.
- Xu, P. (1990). Monitoring sea level rise. Technical report, Faculty of Geodetic engineering, TU Delft.
- Xu, P. and Rummel, R. (1991). A quality investigation of global vertical datum connection. Technical Report 34, Netherlands Geodetic Commission.
- Zerbini, S., Plag, H.-P., Baker, T., Becker, M., Billiris, H., Bürki, B., Kahle, H.-G., Marson, I., Pezzoli, L., Richter, B., Romagnoli, C., Sztobryn, M., Tomasi, P., Tsimplis, M., Veis, G., and Verrone, G. (1996). Sea level in the Mediterranean: a first step towards separating crustal movements and absolute sea-level variations. *Global and Planetary Change*, **14**, 1–48.
- Zwick, A. (1997). Monitoring and assessment of recent research results on global climate change with a special solution on sea-level rise and joint implementation. In *Climate change research and policy*, number Update N. 9 in Periodic survey for the Commission of the European Communities. Joint Research Centre, Sevilla.

